The geochemistry of naturally occurring methane and saline groundwater in an area of unconventional shale gas development

Jennifer Harkness, Thomas Darrah, Nathaniel Warner, Colin Whyte, Myles Moore, Romain Millot, Wolfram Kloppmann, Robert Jackson, Avner Vengosh

The Geochemistry of Naturally Occurring Methane and Saline Groundwater in an Area of Unconventional Shale Gas Development

Jennifer S. Harkness[a], Thomas H. Darrah[b], Nathaniel R. Warner[c], Colin J. Whyte[b], Myles T. Moore[b], Romain Millot[d], Wolfram Kloppman[d], Robert B. Jackson[e], Avner Vengosh[a*]

[a] *Division of Earth and Ocean Sciences, Nicholas School of the Environment, Duke University, Durham, NC 27708, USA*

[b] *Divisions of Solid Earth Dynamics and Water, Climate and the Environment, School of Earth Sciences, The Ohio State University, Columbus, OH 43210, USA*

[c] *Department of Civil and Environmental Engineering, Pennsylvania State University, College Park, PA 16802, USA*

[d] *BRGM, French Geological Survey, Laboratory Division, Orléans, France*

[e] *Department of Earth System Science, Stanford University, Stanford, CA 94305, USA*

* Corresponded author (vengosh@duke.edu)

Abstract

Since naturally occurring methane and saline groundwater are nearly ubiquitous in many sedimentary basins, delineating the effects of anthropogenic contamination sources is a major challenge for evaluating the impact of unconventional shale gas development on water quality. This study investigates the geochemical variations of groundwater and surface water before, during, and after hydraulic fracturing and in relation to various geospatial parameters in an area of shale gas development in northwestern West Virginia, United States. To our knowledge, we are the first to report a broadly integrated study of various geochemical techniques designed to apportion natural and anthropogenic sources of natural gas and salt contaminants both before and after drilling. These measurements include inorganic geochemistry (major cations and anions), stable isotopes of select inorganic constituents including strontium ($^{87}Sr/^{86}Sr$), boron ($\delta^{11}B$), lithium ($\delta^{7}Li$), and carbon ($\delta^{13}C$-DIC), select hydrocarbon molecular (methane, ethane, propane, butane, and pentane) and isotopic tracers ($\delta^{13}C$-CH_4, $\delta^{13}C$-C_2H_6), tritium (^{3}H), and noble gas elemental and isotopic composition (He, Ne, Ar) in 112 drinking-water wells, with repeat testing in 33 of the wells (total samples=145). In a subset of wells (n=20), we investigated the variations in water quality before and after the installation of nearby (<1 km) shale-gas wells. Methane occurred above 1 ccSTP/L in 37% of the groundwater samples and in 79% of the samples with elevated salinity (chloride >50 mg/L). The integrated geochemical data indicate that the saline groundwater originated via naturally occurring processes, presumably from the migration of deeper methane-rich brines that have interacted extensively with coal lithologies. These observations were consistent with the lack of changes in water quality observed in drinking-water wells following the installation of nearby shale-gas wells. In contrast to groundwater samples that showed no evidence of anthropogenic contamination, the chemistry and isotope ratios of surface waters near known spills or leaks occurring at disposal sites (n=8) mimicked the composition of the Marcellus flowback fluids, and show direct evidence for impact on surface water by fluids accidentally released from nearby shale-gas well pads and oil and gas wastewater disposal sites. Overall this study presents a comprehensive geochemical framework that can be

used as a template for assessing the sources of elevated hydrocarbons and salts to water resources in areas potentially impacted by oil and gas development.

Keywords
Water quality, hydraulic fracturing, methane, isotope tracers, shale gas, brines

1. INTRODUCTION

Development of unconventional hydrocarbon resources from previously uneconomical black shales and tight sands through the advent of horizontal drilling and hydraulic fracturing technologies has revitalized the domestic energy industry in the U.S. and reduced dependency on coal combustion for electricity generation (USEIA, 2014). However, numerous environmental concerns, including the potential for compromised drinking-water quality, have tempered public opinions about the economic benefits of unconventional energy development in the U.S. (Jackson et al., 2014; Vengosh et al., 2014). For example, evidence for stray gas contamination in shallow drinking-water wells was reported in a subset of wells located less than 1 km from shale gas sites in Pennsylvania (PA) and Texas (TX) using both geospatial statistics and hydrocarbon and noble gas geochemistry (Darrah et al., 2014; Jackson et al., 2013; Heilweil et al., 2014; Osborn et al., 2011).

The debate around the potential for wide spread contamination from hydraulic fracturing stems from the lack of pre-drilling datasets that include a comprehensive suite of geochemical tracers. The nearly ubiquitous presence of naturally occurring inorganic and hydrocarbon contaminants in many areas of hydrocarbon extraction, and the potential for legacy contamination from conventional oil and gas development and other industries (e.g., coal) can also deteriorate water quality (Vengosh et al., 2014). Several studies have suggested that dissolved methane (CH_4) and saline groundwater in shallow aquifers in the Appalachian Basin likely originated from natural processes (Baldassare et al., 2014; Darrah et al., 2015b; Molofsky et al., 2013; Schon, 2011; Siegel et al., 2015a; Siegel et al., 2015b; Warner et al., 2012).

The intense debate about these issues has been sustained for over five years, highlighting the need to better understand the critical factors that control the elevated levels of hydrocarbon gas and salts in groundwater systems globally. Indeed, answering these questions is a critical challenge in assessing the impacts of unconventional energy development and hydraulic fracturing on the quality of water resources. To address this debate, we must first develop a

robust understanding of the fundamental geochemical, hydrogeological, and environmental factors that control the composition and behavior of hydrological systems in a given area.

This presents a comprehensive suite of geochemical tracers that interrogates the fundamental geochemical interactions and crustal fluid flow processes that control groundwater geochemistry, using a case study in the North Appalachian Basin (NAB) of northwestern West Virginia. The Appalachian Basin is an archetypal energy basin with diverse tectonic and hydrological characteristics and energy development activities, and therefore constitutes an important area to study the potential impacts to water quality from shale gas development (Warner et al., 2012; Darrah et al., 2015b; Engle and Rowan, 2014; Ziemkiewicz and He, 2015).

While many studies have focused on Pennsylvania, less is known about the distribution of naturally occurring saline groundwater and methane in aquifers overlying the southwestern segments of the Marcellus Basin. Despite the long history of fossil fuel development, including both coal mining and conventional oil and gas drilling, there is limited historical geochemical information about these aquifers, particularly studies that integrate both aqueous concentrations and dissolved gas phase measurements. Two reports, one from the West Virginia groundwater atlas (Shultz, 1984) and another from eastern Kentucky coalfield, have identified saline groundwater in the region (Wunsch, 1992). The legacy of previous energy exploration and naturally occurring migration of saline water and natural gas to shallow aquifers are a set of additional factors that could complicate the delineation of potential contamination from recent shale gas development (Vengosh et al., 2014).

Previous applications of inorganic and isotopic tracers of dissolved salts and hydrocarbon and noble gas geochemical tracers have revealed the influence of the tectonic and hydrogeological setting on water quality and natural contamination in areas of oil and gas development both in the NAB and elsewhere (Darrah et al., 2015b; Engle and Rowan, 2014; Llewellyn, 2014, Lautz et al, 2014; Molofsky et al., 2013; Mortiz, 2015; Revesz et al., 2010; Schon, 2011; Sharma and Baggett, 2011; Siegel et al., 2015a; Siegel et al., 2015b; Warner et al., 2012, Warner et al., 2013b, Wunsch, 1992).

Here, we present a combination of integrated techniques applied to a longitudinal dataset as an improved framework to assess the geochemical processes that control groundwater geochemistry, as well as changes to surface water geochemistry during unconventional oil and gas operations. While we apply our framework to a specific area in this study, the ultimate aim

of this study is to contribute to the emerging body of knowledge about the risks to water resources from unconventional oil and gas development and to develop a standardized assessment tool for a more broad application to study the sources and migration of hydrocarbon-rich brines to water resources in the NAB and other hydrocarbon-rich basins.

2. BACKGROUND

2.1. Hydrological Background

The study area in northwestern West Virginia is part of the Appalachian Plateau Physiographic Province, where irregular, steeply sloping ridges, separated by narrow valleys and mountainous terrain characterize the topography. Bedrock in the region is dominated by cyclic sequences of sandstone, siltstone, shale, limestone and coal, which vary in thickness and lateral extent throughout the Appalachian Plateau (Wunsch, 1992). The aquifer rocks are composed of the Permian/Upper Pennsylvania Drunkard Group and the Upper Pennsylvanian Monongahela Group (Fig. 1 and 2). Locally, perched water tables are typical in some upland regions where intermittent shale layers act as local aquitards, which result in horizontal flow through cleated coal seam layers (Wunsch, 1992).

Where present, the unconsolidated alluvium provides the highest yields for domestic wells, while secondary fractures and bedding planes transmit water in the bedrock and the flow is highly variable (3.7 to 757 liters per minute) spatially because of vertical and lateral changes in fracture density, but with little variability across different geologic units. Shallow groundwater flow is dominated by shallow sets of vertical neotectonic fractures in the sandstone layers, with more intense fractures and thus higher hydraulic permeability in the valley bottoms (Wyrick and Borchers, 1981). Wells located in valley settings generally yield higher flow rates (~22.7L/min) than those in hillslopes and uplands (7.5 to 11.4 L/min). Lineaments, which experience the highest fractures and joint system intensity, are associated with the highest groundwater flow rates (Bain, 1972) and can be pathways for gas and brine migration.

In Tyler, Doddridge and Harrison counties groundwater is generally hard (hardness>120 mg/L) with high manganese (Mn>50 ug/L) and iron (Fe>300 ug/L). However, similar to groundwater flow rates, hardness and metal levels are highly variable with some topographic controls. Groundwater wells located in valleys generally have higher alkalinity, pH, and total dissolved solids (TDS). Sodium (Na), pH, alkalinity, chloride (Cl) and total dissolved salt (TDS)

concentrations increase with well depth, while calcium and magnesium decrease. Generally, there is little difference in water quality and water type between different geologic units, with dominantly Ca-HCO_3 composition in most areas, followed by a Na-HCO_3 water type.

Based on the data from Shultz (1984), dissolved solutes in the shallow groundwater varied greatly from low salinity with Cl <10 mg/L to saline waters with Cl up to 2,200 mg/L. Na concentrations had positive correlations with increasing Cl concentrations (r^2 = 0.57, $p<0.05$), with Na concentrations reported up to 970 mg/L. Groundwater with Cl> 250 mg/L has been observed in the area ranging from a few hundred to several thousand feet deep. Elevated Cl concentrations are found at shallower depths mainly in valley floors. Densely fractured zones provide nearly vertical highly permeable conduits for upward migration of deep-seated saline water. High Cl concentrations in groundwater have been also reported in areas of oil and gas development. Old deteriorating oil and gas wells can short-circuit the natural flowpaths and provide an area of localized contamination of groundwater (Shultz, 1984). Cl> 50 mg/L was reported in roughly 23% of wells surveyed (n=32 out of 139) conducted prior to shale gas development. A USGS survey of CH_4 in WV groundwater between 1997 and 2006 reported CH_4 contents up to 15 mg/L (21 ccSTP/L) (White and Mathes, 2006).

2.2 Background of Study Design and Geochemical Techniques

Previous studies in the NAB (northeastern PA) have demonstrated compelling evidence for naturally occurring gas and saline groundwater in regional aquifers. However, prior to the rapid rise of shale gas development and hydraulic fracturing, there was a lack of sufficient baseline water quality datasets in many of the areas of active unconventional energy development. Even when baseline water quality databases do exist, they typically consist of only major elements. For this reason, it can still be challenging to distinguish between naturally occurring salts and hydrocarbon gases in shallow groundwater and any possible anthropogenic contamination that could result from poor shale-gas well integrity (e.g., stray gas contamination) or accidental releases (e.g., surface spills of hydraulic fracturing fluids, produced water, or flowback fluids; Vengosh et al., 2014).

Several geochemical tools such as hydrocarbon isotopic and noble gas tracers have been previously developed to identify and distinguish water contamination from unconventional hydrocarbon production (Baldassare et al., 2014; Chapman et al., 2012; Darrah et al., 2014; Phan

et al., 2016; Sharma et al., 2014; Warner et al., 2014; Ziemkiewicz and He, 2015). In addition, Br/Cl ratios have been successfully employed to identify deep formation brines as the source of saline groundwater in the NAB, however they do not sufficiently distinguish naturally sourced brines from brines released from oil and gas activity (Warner et al., 2012; Ziemkiewicz and He, 2015). Similarly, oxygen and hydrogen stable isotopes are typically enriched in brines (Sharma et al., 2014; Warner et al., 2014), however the relative proportion of a typical brine contribution to a blend that would generate saline groundwater is too small (i.e., <20% contribution) to observe significant changes in the stable isotope composition of salinized groundwater (Warner et al., 2014).

In contrast, the stable isotopes of strontium (Sr), boron (B) and lithium (Li) are more sensitive techniques to detect even small contributions of brines to a blend with fresh water (<1%) due to their distinct isotopic compositions in formation brines and the high concentrations of these elements in the brines (Warner et al., 2014). NAB oil and gas brines are typically enriched in radiogenic Sr, ($^{87}Sr/^{86}Sr$ values ranging from 0.71000 to 0.72200), with Marcellus brines being less radiogenic (0.71000 to 0.71212) (Capo et al., 2014; Chapman et al., 2012; Warner et al., 2014) than Upper Devonian brines (0.71580 to 0.72200) (Chapman et al., 2012; Warner et al., 2014). Boron and Li isotope signatures in Marcellus hydraulic fracturing flowback fluids were distinct ($\delta^{11}B$ = 25 to 31‰ and $\delta^{7}Li$ = 6 to 10‰) from most surface waters ($\delta^{11}B$ = 8 to 20‰ and $\delta^{7}Li$ = 17 to 30‰), and depleted compared to conventional NAB oil and gas brines ($\delta^{11}B$ = 36 to 51‰ and $\delta^{7}Li$ = 10 to 23‰; Phan et al., 2016; Warner et al., 2014). However, the application of these isotope systems for identifying groundwater contamination is limited without establishing a systematic dataset of the isotope signatures of pre-drill saline groundwater in the region.

The molecular and isotopic composition of natural gases can also help to distinguish between natural flow and anthropogenic hydrocarbon gas contamination. Natural gases are often classified as thermogenic, biogenic, or "mixed" sources, based on their molecular ratios (e.g., wetness: C_2+/C_1) along with carbon (C) and hydrogen (H) isotopic compositions (e.g., Bernard, 1978; Clayton, 1991; Rice and Claypool, 1981; Schoell, 1980, 1983; Schoell, 1988). Thermogenic natural gases are typically more enriched in ethane (C_2H_6) and heavier aliphatic hydrocarbons, and thermogenic CH_4 is typically more enriched in ^{13}C ($\delta^{13}C$-CH_4>-55‰) and hydrogen (e.g., Schoell, 1983). As thermal maturity increases, the $\delta^{13}C$ of methane and ethane is

204 further increased. Conversely, biogenic gas is almost exclusively composed of CH_4 ($C_1/C_2+ \geq$
205 ~5,000), with a typically light $\delta^{13}C$-CH_4 between -55‰ and -75‰ (Schoell, 1983; Whiticar et
206 al., 1985). However, methanogenesis, aerobic and anaerobic oxidation, sulfate reduction (thermal
207 or bacterially driven), or post-genetic fractionation (e.g., fractionation during gas transport in the
208 subsurface by diffusion) can alter the original composition of natural gases or lead to complex
209 mixtures of natural gases from multiple sources.
210 Based on these considerations, the elemental and isotopic compositions of noble gases
211 (e.g., helium (He), neon (Ne), argon (Ar)) have recently been utilized to provide additional
212 constrains on the source of hydrocarbons gases in shallow aquifers (Darrah et al., 2014a; Darrah
213 et al., 2015a; Darrah et al., 2015b; Jackson et al., 2013; Heilweil et al., 2015). The inert nature,
214 low terrestrial abundance, and well-characterized isotopic composition of noble gases in the
215 mantle, crust, hydrosphere, and atmosphere enhance their utility as geochemical tracers of crustal
216 fluids such as groundwater (Ballentine et al., 2002). The noble gas composition of hydrocarbons
217 and other geological fluids are derived from three primary sources: the mantle, atmosphere, and
218 the crust (Ballentine et al., 2002). Previous work has demonstrated that the abundance of helium
219 (i.e., ^4He) and air-saturated water major (e.g., N_2) and noble gases (e.g., ^{20}Ne, ^{36}Ar) can be used
220 to distinguish the presence of large volumes of gas-phase hydrocarbons and track the source and
221 mechanism of fluid migration (Darrah et al., 2014; Darrah et al., 2015; Gilfillan et al., 2009;
222 Heilweil et al., 2015).
223 Northwestern West Virginia is an area that has seen a rapid rise in unconventional oil and
224 gas development, with over 3,000 unconventional gas wells drilled since 2008 (Fig. S1)
225 (WVGES, 2012). With knowledge that shale gas development was imminent in the study area,
226 we hypothesized that the collection and analyses of groundwater samples collected pre-, during-,
227 and post-drilling would allow us to 1) evaluate temporal changes in groundwater geochemistry
228 throughout the drilling processes; 2) determine the most sensitive geochemical parameters that
229 can detect anthropogenic contamination relative to naturally occurring geochemical processes; 3)
230 evaluate the source of the salinity and natural gas in shallow aquifers in this region; and 4)
231 determine whether groundwater near shale gas development in this area is becoming
232 contaminated by stray gas and other contaminants following shale gas development.
233 We conducted an extensive geochemical and isotopic analysis that included: (1) major
234 and minor ions; (2) trace elements; (3) water isotopes ($\delta^{18}O$, δ^2H); (4) isotopic ratios of dissolved

constituents ($^{87}Sr/^{86}Sr$, $\delta^{11}B$, $\delta^{7}Li$, $\delta^{13}C$-DIC); (5) molecular and isotopic composition of select dissolved gases (CH_4, C_2H_6+, N_2, $\delta^{13}C$-CH_4, $\delta^{13}C$-C_2H_6); (6) tritium (^{3}H); and (7) noble gas elemental and isotopic compositions (He, Ne, Ar). To better address these questions, we integrate our geochemical data with time-series and geospatial analysis with respect to shale-gas wells and geological deformational features such as faulting, folding, and proximity to valley bottoms.

In parallel with the groundwater study, we also collected surface water samples near storage and disposal of oil and gas wastewater (OGW) areas in order to characterize the geochemical fingerprints of OGW in the research area. We used the geochemical composition of Marcellus flowback and produced waters (Warner et al., 2013a; Warner et al., 2014) as references to determine the source and magnitude of contamination of surface water from OGW. These geochemical fingerprints were also used as references to determine whether the saline and CH_4-rich groundwater in northwestern West Virginia is derived from geogenic process or from direct contamination of leaking from nearby shale-gas wells.

3. MATERIALS AND METHODS

3.1 Sample Survey

We examine the inorganic chemistry (anions, cations, trace metals), stable isotopes (O, H, B, Sr, Li), noble gas, tritium, and hydrocarbon (molecular (C_1 to C_5) and stable isotopic $\delta^{13}C$-CH_4 and $\delta^{13}C$-C_2H_6) compositions of 145 samples from 112 domestic groundwater wells in Doddridge, Harrison, Ritchie, Tyler and Wetzel counties in West Virginia, USA (Table 1). The typical depth of shallow drinking-water wells in our study was 35 to 90 m. A subset of wells (n=31) was tested prior to shale gas drilling in Doddridge County starting in summer 2012 (open circle, triangle, and square according to water type defined below). Groundwater wells were selected based on their location in an area targeted for shale gas development and homeowner participation. An additional 79 wells were sampled in Doddridge (n=56), Harrison (n=9), Ritchie (n=5), Tyler (n=6) and Wetzel (n=3) counties between 2012 and 2014, following installation of shale-gas wells and hydraulic fracturing in the area (crossed circle, inverted triangle, and diamond according to water type defined below). 55% of wells were located within 1 km of a shale-gas well. 20 wells were more than 1 km from a shale gas well when first sampled, but

retested at least once following installation of a shale gas well within 1 km during the study period. 8 wells that were less than 1 km of from a shale gas when initially sampled were retested during the study period.

Neither geological features, nor previous knowledge of water chemistry were considered during water well selection. Instead, we tried to randomly sample domestic water wells from across the study area to get a diverse suite of sample types. Four of the groundwater wells were located near OGW disposal or spill sites in the study area. Modern data was compared to groundwater data from 1982 reported by the West Virginia Department of Natural Resources (Shultz, 1984). We present data from this study with color-coded symbols, while historical data are identified by grey symbols. Pre- and post-drilling samples are indicated by symbol shape within the colors of the three water types identified in this study. An open circle denotes Type 1 pre-drilling samples and post-drilling samples are denoted as a crossed-circle. Type 2 pre-drilling samples are denoted by a triangle and post-drilling samples are denoted as an inverted triangle. Type 3 pre-drilling samples are denoted by a square and a diamond denotes post-drilling samples.

Surface samples were collected from three spill sites, at the point nearest the origin (n=5) and in surface water downstream (n=8) and upstream (n=2) of the spill (Fig. 1; Table 3). We sampled streams near two deep well injection sites and one flowback spill that occurred on a well pad in Tyler County. The first injection well site in Lochgully, WV was sampled in October 2013 and the second site in Ritchie County, WV was sampled in December 2013. The spill in Tyler County was identified on January 3, 2014 and the spill water was sampled directly on the same day and three days after the spill. Surface waters from Big Run Creek were collected upstream and at the point of entry for the spill water into the stream on January 6th and at points adjacent to the pad and downstream along Big Run Creek on February 23rd, 2014 along with water from Middle Island Creek, which is a drinking water source for the area.

3.2. Field Methods

Water samples from wells were collected prior to any treatment systems and were filtered and preserved in high density polyethylene (HDPE), air tight bottles following USGS protocols

(USGS, 2011). Samples were filtered through 0.45 micron filters for dissolved anions, cations and inorganic trace element isotopes (B, Sr, Li). Trace metal samples were preserved in 10% Optima nitric acid following filtering through a 0.45 micron filter. Samples bottles collected for stable isotopes of O, H and DIC were completely filled to minimized interaction with air or air bubbles and were kept sealed until analysis. Water chemistry samples were stored on ice or refrigerated until the time of their analysis.

Hydrocarbon gas samples for concentration and isotopic analyses were collected in the field using Isotube bottles obtained from Isotech Laboratories by procedures detailed by Isotech Laboratories (Isotech, 2011), stored on ice until delivery to Duke University, and analyzed for CH_4 (and where applicable C_2H_6) isotopic compositions of carbon. Dissolved gas samples for gas concentrations and noble gas measurements were collected in refrigeration-grade copper tubes that were flushed in-line with at least 50 volumes of sample water prior to sealing with stainless steel clamps according to standard methods reported previously (Darrah et al., 2013; Darrah et al., 2015;).

3.3 Analytical Methods

3.3.1 Water Chemistry

Major anions (e.g., Cl^-, SO_4^{2-}, Br^-) were measured by ion chromatography and major cations (e.g., Na, Ca, Mg) were measured by direct current plasma optical emission spectrometry. Trace elements (i.e., Li, B, V, Cr, Fe, Mn, As, Se, Sr, Ba) were analyzed by ICP-MS on a VG PlasmaQuad-3 calibrated to the NIST 1643e standard. The detection limit of the ICP-MS of each element was determined by dividing three times the standard deviation of repeated blank measurements by the slope of the external standard.

3.2.2. Isotope Chemistry

$^{11}B/^{10}B$ ratios were measured as BO_2^- in negative mode and reported as $\delta^{11}B$ normalized to NIST NBS SRM-951. Long-term measurements (n=60) of NBS SRM 951 standard yielded a precision of 0.6‰. Sr in the water samples was pre-concentrated by evaporation in a HEPA-filtered clean hood and re-digested in 3.5N HNO_3. Sr was separated using Eichrom Sr-specific resin. The $^{87}Sr/^{86}Sr$ ratios were collected in positive mode on the TIMS and the standard NIST SRM 987 had an external reproducibility of 0.710265±0.000006. Li isotopes were measured by a

ThermoFisher Neptune MC-ICP-MS at BRGM (French Geological Survey) in France. $^{7}Li/^{6}Li$ ratios were normalized to the L-SVEC standard solution (NIST SRM 8545) and presented as $\delta^{7}Li$. Long-term replicate measurements of NIST SRM 8545 standard yielded a precision of 0.5% (Millot et al., 2004).

The stables isotopes of water (i.e., $\delta^{2}H$ and $\delta^{18}O$) were analyzed in the Duke Environmental Isotope Lab. These gases are chromatographically separated in the TCEA, and carried to a ThermoFinnigan Delta+XL ratio mass spectrometer via a Conflo III flow adapter. Raw delta values were normalized offline against known vs. measured isotope values for international reference waters VSMOW, VSLAP and IAEA-OH16. The $\delta^{2}H$ and $\delta^{18}O$ values are expressed in per mil versus VSMOW, with standard deviations of ±0.5 ‰ and ±0.1, respectively.

Carbons isotopes in dissolved inorganic carbon ($\delta^{13}C$-DIC) were measured at Duke University. Glass septum vials (Labco 11 mL Exetainers) were loaded into the thermostated sample tray of a ThermoFinnigan GasBench II and flushed for ~20 minutes each by autosampler with a two-way flushing needle and a carrier stream of UHP helium at ~30 mL/min. to remove air, and then were each injected with 100 µL of liquid ortho-phosphoric acid. Sample waters were analyzed by ThermoFinnigan Delta+XL ratio mass spectrometer. Reference CO_2 pulses are injected automatically before and after the six sample peaks. The calculated raw $\delta^{13}C$ values of samples were then normalized offline against known vs. measured values for three carbonate standards that were analyzed during the run using the same acid reaction (NBS19, IAEA CO8, and Merck calcium carbonate). The first two are international reference materials and the third is an internal standard previously calibrated against the first two. The $\delta^{13}C$ is expressed in per mil vs. VPDB, and the standard deviation is ±0.2 ‰.

3.3.3. Dissolved Gas and Gas Isotope Geochemistry

For samples where copper tube samples were not available, dissolved CH_4 concentrations were calculated using headspace equilibration, extraction and subsequent concentration calculation by a modification of the Kampbell and Vandegrift (1998) method (Kampbell and Vandegrift, 1998) at Duke University. Calculated detection limits of dissolved CH_4 were 0.002 mg/L water. Procedures for stable isotope analyses of gas are summarized in Jackson et al. (2013). Reporting limits for reliable stable carbon isotopic compositions of methane ($\delta^{13}C$-CH_4) and ethane ($\delta^{13}C$-C_2H_6) were consistent with Isotech Laboratories (Illinois, USA). Stable carbon

isotopes of methane and ethane were determined for all samples with CH_4 exceeding 0.1 cm^3 STP/L (n=97) and 0.001 cm^3 STP/L, respectively. The $\delta^{13}C$-CH_4 were determined by cavity ring-down spectroscopy (CRDS) (Busch and Busch, 1997) at the Duke Environmental Stable Isotope Laboratory (DEVIL) using a Picarro G2112i or newer generation G-2132i (NOTE: after May 2014, the G221i was replaced with the newer generation G-2132i) or gas chromatographic separation using a Trace Ultra ThermoFinnigan followed by combustion and dual-inlet isotope ratio mass spectrometry using a Thermo Fisher Delta XL.For samples in which copper tubes were available, dissolved gas samples were measured by extracting the fluid from the copper tube on a vacuum line (Darrah et al., 2015). Copper tube samples were prepared for analysis by attaching the copper tube to an ultra-high vacuum steel line (total pressure= 1-3 $x10^{-6}$ torr), which is monitored continuously using a four digit (accurate to the nearest thousandths) 0-20 torr MKS capacitance monometer, using a 3/8" (0.953 cm) Swagelok ferruled connection. After the sample connection had sufficiently evacuated and pressure was verified, the fluid sample was inlet to the vacuum line by re-rounding the copper (Kang et al., 2016). After the fluid pressure had equilibrated, the sample was sonicated for ~30 minutes to ensure complete transfer of dissolved gases to the sample inlet line (Solomon et al., 1995).

From this gas volume, splits of samples were taken for the measurement of major gas components (e.g., N_2, O_2, Ar, CH_4 to C_5H_{12}) using an SRS quadrupole mass spectrometer (MS) and an SRI gas chromatograph (GC) at Ohio State University with standard errors of <3% (Cuoco et al., 2013; Hunt et al., 2012; Kang et al., 2016). The average external precision was determined by measurement of a "known-unknown" standard, including an atmospheric air standard (Lake Erie, Ohio Air) and a series of synthetic natural gas standards obtained from Praxair. The results of the "known-unknown" average external precision analysis are as follows: CH_4 (1.27%), C_2H_6 (1.68%), C_3H_8 (1.34%), C_4H_{10}-n (2.08%), C_4H_{10}–i (2.11%), C_5H_{12}-n (2.78%), C_5H_{12}–i (2.81%), N_2 (1.25%), CO_2 (1.06%), H_2 (3.41%), O_2 (1.39%), and Ar (0.59%). CH_4 concentrations are reported as cc/L (the SI molar unit for gas abundance in water) at standard temperature and pressure (STP) where 1 mg/L of gas is equivalent to 1.4 cc STP/L.

An additional split of the gas was taken for the isotopic analysis of noble gases using a Thermo Fisher Helix SFT Noble Gas MS at Ohio State University following methods reported previously (Cuoco et al., 2013; Darrah and Poreda, 2012; Hunt et al., 2012). The average external precision based on "known-unknown" standards were all less than +/- 1.46% for noble

gas concentrations with values reported in parentheses (^{4}He (0.78%), ^{22}Ne (1.46%), and ^{40}Ar (0.38%)). These values were determined by measuring referenced and cross-validated laboratory standards including an established atmospheric standard (Lake Erie Air) and a series of synthetic natural gas standards obtained from Praxair including known and validated concentrations of C_1 to C_5 hydrocarbons, N_2, CO_2, CO, H_2, O_2, Ar, and each of the noble gases. Noble gas isotopic standard errors were approximately ±0.0091 times the ratio of air (or 1.26 x10^{-8}) for ^{3}He/^{4}He ratio, <±0.402% and <±0.689% for ^{20}Ne/^{22}Ne and ^{21}Ne/^{22}Ne, respectively, less than ± 0.643% and 0.427% for ^{38}Ar/^{36}Ar and ^{40}Ar/^{36}Ar, respectively (higher than typical because of interferences from C_3H_8 on mass=36 and 38).

To evaluate the potential for *in-situ* radiogenic production and/or release of ^{4}He, we analyzed the U and Th in various aquifer outcrop samples collected in Doddridge County, WV. Analyses were conducted by standard methods using inductively coupled plasma mass spectrometry (ICP-MS) (Cuoco et al., 2013). Additionally, tritium (^{3}H) analyses were performed on 56 groundwater samples to evaluate the contributions from modern meteoric water. Tritium (^{3}H) concentrations were measured by the in-growth of ^{3}He using a ThermoFisher Helix SFT noble gas MS at The Ohio State University following methods reported previously (Darrah et al., 2015; Solomon et al., 1995; Solomon et al., 1992).

3.4. Graphical and Statistical Treatment of Data

All maps, cross-sections, and well coordinates are plotted using ArcMap GIS 10.2.2. Geological and oil and gas well data were available from the West Virginia Geological and Economic Survey (WVGES, 2012). All graphics are plotted using R v. 3.2.0. Statistical evaluations including mean, minimum, maximums, Spearman correlations, standard deviations, and analysis of variance (ANOVA) were performed using R v. 3.2.0. Correlation coefficient, *r* reported in the text was calculated as Spearman's rank correlation coefficient, ρ.

We present data from this study with color-coded symbols, while data from previous studies are identified by orange hexagon. Within all figures, the abundance of methane is preserved using a color intensity scale, where low methane concentrations close to 0 ccSTP/L are blue and range up to red for methane concentrations > 40 ccSTP/L. Samples for which methane samples were not analyzed are shown as a grey symbol.

4. RESULTS

4.1 Groundwater quality

The dissolved solutes in the shallow groundwater in the study area varied from low salinity (Cl <50 mg/L) to saline waters (Cl up to 2400 mg/L), mostly in the deeper wells (depths ~100 m). Cl concentrations >50 mg/L were detected in 19% of wells surveyed in our study (n=27/145). Saline waters were typically also elevated in other major constituents (Fig. 3). For example, Br and Na concentrations had strong positive correlations with Cl ($r = 0.79$, $p<0.05$ and $r = 0.62$, $p<0.05$, respectively; Fig. 4). Br concentrations ranged from below detection limits (<0.02 mg/L) to 15.2 mg/L, and Na concentrations ranged from below detection limits (<0.1 mg/L) to 1,362 mg/L. DIC in groundwater was also positively correlated with Cl ($r = 0.35$, $p<0.05$) and concentrations ranged from 42 to 836 mg/L (Fig. 4). Ca, Mg and SO_4 in the groundwater, however, did not show any correlation with salinity (Fig. 4). SO_4 concentrations were relatively low in groundwater, ranging from below detection limits up to 50 mg/L, while Ca concentrations ranged from below detection limits up to 346 mg/L, and Mg concentrations ranged from below detection limits up to 233 mg/L.

Some trace elements were strongly associated with the salinity of the groundwater (Fig. S2). B and Li, specifically, had higher concentrations in the saline water. Li concentrations ranged from below detection limits (0.1 µg/L) to 72 µg/L, and were positively correlated to Cl ($r = 0.54$, $p<0.05$), while B concentrations ranged from 6 to 232 µg/L and correlated to Cl ($r = 0.60$, $p<0.05$; Fig. S2). Arsenic (As) was weakly correlated with Cl ($r = 0.18$, $p<0.05$), while other trace elements, such as Ba and Sr, were not significantly correlated with Cl (Fig. S2 and S3). Sr concentrations were relatively high in the study area and ranged from below detection limits (<0.1 µg/L) to 2,782 µg/L, while Ba concentrations ranged from below detection limits (<0.1 ug/L) to 4.2 mg/L. Ba and Sr were both correlated with Ca ($r = 0.53$, $p<0.05$ and $r = 0.68$, $p<0.05$, respectively; Fig. S3). These high correlations with Ca suggest that Sr and Ba concentrations are more likely influenced by water-rock interactions in the shallow subsurface than from the migration of a brine.

The Br/Cl (molar) ratios in the saline water (Cl>50 mg/L) ranged from very low values around $2x10^{-4}$ to brine-type waters with Br/Cl > $1.5x10^{-3}$ (up to $7.8x10^{-3}$). These ratios are similar to ranges found in saline groundwater that have been impacted by deep formation brines in other regions of the Appalachian Basin (Warner et al., 2012; Wunsch, 1992). Based on the Cl

concentrations and Br/Cl ratios (Warner et al., 2012), we divide the water samples into three major water types. The first type (Type 1) is characterized by Cl< 50 mg/L and has Ca-Na-HCO_3 composition (n=118 samples) (Fig. 3). Type 2 (n=17) has elevated salinity (Cl>50 mg/L) and is a Ca-Na-Cl type, with Br/Cl molar ratio between $1.0x10^{-3}$ and $2.5x10^{-3}$ and high correlation between Br and Cl ($r = 0.97$ $p<0.05$). Type 3 (n=10) also has elevated salinity (Cl>50 mg/L) and is a Ca-Na-Cl type, but has a Br/Cl molar ratio $>2.5x10^{-3}$ and a lower correlation between Br and Cl ($r = 0.56$; $p<0.05$; Fig. 4). In addition to the difference in Br/Cl, Type 3 had lower Na/Cl (0.99±0.28) and B/Cl ($0.97±5.4x10^{-4}$) ratios relative to those in Type 2 (2.68±1.87 and $4.4±3.5x10^{-3}$, respectively) (Fig. 4). All Type 3 groundwater samples occurred within 750 m of a valley bottom. The majority of these Type 3 water samples were located in valley bottom characterized by the hinge of the Burchfield syncline (Fig. 2) (Hennen, 1912; Ryder et al., 2012).

The stable isotopes ($\delta^{18}O = -5.9$ to -9.2‰; $\delta^{2}H = -24.1$ to -55.0‰) of the shallow groundwater in the study area primarily fall along the local meteoric water line (LMWL = 6.6 $\delta^{18}O$ + 2.4) (Kendall and Coplen, 2001), with low deuterium excess relative to the LMWL in the more saline samples (Fig. S4). $\delta^{7}Li$ values in groundwater from the study area ranged from 10.9‰ to 21.3‰, which are higher than the $\delta^{7}Li$ of Middle Devonian-age brines (6-10‰; Phan et al., 2016; Warner et al., 2014). The $\delta^{11}B$ values of the groundwater were between 12.7‰ and 25.2‰, which are lower relative to the $\delta^{11}B$ of the Devonian-age brines (25-31‰) (Warner et al., 2014).

The saline groundwater had higher $\delta^{11}B$ values (19.9±5.9‰) than that of the low-saline ground water of Type 1 (16.1±5.8‰, $p<0.001$), and also had lower B/Cl ratios ($p<0.001$) (Fig. 5). The $\delta^{11}B$ was statistically indistinguishable between Types 1 and 2 ($p= 0.75$). The Li/Cl ratios were similar to B/Cl ratios, with lower ratios in the saline water ($p<0.001$). However, $\delta^{7}Li$ values were only significantly higher in Type 2 water (mean = 19.7±1.4‰, $p<0.05$) compared to both Type 1 (16.8±5.3‰) and Type 3 (16.4±5.2‰) water. $\delta^{7}Li$ in groundwater of types 1 and 3 were statistically indistinguishable ($p=0.83$).

Sr/Ca molar ratios were lower than values typically reported in the Appalachian brines (0.002 to 0.17) (Warner et al., 2012), with values in the saline water ranging from 0.0004 to 0.022 (Fig. 5). The $^{87}Sr/^{86}Sr$ ratios ranged from 0.71210 to 0.71333, and mean ratios were 0.71287±0.0002 for Type 1, 0.71279±0.0001 for Type 2 and 0.71294±0.0002 for Type 3 (Table 1). These $^{87}Sr/^{86}Sr$ ratios are more radiogenic than typical Marcellus age brines (0.71000 to

0.71212), but still less radiogenic than the Upper Devonian conventional produced water (0.71580 to 0.72200). The Sr/Ca and $^{87}Sr/^{86}Sr$ ratios of the three-groundwater types were statistically indistinguishable from each other (in spite of the differences in salinity and Sr concentrations).

High concentrations of Ba and other trace metals were also observed in the saline groundwater (Table 1). Type 3 groundwater had higher Ba (1.9±1.3 mg/L, $p<0.05$) than either Type 1 or 2, with concentrations exceeding the U.S. EPA maximum contaminant level (MCL) of 2 mg/L in 4 out of 10 Type 3 saline waters, and 1 out of 17 Type 2 waters. Likewise, the saline groundwater of Type 3 had distinctively higher As concentrations (14.3±15.7 μg/L) relative to either Type 1 (5.4±6.7 μg/L) or Type 2 (4.9±3.7 μg/L) samples, but it was not statistically significantly ($p=0.16$), and the MCL of 10 ug/L was exceeded in 5 of the 10 Type 3 waters and 2 out of 17 Type 2 waters. The MCL was also exceeded in 18 of the 119 low-salinity Type 1 groundwater. Overall, arsenic exceeded the MCL level of 10 μg/L in 25 well samples (17%).

4.2 Dissolved Gas Geochemistry

CH_4 concentrations in groundwater from the study area ranged from below detection limits (~0.01 cm^3 STP/L) to 36.9 cm^3 STP/L (Table 2). Similar to previous studies in the Appalachian Basin, the upper limit is near saturation conditions for CH_4 in fresh water (saturation for CH_4 is ~35-40 cm^3STP/L at $p(CH_4)$= 1 atm at 10^{o}C) (Darrah et al., 2014; Darrah et al., 2015b). Samples from this study area had C_2H_6 concentrations that ranged from below detection limits (~0.0005 cm^3 STP/L) to 0.037 ccSTP/L, C_3H_8 concentrations that ranged from below detection limits (~0.0005 ccSTP/L) to 6.65 x 10^{-4} ccSTP/L, C_4H_{10}-i concentrations that ranged from below detection limits (~0.0001 ccSTP/L) to 2.68 x 10^{-6} ccSTP/L, C_4H_{10}-n concentrations that ranged from below detection limits (~0.0001 ccSTP/L) to 2.24 x 10^{-6} ccSTP/L, C_5H_{12}-i concentrations that ranged from below detection limits (~0.0005 ccSTP/L) to 4.65x10^{-7} ccSTP/L, and C_5H_{12}-n concentrations that ranged from below detection limits (~0.0005 ccSTP/L) to 4.32x10^{-7} ccSTP/L (Table 2).

A one-way analysis of variance of all data from each water type found that groundwater Types 2 and Type 3 (high salinity types) had significantly higher ($p<0.05$) CH_4 concentrations (13.4±15 and 14.3±15 ccSTP/L, respectively) relative to the low salinity Type 1 (1.7±3.2 ccSTP/L), but were not significantly different from each other. CH_4 and Cl contents were

positively correlated when including all samples (r^2 = 0.70, $p<0.05$; Fig. 6). CH_4 was also correlated with Br (r^2= 0.68, $p<0.05$), B (r= 0.47, $p<0.05$), and Li (r= 0.71, $p<0.05$; Fig. S5) across the whole dataset. In the saline samples, CH_4 was correlated with Cl (r=0.60, $p<0.05$), Br (r=0.59, $p<0.05$), and Li (r= 0.67, $p<0.05$).

Most of the Type 1 samples had CH_4 below 1.4 ccSTP/L, with a wide $\delta^{13}C$-CH_4 range of -96‰ to -19‰ and elevated C_1/C_2+ ratios (mean = 10,389 ± 45). A subset (30 out of 145) of low-salinity groundwater samples had CH_4 above 1.4 ccSTP/L, with most of these samples having $\delta^{13}C$-CH_4= <-55‰. Types 2 and 3 groundwater with elevated salinity had much higher CH_4 contents on average, but had relatively low $\delta^{13}C$-CH_4 (mean= -63.0±18.3‰ in Type 2 and mean= -69.0±28.6‰ in Type 3), an isotopic composition that is consistent with biogenic sources (Fig. 6) (Schoell, 1983; Whiticar and Faber, 1986). Types 1, 2 and 3 samples did display significantly heavier ethane isotope values, where sufficient ethane concentrations were available for isotopic analysis. The mean $\delta^{13}C$-C_2H_6 were -35.87±1.80, -38.25±0.87, and -37.60±0.54‰ for Types 1, 2, and 3, respectively. These values are consistent with the ranges observed for thermogenic gases derived from marine (e.g., shale) or terrestrial (e.g., coal) of organic matter.

Groundwater samples from the current study display N_2 (8.94 cm^3 STP/L to 20.50 cm^3 STP/L; average=12.71 cm^3 STP/L) and Ar (0.21 cm^3 STP/L to 0.41 cm^3 STP/L; average=0.30 cm^3 STP/L) concentrations that vary within 9% and 19% of air-saturated water (ASW) values (13.9 and 0.37 cm^3 STP/L, respectively) on average, assuming Henry's Law solubility equilibration conditions at atmospheric pressure (1 atm), 10^{o}C, and ~600 meters of elevation (average elevation in the study area) (Table 2; Fig. 7). In fact, the majority of samples have N_2 and Ar that plot within 14% of the temperature-dependent ASW solubility line (Fig. 7).

In the current study, ^{4}He concentrations ranged from near ASW values (~37.49 x10^{-6} cm^3 STP/L) up to 0.357 cm^3 STP/L, similar to the range observed in other parts of the Appalachian Basin (Darrah et al., 2015). All of the samples displayed $^3He/^4He$ ratios that decreased from 1.021 R_A (ASW values plus small contributions from the in-growth of tritiogenic ^{3}He; Table 2) to a uniformly crustal isotopic composition of 0.0166R_A (where R_A = the ratio of air=1.39 x 10^{-6}) with increasing [^{4}He] and $^4He/^{20}Ne$ (Fig. 8). Note that this trend is largely consistent with other areas in the NAB, with the exception that the WV dataset do not show any evidence for a subset of samples with an anomalous mantle-derived composition as was seen in northeastern PA (Darrah et al., 2015b). The $^{20}Ne/^{22}Ne$ and $^{21}Ne/^{22}Ne$ values ranged from 9.757 to 9.914 and

0.0276 to 0.0310, respectively. These values are within 1.4% and 7.3% of the anticipated air-saturated water values, respectively. The small increase in $^{21}Ne/^{22}Ne$ reflects minor contributions of nucleogenic $^{21}Ne^*$, which is significantly higher in Type 2 and Type 3 waters as compared to Type 1. Similarly, $^{40}Ar/^{36}Ar$ and $^{38}Ar/^{36}Ar$ values ranged from 294.50 to 308.77 and 0.1781 to 0.1909, respectively. These values are within 4.5% and 1.3% of the anticipated air-saturated water values, respectively. The small increase in $^{40}Ar/^{36}Ar$ reflects minor contributions of radiogenic $^{40}Ar^*$, which is significantly higher in Type 2 and Type 3 waters, as compared to Type 1.

4.3 Spatial and statistical relationship between hydrogeological location and groundwater geochemistry

Previous studies have identified valley bottoms as an area with high occurrences of naturally saline, hydrocarbon-rich groundwater. Eight out of ten Type 3 drinking-water wells, were located less than 750m from the same valley bottom in the northwest corner of Doddridge County. The remaining Type 3 well (WV-503) was located in the valley bottom of an adjacent valley in west Tyler County. Both of these valleys intersect the Burchfield Syncline that runs through the study area. Seven of the Type 2 waters were also found within 750m of a valley bottom in northwest Doddridge County. The remaining Type 2 wells were located between 1,016 and 8,241 m distance to a valley bottom.

The correlations of Cl ($r=0.36$, $p<0.05$) and Br/Cl ($r=0.37$, $p<0.05$) to valley bottoms were not high, but higher Cl concentrations and Br/Cl ratios were recorded in groundwater wells located closest to valley bottoms (Fig. S8). CH_4 and C_2H_6 concentrations were also weakly correlated with proximity to valley bottoms ($r=0.15$, $p<0.05$ and $r=0.16$, $p<0.05$ respectively). The C_1/C_2+ ratio, on the other hand, was negatively correlated with distance to a valley bottoms (i.e. the ratio increased further away from the valley bottom) ($r=0.4$, $p<0.05$). The N_2 and ^{36}Ar concentrations of groundwater from this study were also negatively correlated to valley bottoms ($r= -0.13$, $p<0.05$ and $r= -0.24$, $p<0.05$), with the lowest concentrations in groundwater wells closest to valley bottoms (Fig. S8). The carbon stable isotopes of methane showed no correlation with distance from valley bottoms ($p=0.23$). Tritium showed no correlation with distance to a valley bottom.

The noble gases concentrations and gas ratios were also correlated with distance to valley bottoms (Fig. S8). For example, the ^{4}He ($r = 0.33$, $p<0.05$), the $^{4}He/CH_4$ ($r=0.42$, $p<0.05$), and the $^{20}Ne/^{36}Ar$ ($r=0.39$, $r<0.05$) were all weakly, but significantly correlated with proximity to valley bottoms so that higher values occurred in groundwater wells close to valley bottoms and are associated with more saline samples (Fig. S8). However, it is important to note that there is significant overlap between distances to the Burchfield Syncline and valley bottom in the current data set. Although the trends in $^{20}Ne/^{36}Ar$ and ^{36}Ar could relate to gas-water interactions in the presence of a relatively low volume of free-gas phase hydrocarbons or the migration of an exogenous hydrocarbon-phase in the valley bottom, the lack of coherent fractionation between $^{20}Ne/^{36}Ar$ and N_2/Ar suggests that phase-partioning during fluid migration from depth to the shallow aquifer is more likely.

4.4 Spatial and statistical relationship between conventional and unconventional energy development and water quality

We did not observe any relationship between Cl and proximity of the drinking-water wells to the nearest shale gas drilling sites for any of the water types ($r= 0.04$, $p=0.70$; Fig. 9). A Kruskal-Wallis test found that Cl concentrations in drinking-water wells <1km from a shale gas well pad were statistically indistinguishable to values in drinking-water wells >1 km away from a well pad ($p=0.88$). CH_4 concentrations did not increase with proximity to the nearest shale gas drilling sites ($r = 0.10$, $p=0.89$; Fig. 9), and the CH_4 concentrations in wells located <1km from drilling were statistically indistinguishable from concentrations >1km from drilling ($p=0.51$). However, the carbon isotopes of CH_4 ($\delta^{13}C\text{-}CH_4$) had a weak correlation with distance to a shale gas well ($r=0.28$, $p<0.05$), with significantly more negative values of $\delta^{13}C\text{-}CH_4$ in drinking-water wells <1km from a well pad (mean = -66.4‰) than those located >1km from a well pad (mean = -59.8‰, $p<0.05$). Conversely, there was no significant correlation between $\delta^{13}C\text{-}C_2H_6$ and distance to a shale-gas well ($r=0.124$, $p=0.73$). The C_1/C_2+ ratio had no relationship with proximity to a shale-gas well ($p=0.38$) (Fig. 9). However, the C_1/C_2+ ratios were significantly higher than either the Marcellus or other productive natural gas horizons in the region or groundwater wells that experienced fugitive gas contamination in northeastern PA or elsewhere. Additionally, mean C_1/C_2+ ratios in wells <1 km were not significantly different to the mean ratios in wells >1 km from a shale-gas well ($p=0.60$).

The only other parameter that showed a weak, but significant correlation to distance from oil and gas wells and valley bottoms was $^{87}Sr/^{86}Sr$ ($r=0.32$, $p<0.05$ and $r=0.41$, $p<0.05$). The $^{87}Sr/^{86}Sr$ ratio increased in drinking-water wells with increasing distance from a shale-gas well and from valley bottoms (Fig. 9). Saline groundwater wells (both Type 2 and Type 3) within 1km of a well pad had significantly lower $^{87}Sr/^{86}Sr$ ratios than wells located >1km from a well pad ($p<0.05$, Kruskal-Wallis test). When considering all groundwater wells, there was no statistically significant difference in $^{87}Sr/^{86}Sr$ ratios in wells greater than or less than 1 km from a well pad ($p=0.24$, Kruskal-Wallis test). No significant ($p= >0.10$) correlations were observed between distance from a shale-gas well and any other isotope or noble gas parameters (e.g., $\delta^{11}B$, $\delta^{7}Li$, $^{13}C\text{-}CH_4$, $^{4}He/CH_4$, ^{36}Ar, $^{20}Ne/^{36}Ar$, and ^{4}He). There was also no correlation observed for any parameters and number of shale-gas wells in a 1km radius.

It is also important to consider the legacy impact of other forms of conventional oil and gas development on water quality in the study area. Considering there are over 130,000 active, plugged, or abandoned conventional oil and gas wells in West Virginia, the extensive hydrocarbon production in West Virginia over the past 100 years could be a major influence on water chemistry and contamination, especially compared to the relatively short period (~10 years) that hydraulic fracturing has been employed in the area. Only 7 of the 112-groundwater wells sampled in this study were located more than 1 km from a conventional (active or inactive) well. The ^{36}Ar were weakly, positively correlated with distance to a conventional well ($r=0.22$, $p<0.05$), but no other parameters showed any relationship with distance to the nearest conventional gas well. There were no significant correlations between the geochemical and gas parameters with the number of conventional wells within a 1km radius. The lack of correlations suggests that conventional oil and gas wells do not play a role in affecting the groundwater geochemistry in this study area in West Virginia, while a previous study in Colorado has suggested stray gas contamination associated with conventional oil and gas wells (Sherwood et al., 2016).

4.5 Pre- and post–drilling groundwater quality

The data indicate that none of the 17 Type 1 wells that were retested after the installation of nearby shale gas wells showed any change in Cl as compared to the Cl measured in the initial Type 1 baseline testing (slope=0.9; $r=0.79$; $p<0.05$; Fig. 10), even in those located near shale gas

drilling sites. However, some groundwater wells with Type 2 and 3 water showed both significant increases and decreases in Cl after drilling, which are discussed further below. CH_4 contents of wells collected after installation of nearby shale gas wells did not change for the majority of the wells (for all 3 water types) relative to the baseline CH_4 data in wells collected prior to the shale gas drilling (slope=1.1; r=0.90; $p<0.05$; Fig. 10). Likewise, the $\delta^{13}C$-CH_4 of water collected after hydraulic fracturing was statistically indistinguishable to their respective values before drilling (slope=0.92, r=0.84; $p<0.05$; Fig. 10). $\delta^{13}C$-C_2H_6 was only measured before and after in four samples but the isotope ratios all fall close to the 1:1 line between the pre and post-drilling samples.

These trends were also consistent for stable and noble gas isotopes (Fig. 10). Li and Sr isotopes ratios showed no changes in groundwater sampled post-drilling (slope=0.96, r=0.89; $p<0.05$ and slope=0.87, r=0.84; $p<0.05$, respectively). Neither the abundance of ^{20}Ne nor $CH_4/^{36}Ar$ changed significantly over time either (slope =1.1, r=0.90, $p<0.05$ and slope =1.1, r=0.95, $p<0.05$, respectively), but other noble gas parameters did show some changes after drilling (Fig. 10). The $^4He/^{20}Ne$ (slope = 0.97, $r^2=0.99$, $p<0.05$), N_2 (slope =1.0, $r^2= 0.29$, $p<0.05$), and ^{36}Ar (slope =1.0, $r^2=0.28$, $p<0.05$) also do not show significant change with time, but the variability was much higher. The $^4He/^{20}Ne$ is well WV-58, however, showed a dramatic increase from 179 to 503. The $^4He/CH_4$ ratios showed little change in the saline samples (slope=0.93, $r^2=0.50$, $p<0.05$), but either a large increase (up to 2x) or large decrease (up to 5x) in some of the freshwater samples (Fig. 10).

In two of the saline water samples (WV-36 and WV-38), we observed a >100% increase in Cl following shale gas drilling and hydraulic fracturing (Table 1), yet no changes were observed in the overall chemical composition for well WV-36 or in the B, Li, and Sr isotopes ratios of the saline groundwater collected after unconventional energy development. Groundwater in well WV-38 showed an increase in the Br/Cl ratio from Type 2 ($Br/Cl=1.9x10^{-3}$) to Type 3 ($2.9\ x10^{-3}$). None of the diagnostic gas tracers (e.g., CH_4, ^4He, $^4He/CH_4$, $^{20}Ne/^{36}Ar$, ^{36}Ar) showed any marked changes between sampling before and after installation of shale gas wells. One exception is a Type 1 well WV-3, which showed an increase in CH_4 from 2.8 to 21.0 ccSTP/L after hydraulic fracturing, which is above the U.S. Dept. of Interior advisory limit, and yet did not correlate with an increase in Cl (Table 1) or other parameters. Despite the increase in

663 CH_4, the $\delta^{13}C$-CH_4 for this drinking-water well was very negative (-93‰) and, like other gas
664 parameters (hydrocarbon composition, noble gases) did not change significantly through time.

665 **4.6. Surface water contamination**

666 A spill on January 3rd, 2014 at a well pad in Tyler County was characterized by high
667 salinity (Cl up to 18,000 mg/L), Br (278 mg/L), B (25.7 mg/L), Cr (679µg/L), and Sr (76 mg/L)
668 (Table 3). The variations of Br/Cl=($6.8x10^{-3}$), $\delta^{11}B$ (27‰), $\delta^{7}Li$ (11‰), and $^{87}Sr/^{86}Sr$ (0.70981)
669 were consistent with the composition of Marcellus flowback waters (Chapman et al., 2012;
670 Warner et al., 2014). We show that all of the downstream water collected at different dates had
671 elevated Cl compared to the upstream values (2 mg/L), and high Br/Cl ratios similar to the spill
672 waters (Fig. S9). Surface water directly adjacent to the spill site in Tyler County collected at two
673 dates had up to twice the upstream Cl values (14 and 21 mg/L) and Br/Cl ratios that reflect
674 mixing between the flowback and upstream surface water (Fig. S9). Run-off into Big Run Creek
675 and the surface water at the run-off point sampled in February (more than a month after the spill)
676 also had values that correspond to a mixing line between the flowback and upstream creek values
677 (Fig. S9), indicating continued contamination of the stream from the spilled water. The $\delta^{11}B$ and
678 $\delta^{7}Li$ values in the run-off to Big Run creek were consistent with values in WV flowback (27 and
679 14‰, respectively).

680 Surface water was also sampled near two disposal (i.e., injection) wells known to accept
681 OGW; these surface waters also showed evidence of contamination. At both injection well sites,
682 the oil and gas wastewater are stored in holding ponds prior to injection. Here, we sampled
683 streams running adjacent to the injection pad and storage ponds, along with background surface
684 water in the area. Two small streams directly downstream of the injection well in Lochgully and
685 surface holding ponds had high Cl (mean = 470 mg/L), Sr (2 mg/L), Ba (2 mg/L), and Br/Cl (2.6
686 x 10^{-3}), as well as $\delta^{11}B$ (20‰) that are consistent with the Devonian-age brine (Warner et al.,
687 2014). The injection well was permitted in 2002 and renewed for another five years in 2007. The
688 surface storage ponds were closed in 2014, after we sampled in October 2013. Likewise, surface
689 water next to the Hall injection well site in Ritchie Co. had elevated Cl (87 mg/L compared to an
690 upstream of 16 mg/L) and Br/Cl (4.4 x 10^{-3}) and low Na/Cl (0.60) indicating possible
691 contamination from the injection well site (Fig. S9). The Hall injection well is much recent and

692 was first permitted in 2013.

693

694 # 5. DISCUSSION

695 ## 5.1 Tracing the source of the salinity and hydrocarbons in groundwater

696 The complex geology and tectonic history of the Northern Appalachian Basin (NAB) has
697 led to diverse groundwater quality in the shallow aquifers. Saline groundwater in the NAB
698 aquifers is relatively common and is frequently associated with the presence of hydrocarbon
699 gases. However, findings of elevated salts and CH_4 in drinking-water wells near oil and gas
700 development have prompted concerns about groundwater quality impacts from unconventional
701 exploration of the Marcellus Shale. In some areas, stray gas from leaky, faulty, or damaged wells
702 has been identified, but hydrocarbon-rich saline groundwater has typically only been associated
703 with naturally occurring migration of deep formation brines (Darrah et al., 2014; Jackson et al.,
704 2013b; Warner et al., 2012; Warner et al., 2013b). The timeline data in this study show that
705 saline and hydrocarbon-rich groundwater was present in drinking-water wells prior to
706 unconventional oil and gas development in the region, and the inorganic and gas geochemistry of
707 both fresh and saline groundwater generally went unchanged in the first three years post-
708 development in the suite of samples evaluated in this study. These observations suggest a natural
709 source of hydrocarbon-rich brine mixing with shallow, young meteoric groundwater rather than
710 contamination from nearby unconventional oil and gas development.

711 Salinity in the groundwater wells in the study area was lower (maximum Cl ~ 2,400
712 mg/L) compared to groundwater sampled in northeastern Pennsylvania (Cl up to ~4,000 mg/L);
713 however the range of Cl concentrations was very similar to the results of groundwater wells
714 analyzed within the study area in a pre-existing1982 study (Shultz, 1984). Additionally, the
715 frequency of saline water wells was consistent with this historical data. Type 2 and Type 3 saline
716 waters had Ca-Na-Cl composition with $Br/Cl>1.5x10^{-3}$ that differ from the Type 1 fresh water
717 with Ca-Na-HCO_3 composition, which is consistent with the brine compositions in Devonian-age
718 produced waters in the NAB (Chapman et al., 2012; Dresel and Rose, 2010; Haluszczak et al.,
719 2013; Warner et al., 2012). Ca-Na-Cl type water was also reported in the 1984 study, further
720 supporting the presence of brine in groundwater prior to shale gas development in West Virginia
721 (Shultz, 1984). The higher Br/Cl found in Type 3, but not in Type 2 water, with ratios up to

722 ~$4x10^{-3}$ are similar to the ratios reported in Marcellus flowback water and accidental spills in
723 northern West Virginia (Fig. 4; Ziemkiewicz and He, 2015; Harkness et al., 2015). Additionally,
724 Type 3 waters were not present in groundwater sampled prior to shale gas development in the
725 study area; however, it was detected in groundwater located more than 2 km from a shale-gas
726 well.
727 Our data show that both Cl and Br/Cl ratios decrease with increasing elevation. Thus, the
728 data show that saline waters with high Br/Cl ratios (mainly Type 3 waters) are more likely to
729 occur in valley bottoms in this study area (Fig. S8). The relationships between salinity, brine
730 contribution and location at the valleys have been observed in other parts of the NAB
731 (Llewellyn, 2014; Warner et al., 2012). The increased fracturing in geologic formations below
732 these features can induce higher hydraulic permeability and promote migration of deep fluids
733 into the shallow aquifers, which supports natural migration of deep brines as the primary source
734 of saline water. Additionally, several previous studies have suggested that increased levels of
735 saline-rich and hydrocarbon-gas-rich fluids occur in valley bottoms assigned either based on
736 topography or distances to nearest stream or river (Baldassare et al., 2013; Molofsky et al., 2013;
737 Darrah et al., 2015; Siegel et al., 2015; Warner et al., 2012). By comparison, other studies have
738 suggested the saline and hydrocarbon gas-rich fluids specifically occur within valley bottoms
739 related to the eroded cores of highly fractured anticlinal structures (e.g., Darrah et al., 2015). The
740 eroded cores of anticlines are not commonly observed in this region of WV because of the low
741 amplitude nature of folding in this area.
742 CH_4 also had a significant relationship to valleys in the region (Fig. S6 and S7).
743 Hydrocarbon gases may result from *in-situ* microbial or thermogenic production, and/or the
744 migration of hydrocarbons from an exogenous biogenic or thermogenic source (e.g., Darrah et
745 al., 2015). In general, results from this study are consistent with previously observed
746 relationships between CH_4 and elevated salinity. The strong correlation between Cl and CH_4 in
747 groundwater, particularly for Type 2 water ($r = 0.76$, $p < 0.05$), suggests that elevated CH_4 is
748 mainly arriving in the shallow groundwater along with a migrated brine (Fig. 4). Importantly, the
749 high CH_4 (>1 ccSTP/L) identified in groundwater wells is associated with elevated salinity, but
750 not with distance to shale gas wells (Fig. 9), which appears to preclude an anthropogenic source
751 for both hydrocarbon gases and salts. Historical data from WV also shows naturally high CH_4
752 (up to 21 ccSTP/L), and thus the values that were observed in this study do not appear atypical

753 for historical groundwater in the region (White and Mathes, 2006). Similar to what was shown
754 by Darrah et al (2014; 2015b), we find that although CH_4 concentrations increase with Cl content
755 until the point of methane saturation in groundwater. As CH_4 concentrations approach the
756 saturation level (i.e., "bubble point" or CH_4 partial pressure of 1atm ($p(CH_4)$=1atm) of methane
757 (35-40 cm^3 STP/L) in groundwater at 1atm and 10^{o}C for groundwater, there is a noticeable "roll
758 over" in the plot of CH_4 versus Cl (Fig. 6). This roll over demonstrates how the conditions of gas
759 saturation in water regulate the concentrations of CH_4 in groundwater.
760 By comparison to previous studies of the NAB, samples from this study area have lower
761 C_2H_6 concentrations (higher C_1/C_2+) on average and much more negative $\delta^{13}C\text{-}CH_4$ values.
762 Although the Type 2 and Type 3 waters display heavier $\delta^{13}C\text{-}CH_4$ than Type 1 on average, the
763 more negative $\delta^{13}C\text{-}CH_4$ signature in the saline groundwater of Type 2 and Type 3 indicates
764 significant biogenic contributions of methane in all groundwater samples (Fig. 6), which is
765 different from the more thermogenic-dominated (i.e., enriched in $\delta^{13}C\text{-}CH_4$,) sources of
766 hydrocarbon gases in groundwater from other regions of the Appalachian Basin (Baldassare et
767 al., 2014; et al., 2014c; Jackson et al., 2013a; Molofsky et al., 2013; Osborn et al., 2011).
768 Nonetheless, saline Type 3 groundwater samples showed positive linear correlations between
769 CH_4 and $\delta^{13}C\text{-}CH_4$ ($r=0.60$, $p<0.05$) with Cl ($r= 0.67$, $p<0.05$; Fig. 6). Similar correlations were
770 observed in earlier studies for the northeastern part of the Appalachian Basin, and are consistent
771 with post-genetic fractionation during migration of CH_4–rich brines to shallow aquifers (Darrah
772 et al., 2015b; Darrah et al., 2014).
773 While $\delta^{13}C\text{-}CH_4$ <-55‰ and elevated C_1/C_2+ can readily be interpreted as biogenic, as
774 opposed to thermogenic in origin, the persistent presence of ethane (and in some cases propane),
775 elevated helium, and the presence of methane with a more enriched $\delta^{13}C\text{-}CH_4$ have a less certain
776 mode of formation (Fig. 6). The most confounding issue with the interpretation of a biogenic
777 source of natural gases in this study area is the low, but persistent presence of higher aliphatic
778 hydrocarbons such as ethane, propane, and in some samples trace amounts of butane and
779 pentane. Further, the abundance of these higher order aliphatic hydrocarbons increases with
780 increasing salinity and helium content, and is associated with a general increase in $\delta^{13}C\text{-}CH_4$
781 (discussed below) (Table 2; Fig. 6; 8). This trend is consistent with the presence of a mixture of
782 thermogenic hydrocarbon gas in samples from this area (Darrah et al., 2014; 2015). Moreover,
783 although there is a broad range of $\delta^{13}C\text{-}C_2H_6$ (approximately -39 to -34 per mil) in groundwater

784 from Types 1, 2, and 3, ethane and isotopic values of $\delta^{13}C\text{-}C_2H_6$ are consistent with the expected
785 composition of thermogenic gases derived from either marine (e.g., shale) or terrestrial (e.g.,
786 coal) organic matter (Faber and Stahl, 1984; Whiticar et al., 1994) throughout all sample types
787 (Figure 6E).
788 In order to find a consistent explanation for all of the geochemical observations, we must
789 first consider the series of geochemical processes that may change the molecular and isotopic
790 composition of natural gas. Given the persistent presence of thermogenic natural gas, we start
791 with the evolution of hydrocarbon stable isotopes during thermal maturation. During the
792 generation of hydrocarbon gases by the thermocatalytic degradation of marine or terrestrial
793 organic matter, there is an approximately linear, temperature-dependent relationship between the
794 $\delta^{13}C$ values of methane, ethane, propane, and higher aliphatic hydrocarbons (Faber and Stahl,
795 1984; Whiticar et a., 1985; Whiticar and Faber, 1986; Whiticar et al., 1994). Since only stable
796 carbon isotopes of methane and ethane were available in the current study, we plot $\delta^{13}C\text{-}CH_4$ vs.
797 $\delta^{13}C\text{-}C_2H_6$ and the temperature-dependent relationship between these parameters, illustrated by
798 the green line in Figure 6E. The classic interpretation of this plot is that samples that fall above
799 the line represent mixing of various thermogenic components or methane oxidation, whereas
800 samples that fall below the line indicate the addition of biogenic methane (Whiticar et al., 1994).
801 Note that all of the samples fall below the line, indicating a significant mixture of biogenic
802 methane with an apparently ubiquitous, and in this case, relatively low proportion of natural gas
803 derived from a thermogenic source (Figure 6E).
804 Because $\delta^{13}C\text{-}CH_4$ and $\delta^{13}C\text{-}C_2H_6$ values are expected to increase with increasing thermal
805 maturity (Faber and Stahl, 1984; Whiticar et a., 1985; Whiticar and Faber, 1986; Whiticar et al.,
806 1994), decreasing $\delta^{13}C\text{-}CH_4$ paired with the extent of increase in C_1/C_2+ ratios may appear to be
807 inconsistent with the anticipated trends for hydrocarbon maturation. However, we suggest that
808 one potential parsimonious explanation may relate to a multiple stage process that progresses as
809 follows: (1) initially a thermogenic natural gas migrates to shallow aquifers over geological time;
810 (2) the range of $\delta^{13}C\text{-}C_2H_6$ can be accounted for by *either* a) differences in the thermal maturity
811 of natural gas that migrates to shallow aquifers over time (increasing the $\delta^{13}C\text{-}C_2H_6$ with a
812 progressive increase in thermal maturity); b) the migration of multiple sources of thermogenic
813 natural gas (e.g., shale gas plus thermogenic gas derived from coals); or c) aerobic oxidation of
814 hydrocarbons after introduction to oxic/anoxic boundaries in shallow aquifers (Darrah et al.,

2015b); followed by (3) mixing with biogenic methane in the shallow subsurface following methanogenesis.

This processes would involve (1) the migration of a thermogenic natural gas with relatively enriched values of $\delta^{13}C\text{-}CH_4$ and $\delta^{13}C\text{-}C_2H_6$ and relatively low C_1/C_2+ (as compared to groundwater geochemical composition observed in this study); (2) the C_1/C_2+ composition of this natural gas would increase during fluid migration, potentially by a combination of solubilty fractionation and aerobic oxidation during migration to the shallow aquifers (producing a range of progressivley enriched $\delta^{13}C\text{-}CH_4$ and $\delta^{13}C\text{-}C_2H_6$ and elevated C_1/C_2+); (3) mixing of thermogenic natural gases from either multiple sources *or* natual gas from varying thermal maturities, potentially followed by aerobic oxidation (both which would further increase the range of $\delta^{13}C\text{-}CH_4$ and $\delta^{13}C\text{-}C_2H_6$ and elevate C_1/C_2+); followed by (4) the introduction of biogenic methane with depleted $\delta^{13}C\text{-}CH_4$ (^{12}C enriched) and elevated C_1/C_2+, but without additional changes in $\delta^{13}C\text{-}C_2H_6$.

Based on the summation of data, we hypothesize that the persistent occurrence of ethane (and in some cases propane) and the ethane with this isotopic $\delta^{13}C\text{-}C_2H_6$ values ranging from -39 to -34 ‰ reflect an unambiguous presence of thermogenic natural gas that apparently migrated to the shallow aquifers, followed by the addition of biogenic methane. In combination, these coupled processes produce a distinguished geochemical composition of natural gas composed of a mixture of both post-genetically altered thermogenic natural gas and biogenic methane.

In support of this *ad hoc* hypothesis, is the presence of highly elevated [^4He], $^4He/CH_4$, and $^{20}Ne/^{36}Ar$ (discussed further below) in the gas-rich end-member with relatively elevated $\delta^{13}C\text{-}CH_4$ and $\delta^{13}C\text{-}C_2H_6$. The majority of the data can be accounted for by simple two component mixing between a biogenic end-member and a thermogenic end-member that previously experienced post-genetic modification that increased the C_1/C_2+ ratio without major changes in the $\delta^{13}C\text{-}CH_4$ or $\delta^{13}C\text{-}C_2H_6$; these conditions can be met by solubility partitioning during hydrocarbon gas migration (depicted by the dashed red line in Figure 6D).

In addition to the natural gas, this study investigates the origin of the saline groundwater. Boron and Li isotope variations in the saline groundwater reflect intensive water-rock interactions, which is consistent with this hypothesis. Thus, we hypothesize that the saline water originated from Upper Devonian brines with $\delta^{11}B$ >40‰ and low B/Cl (Warner et al., 2014), but was modified through extensive water-rock interactions to form saline groundwater with lower

846 $\delta^{11}B$ of Type 2 and Type 3 water (Fig. 5). The high correlation of B/Cl with Na/Cl for Type 3
847 water suggests that the B modification was induced by base-exchange reactions with the coal and
848 shale rocks that also compose the aquifer, with typically lower $\delta^{11}B$ (i.e., $\delta^{11}B$~15‰ in
849 desorbable B from marine clays; Spivack and Edmond, 1987). The $\delta^{7}Li$ values in the
850 groundwater wells mimic the composition of the Upper Devonian produced waters (Warner et
851 al., 2014), which suggests lower contribution of Li from water-rock interaction. Nonetheless,
852 these isotopic values were higher than the $\delta^{7}Li$ fingerprints of the Marcellus flowback water
853 ($\delta^{7}Li$<10; Fig. 5), which is consistent with the lack of evidence for contamination from
854 unconventional energy development (Phan et al., 2016; Warner et al., 2014).

855 The $^{87}Sr/^{86}Sr$ ratios in groundwater from the study area were less radiogenic than the
856 typical high $^{87}Sr/^{86}Sr$ measured in Upper Devonian brines (>0.716) and slightly higher than the
857 $^{87}Sr/^{86}Sr$ Marcellus flowback and produced waters (0.71121±0.0006) and spill water reported in
858 this study (0.70981; Table 3; Fig. 5; Chapman et al., 2012; Warner et al., 2012). The
859 groundwater data are also different from the composition of Marcellus-like saline groundwater in
860 northeastern PA reported by Warner et al. (2012). $^{87}Sr/^{86}Sr$ ratios reported for coals from the
861 Pittsburgh, Allegheny and Kanawha formations in West Virginia (Vengosh et al., 2013) and
862 Pennsylvania (Chapman et al., 2012), as well as leaching of U.S coals (Brubaker et al., 2013;
863 Ruhl et al., 2014; Spivak-Birndorf et al., 2012), had a range of 0.70975 to 0.71910. Both
864 leaching experiments of WV surface rocks and streams that discharged from valley fills in WV
865 found that coal-bearing rocks have $^{87}Sr/^{86}Sr$ ratio ~0.7124 (Vengosh et al., 2013), which is
866 similar to the values measured in groundwater in this study. This similarity suggests that the
867 deep-source of saline groundwater has interacted with the coal units imbedded in the deep or
868 surface geology, causing the observed isotopic shift from the original isotope composition of the
869 brine. Wunsch (1992) presented a hypothesis that groundwater in the lower NAB likely migrates
870 along coal seams that have higher permeability than the interbedded shale layers found through
871 shallow aquifers in the region. This preferential flowpath would induce intensive interaction with
872 coal seams.

873 Overall, the integration of the isotope systematics of Sr, B, and Li in the investigated
874 groundwater suggests that the saline groundwater originated from the Appalachian brines, but
875 was modified by interactions with the local coal-bearing aquifer rocks. The difference in Br/Cl

ratios of Type 2 and 3 could be related to a different origin of the source brines. Produced waters from different geological formations in northern Appalachia have shown large variations in Br/Cl ratios, reflecting different degrees of evaporation and/or later modification by halite dissolution (Chapman et al., 2012; Dresel and Rose, 2010; Warner et al., 2012). The long-term migration of these presumably two different brine sources to the shallow aquifer in WV has involved interactions with the rock formations and modification of the original composition. In any case, the Li and Sr isotope compositions of the saline groundwater of Type 2 and 3 are different from those of the Marcellus brines and spill waters collected in this study, and clearly rule out the possibility of contamination from flowback or produced waters associated with unconventional energy development in the area. This interpretation is further strengthened by the fact that the chemistry of the saline groundwater prior to the shale gas drilling in the area was not modified throughout time following shale gas drilling and hydraulic fracturing.

5.2 Determining transport mechanisms using noble gas geochemistry

Geochemical studies in other regions of the NAB (northeast Pennsylvania, eastern Kentucky) identified mixing of shallow groundwater with possible deep brines with chemistry similar to that found in the Marcellus Shale (Warner et al., 2012). The flow paths that allow the migration from depth was attributed to a combination of deep high hydrodynamic pressure and enhanced natural flow paths (i.e. fracture zones) (Engelder et al., 2009). This model is particularly relevant in valleys due to increased regional discharge to lower hydrodynamic pressure in the valleys and greater fracturing and thus permeability of the subsurface in valleys. The presence of naturally occurring flow paths for fluid migration is important as it suggests there are connective pathways between shallow groundwater and oil and gas bearing formations that could allow for migration of hydraulic fracturing fluids. Noble gas studies in the Appalachian region support the model for long-range migration of hydrocarbon-rich brines over geological time from depth and mixing with shallow groundwater (Darrah et al., 2015; Darrah et al., 2014).

The abundance of dissolved atmospheric (ASW) gases (i.e., ^{20}Ne, ^{36}Ar, N_2) can also help to constrain the behavior of hydrocarbon gases (Aeschbach-Hertig et al., 2008; Gilfillan et al., 2009; Holocher et al., 2002; Holocher et al., 2003; Solomon et al., 1992). Previous research has shown that quantitative “stripping” of air-saturated water noble gases provide evidence for

fugitive gas contamination in some shallow drinking-water wells (Darrah et al., 2014). In contrast, *none* of the samples in this study, collected before or after shale gas drilling showed evidence for stripping or fugitive gas contamination (Fig. 7). The most obvious deviations from ASW composition in this study include concomitantly elevated levels of ^{4}He, ^{20}Ne, CH_4, and C_2H_6, which generally correspond to increasing salinity (Fig. 8 and S6) as was observed previously (Darrah et al., 2014; 2015).

The extent of "bubble enrichment" or "excess air" entrainment observed here is common in many aquifers (Aeschbach-Hertig et al., 2008; Heaton and Vogel, 1981) and reflects normal equilibration between the atmosphere and meteoric water during groundwater recharge. These findings were as expected for a typical shallow aquifer and consistent with an absence of obvious evidence for extensive gas-water interactions in this dataset (i.e., stripping related to fugitive gas contamination) (Weiss, 1971a, b). One noticeable difference from previous studies, is the lower ^{36}Ar, on average, for samples with the elevated CH_4 concentrations in Types 2 and 3, which suggests the addition of CH_4 may have induced minor two-phase effects (gas–liquid interactions) during transport in the aquifer (Fig. 7).

Noble gas isotopes and ^{3}H data also provide additional insights for the origin of the different water types. Similar to other studies, all water types apparently reflect contributions from relatively young meteoric water as demonstrated by the presence of statistically indistinguishable ($p<0.05$) quantities of ^{3}H (half-life ~12.4 years) in all three subsets. In general, Type 1 water samples appear to reflect relatively young (^{3}H-active; <~80 years), low-CH_4, and low salinity groundwater. By comparison, both Type 2 and 3 waters contain lower ^{3}H levels (mean ^{3}H = 4.5 compared to 5.9 for the whole dataset), and thus indicate the likely migration of an old exogenous fluid into, and subsequent mixing with, fresh water in shallow aquifers on undetermined time scales. For these reasons, we conclude that the salinity and the majority of the dissolved CH_4 reflect the migration of a deeper, exogenous source of CH_4-rich brines into the shallow aquifers over geological time coupled with the additaion of methanogenic methane in the shallow subsurface. This argument conflicts with models of elevated CH_4 controlled by hydrodynamic pressure (Molofsky et al., 2013; Siegel et al., 2015a) and instead suggests that valley bottoms with higher hydraulic permeability induced from higher fault and fracture intensity along deformational features, which may result in preferential pathways for the migration of deep fluids to shallow aquifers.

Important distinctions between Type 2 and 3 waters include the resolvable differences in the $^{4}He/CH_4$ and $^{20}Ne/^{36}Ar$ ratios, which suggests a longer range of fluid transport for Type 3 waters (Fig. 8). We interpret the noble gas differences as the result of the migration of a deeper source for Type 3 waters relative to Type 2 waters, potentially from an organic-rich shale-like source rock. This distinction is supported by the relatively higher Br/Cl of Type 3 groundwater, indicating a brine-rich source. This mechanism is consistent with the other geochemical and isotope differences observed between Type 2 and Type 3 waters. The B/Cl and Na/Cl ratios and $\delta^{11}B$ suggest that the Devonian brines that formed Type 3 waters had fewer interactions with the shallow aquifer host rocks relative to Type 2 waters.

Although we do observe a general trend of concomitantly increasing ^{4}He and $^{4}He/^{20}Ne$ and low $^{3}He/^{4}He$ in samples that are rich in Cl and CH_4, we also found significant scatter in these relationships within the current dataset (Fig. 8 and S6). These data provide an important parameter by which to differentiate Types 2 and 3 from Type 1, but do not distinguish Types 2 and 3 from each other. All Type 3 and the majority of Type 2 samples do display elevated ^{4}He, ^{20}Ne, and $^{4}He/^{20}Ne$, and low $^{3}He/^{4}He$ in samples rich in Cl and CH_4, which is largely consistent with an exogenous crustal/radiogenic source of natural gas to the aquifer (i.e., a source of He external to the present aquifer lithologies) (Fig. 8 and S6).

By comparison to the He-rich samples, with a few exceptions, the majority of Type 1 and a subset of Type 2 samples have air saturated water-like $^{3}He/^{4}He$ values that decrease with increasing ^{4}He content, but does not decrease with increasing CH_4 or Cl levels (Fig. 8). This trend appears to reflect a variable mixture between air-saturated water and crustal helium at moderate CH_4 and Cl levels, which is consistent with a larger component of younger, biogenic CH_4.

The ^{4}He in groundwater, reflects a combination of: (1) atmospheric inputs; (2) *in-situ* production of ^{4}He from α-decay of U-Th in the aquifer rocks; (3) the release of ^{4}He that previously accumulated in detrital grains; and (4) the flux from exogenous sources (Solomon et al., 1996; Zhou and Ballentine, 2006). The proportion of ^{4}He from atmospheric inputs can be readily estimated from the abundance of other air-saturated water gases and the *in situ* production from α-decay can be determined by measuring the U and Th of aquifer rocks (Table 2). The steady-state production and accumulation for ^{4}He in aquifer minerals (dominated by quartz and clay grains) was estimated as $<2.94x10^{-9}$ cm^3 STP/L of water/yr. Additionally, we

estimate that maximum release of radiogenic helium into aquifer waters that previously accumulated in crustal minerals over geologic time by conducting step-wise heating experiments on aquifers minerals to be on the order of ~0.71×10^{-6} cm^3 STP/L/yr.

Based on these estimates, we find that the ^4He that we observed (up to 0.36 cm^3 STP/L) in the CH_4-rich and high salinity samples greatly exceeds the viable combined concentrations from $^4He_{ASW}$, the maximum $^4He_{in\text{-}situ}$ production, and the expected release from ^4He that previously accumulated in aquifers minerals, unless we assume a groundwater age of greater than 1.4 million years. Because of the consistent presence of ^3H (with a half-life of 12.3 years) observed in groundwater from this study (2.48 to 8.48 ^3H units overall and 3.67 to 5.11 in Type 3 waters), in combination with water isotopes that are consistent with the post-glacial (post-Pleistocene) local meteoric water line (Fig. S4), we suggest that these groundwater samples represent a mixture between young meteoric water and an exogenous source of hydrocarbon-rich diluted brines in the shallow subsurface. We conclude that Type 3 waters unambiguously require an exogenous source of ^4He that mixes with relatively fresh meteoric water, while Type 2 waters likely reflect a mixture of both components. Clearly, on average the majority of Type 1 samples appear to reflect shallow, relatively young meteoric water with some exceptions that have higher ^4He and lower $^3He/^4He$.

In addition to ^4He, other noble gas data are consistent with the hypothesized migration of an exogenous fluid. In others parts of the Appalachian Basin, we previously interpreted strong correlations between ratios of thermogenic to air-saturated water gases to each other and to increasing salt content as variable additions of a thermogenic hydrocarbon gas-rich brine (dominated by CH_4 with minor C_2H_6 and other crustal components such as ^4He) to ^3H-active, and hence, relatively recent meteoric water (dominated by ASW components such as N_2 and ^{36}Ar) in shallow groundwater conditions (Darrah et al., 2014; Darrah et al., 2015b). Although the collection of geochemical data likely indicates a different origin for these gases in this study area (i.e., coal beds or a lower thermal maturity shale gas), in combination, the data suggests the coherent migration of hydrocarbon gases, salts, and radiogenic helium from deeper exogenous sources.

5.4. Surface water impacts due to release of wastewater

The clear evidence for surface water contamination at two injection well sites and from

999 the flowback spill in Tyler County, provide the basis for a geochemical "contaminated"
1000 fingerprint that can be compared to the groundwater geochemistry in the study area. The
1001 flowback spill water was associated with high salinity, high Br/Cl ratios and isotope ratios that
1002 were similar to Marcellus flowback values reported in previous studies (Chapman et al., 2012;
1003 Warner et al., 2014). The spill water was also characterized by relatively high $\delta^{11}B$ (>27‰) and
1004 low $\delta^{7}Li$ (<15‰) values that are similar to the values found in Marcellus flowback and are
1005 distinct from the Upper Devonian produced waters from conventional oil and gas wells. Water
1006 samples collected 1.5 and 8 months after the spill show a continued release of flowback water to
1007 the environment, with pools of water showing elevated salinity, Br/Cl ratios and Marcellus-like
1008 isotope signatures. At 1.5 months after the spill, flowback-like water with elevated salinity, Li,
1009 B, Ba, Sr, and other metals was found still running off into Big Run Creek and downstream of
1010 the spill site in Big Run Creek. These samples had elevated concentrations of various inorganic
1011 components compared to the upstream values, although the absolute concentrations levels were
1012 below any ecological or drinking water standards.

1013 The $\delta^{11}B$ values of the spill water from the Lochgully injection well sites were ~20‰,
1014 which could reflect mixing of flowback water with surface water, or that the OGW released from
1015 the storage ponds at the Lochgully site could be a mixture of both Upper Devonian produced
1016 waters and Marcellus flowback. The streams running through the Lochgully site connect
1017 downstream to Wolf Creek, which is a major drinking water source in the area. Other than
1018 elevated Ba and Sr, no other trace elements contamination was found in the two small streams.
1019 The surface water adjacent to the Hall injection well had elevated Cl, Br, Na, B, Sr and Ba
1020 compared to the background surface water, which indicates possible contamination from the
1021 OGW spills downstream from the injection well. These samples were collected during the winter
1022 and there could be seasonal variations in the contribution of OGW to the environment.

1023 Overall, the surface water chemistry at these spill sites is consistent with the composition
1024 of the Marcellus flowback, providing a strong evidence for contamination due to disposal and
1025 storage of hydraulic fracturing fluids in West Virginia. The $\delta^{7}Li$ values of the leaking flowback
1026 fluid at the Tyler County site were lower compared to the regional saline groundwater in this
1027 study, while the $\delta^{11}B$ values were higher. This suggests that the B and Li isotope values in water
1028 contaminated from unconventional activities should be distinct from naturally occurring brine

1029 salinization. These findings further support the conclusions from the time series data that the
1030 saline groundwater found in the study site is not a result of releases of OGW from
1031 unconventional oil and gas drilling activity in the area.

1032 **6. CONCLUSIONS**

1033 Similar to other areas in the Appalachian Basin, the occurrence of CH_4-rich, saline
1034 groundwater in shallow aquifers was found to be a widespread phenomenon and likely a result of
1035 natural migration of deep brine- and natural gas-rich fluids combined with shallow water-rock
1036 interactions. This three-year study has monitored the geochemical variations of drinking-water
1037 wells before and after the installation of nearby shale gas wells, and provides a clear indication
1038 for the lack of groundwater contamination and subsurface impact from shale-gas drilling and
1039 hydraulic fracturing with the temporal resolution offered by the study. Saline groundwater was
1040 ubiquitous throughout the study area before and after shale gas development, and the
1041 groundwater geochemistry in this study was consistent with historical data reported in the
1042 1980's. We observed significant relationships of Cl and Br/Cl ratios with tectonic and
1043 topographic structures, but not with distance to shale gas wells. The variations of B, Li, and Sr
1044 isotopes ratios in the groundwater samples were not consistent with the signature of hydraulic
1045 fracturing fluids, but rather reflect upflow of Devonian-age brines that have migrated to the
1046 shallow aquifers and were modified by water-rock interactions.

1047 Additional evidence comes from the relative distributions of hydrocarbon gases and air-
1048 saturated water gases. Unlike previous studies that have identified fugitive gas contamination in
1049 groundwater near shale gas wells in the northeastern part of the Appalachian Basin, we did not
1050 observe significant deviations of $CH_4/^{36}Ar$ (gas to water ratio) or $^{4}He/^{20}Ne$ (thermogenic to air-
1051 saturated water ratio) relative to Cl concentration (Fig. 10). While we did observe a subset of
1052 samples with elevated CH_4 at low Cl concentrations, these samples all had very low $\delta^{13}C\text{-}CH_4$,
1053 which is consistent with microbial CH_4 and display near air-saturated water levels of ^{4}He (Darrah
1054 et al., 2015). The occurrence of ethane and propane and the carbon isotope ratios of ethane
1055 indicate that thermogenic gas contributes to the overall mixture of natural gas in the shallow
1056 aquifers of WV. However, groundwater from this study area is dominated by biogenic CH_4.
1057 Importantly, it appears that both biogenic and migrated thermogenic gases in the shallow
1058 groundwater are unrelated to shale gas development.

The abundance of dissolved air-saturated water parameters and ^{4}He, further support this interpretation. With the exception of four samples that have significant excess air (denoted by highly elevated ^{36}Ar), the only notable deviations from normal Henry's Law equilibrium values are the significant excesses of ^{4}He and ^{20}Ne in CH_4- and the salt-rich groundwater samples noted above. Both of these components are likely enriched in these aquifers by the migration of exogenous CH_4- and salt-rich fluids, and potentially altered by minor gas-water interactions in aquifer systems. Importantly, we did observe lower abundances of ^{36}Ar and N_2, on average, in samples with higher CH_4 and Cl content, and thus we do not observe any evidence for quantitative stripping of air-saturated water noble gases. Additionally, because the N_2/Ar does not fractionation coherently with $^{20}Ne/^{36}Ar$, we conclude that the phase-partioning that enriches ^{4}He and ^{20}Ne likely reflects migration of natural gas derived from an exogenous source. These data also suggest that gas-water interactions occur at exceedingly lower volumes of gas with respect to water, which further supports our observation for the lack of fugitive gas contamination in the current study area.

Trace metals, such as As, that are associated with potential health impacts also showed no correlation with proximity to shale gas activities. Arsenic concentrations exceeding national drinking water standards were detected also in wells tested before shale gas development. Wells containing higher As concentrations were generally located in two regions of the study area, and occurred in all 3 types of water, which points to natural (i.e., geogenic) sources of arsenic in the aquifer. This observation is important for evaluating possible contamination processes because some previous studies have associated elevated As with contamination from hydraulic fracturing activities (Fontenot et al., 2013). Our data rules this out for this study area.

It is clear from this and previous studies that risks to water resources from shale gas development vary within and between basins. Stray gas contamination has been identified in northeastern Pennsylvania and Texas (Darrah et al., 2014; Jackson et al., 2013), but not in northeastern West Virginia (this study) or Arkansas (Warner et al., 2013b). However, surface water impacts from spills and accidental release do seem to occur in all areas with hydraulic fracturing such as Pennsylvania (Vengosh et al., 2014) and North Dakota (Lauer et al., 2016). The integrated geochemical data presented herein rule out stray gas or brine contamination from shale gas development in this study area. In contrast, we observed surface water contamination at

three sites that originated directly from surface spills associated with unconventional oil and gas activities. The chemistry of the spill water was identical to the composition of the Marcellus flowback and/or produced waters. These results clearly demonstrate the advantage of integrated geochemical tools for delineating the environmental effects of energy development, in addition to geospatial analysis. The study also shows that surface processes like spills have immediate effects, while groundwater quality is not impacted, even in a time scale of three years conducted in this study. Future studies should adapt these and similar geochemical tools to evaluate the long-term effects of intensive shale gas development in the NAB and other basins, and address the potential for groundwater contamination over longer periods of time.

FUNDING

This study was supported by grants from the National Science Foundation (grants number EAR-1441497 and 1249255) and the Natural Resources Defense Council (NRDC).

CONFLICT OF INTEREST

The authors have no conflicts of interest to declare.

ACKNOWLEDGMENTS

We gratefully acknowledge Mirijana Beram, Diane Pitcock and the Doddridge County Watershed Association for their generous help with recruiting homeowners and field logistics. We thank Gary Dwyer for trace element analysis, Jon Karr for stable isotope analysis, Nancy Lauer, Eleanor Kern, William K. Eymold for fieldwork and sample processing, and Andrew Kondash for GIS mapping.

Figures Captions

Fig. 1. Stratigraphic column of the carboniferous aquifers in the study area based on (Martin, 1998) showing interbedded layers of sandstone, limestone and coal.

Fig. 2. Location of private drinking-water wells and spill sites sampled in northwestern West Virginia, superimposed on the local surface geology. Shale-gas wells and the direction and length of lateral drills are also shown. The Arches Fork anticline (AFA) that divides Doddridge County is show in green, while Burchfield Syncline to the north and Robbison Syncline to the south of the AFA are shown in blue (Hennen, 1912; Ryder et al., 2012). No known faults are described in the study area.

Fig. 3. Ternary diagrams that display the relative percent of (A) cations, and (B) anions in groundwater samples in the study region. Type 1 groundwater (circles) is characterized as Ca-Na-HCO_3 type water, while Type 2 (triangles) and 3 (squares) are Ca-Na-Cl type water. Historical data from West Virginia collected in 1982 (orange hexagons) shows the presence of both fresh and saline-type groundwater prior to shale-gas development in the region and could be the result of natural mixing (Shultz, 1984). The abundance of methane is preserved by using a blue-red color intensity scale, where methane concentrations of 0 ccSTP/L are blue and range up to red for [CH_4] >40 ccSTP/L. For samples from which methane was not analyzed, data is shown with a grey symbol. The same color and label scheme is used for groundwater in all subsequent figures.

Fig. 4. Bromide (A), Ca (B), Na (C), Mg (D), dissolved inorganic carbon (DIC) (E), and SO_4 (F) versus chloride (Cl) concentrations in low-Cl Type 1 water and high-Cl Type 2 and Type 3 groundwater from the study area. Significant ($p<0.05$) positive linear correlations were found for Br ($r = 0.79$), Na ($r = 0.62$), and DIC ($r = 0.35$) with Cl concentrations. Type 2 and Type 3 groundwater had lower Na/Cl ratios but no significant difference was found in the Na/Cl ratio between Type 2 and Type 3 wells. Water types 2 and 3 had high Br/Cl (>0.0015) ratios with a strong linear correlation between Br and Cl ($r = 0.97$ and $r = 0.56$), but with different Br/Cl ratios, reflecting of mixing of freshwater with different brine-like sources.

Fig. 5. Boron (A), lithium (B), and strontium (B) isotope and elemental variations in groundwater from the study area. $\delta^{11}B$ values in the saline water types were high compared to the low-saline groundwater of Type 1 but lower than the composition of Upper Devonian brines, and likely reflect contribution of deep-source brines modified by water-rock interactions with ^{11}B-depleted rocks. $\delta^{7}Li$ values, particularly in Type 2 and Type 1 waters, were mostly consistent with values found in Upper Devonian brines, but not in the Marcellus Formation brines. The $^{87}Sr/^{86}Sr$ rations in the groundwater samples were indistinguishable between the water types, and were more consistent with values found in Appalachian coals (0.70975 to 0.71910) than the Devonian age brines (Chapman et al., 2012; Vengosh et al., 2013).

Fig. 6. Variations of methane (CH_4) (A) and ethane (C_2H_6) (B) concentrations, $\delta^{13}C$-CH_4 values (C) versus chloride concentrations; C_1/C_2+ hydrocarbon ratios versus $\delta^{13}C$-CH_4 (D); $\delta^{13}C$-CH_4 versus $\delta^{13}C$-C_2H_6 (E); and C_1/C_2+ ratios versus $\delta^{13}C$-C_2H_6 (F) in groundwater analyzed in this

study. The majority of groundwater samples had $\delta^{13}C\text{-}CH_4$ <-55‰ and elevated C_1/C_2+ that can be interpreted as biogenic. However, the positive correlations of CH_4 and higher order hydrocarbons (C_2H_6) with Cl, the occurrence of higher order hydrocarbons, and the heavy $\delta^{13}C\text{-}C_2H_6$ all suggest the coherent migration of a gas-rich, saline fluid from deeper formations into shallow aquifers, which is consequently diluted and presumably oxidized by meteoric water. Maximum CH_4 concentration is constrained by the upper level (saturation = 40 ccSTP/L at 10°C and 1 atm) for CH_4, resulting in an observed ''roll over" as CH_4 concentrations approach saturation levels for shallow groundwater. No significant variations in the $\delta^{13}C\text{-}CH_4$ values of the groundwater were observed between different water types, with biogenic and thermogenic signatures found in all three water types. The persistent presence of ethane and the values of $\delta^{13}C\text{-}C_2H_6$ indicate a uniform background of thermogenic natural gas derived from Type II (marine organic matter-shale) or Type III (terrestrial organic matter-coal) kerogen through the study area. However, water samples with more enriched $\delta^{13}C\text{-}CH_4$ (>-55‰) have a reduction in the total amount of hydrocarbons and high C_1/C_2+ in the residual hydrocarbon-phase, which could reflect post-genetic modification of hydrocarbons by migration or oxidation.

Fig. 7. ^{20}Ne (A), N_2 (B), and CH_4 (C) versus ^{36}Ar and CH_4 versus $^{20}Ne/^{36}Ar$ (D) in the shallow groundwater wells in the study area. All Type 1 samples have ^{36}Ar and N_2 within 14% of the temperature-dependent ASW solubility line, while the subset of methane-rich samples showed noticeably elevated excess ^{20}Ne. In contrast, none of the samples in this study, collected before or after shale gas drilling showed clear evidence for stripping or fugitive gas contamination. One noticeable difference from previous studies is the lower ^{36}Ar on average for the samples with elevated CH_4 concentrations in Types 2 and 3, which suggests the addition of CH_4 may have induced minor two-phase effects (gas–liquid interactions) in the aquifer. Note also the elevated $^{20}Ne/^{36}Ar$ in samples with high CH_4; these values indicate significant two-phase migration during transport to shallow aquifers.

Fig. 8. $^{3}He/^{4}He$ versus Cl (A), $^{4}He/^{20}Ne$ (B), CH_4 (C), and $\delta^{13}C\text{-}CH_4$ (D); $^{4}He/CH_4$ versus $^{20}Ne/^{36}Ar$ (E); and $^{4}He/^{20}Ne$ versus $^{4}He/^{36}Ar$ (F) in shallow groundwater samples in the study area. A general trend of concomitantly increasing ^{4}He and low $^{3}He/^{4}He$ in samples rich in Cl and CH_4 suggest a source of ^{4}He external to the aquifer formation, likely due to an exogenous crustal/radiogenic source of natural gas to the aquifer. These data trends clearly distinguish sample Types 2 and 3 from Type 1 ($p<0.01$), but not from each other, and are consistent with the migration of a hypothesized exogenous, two-phase fluid, potentially of thermogenic origin, to these aquifer systems.

Fig. 9. Variations of Cl (A), $\delta^{13}C\text{-}CH_4$ (B), CH_4 (C), C_1/C_2+ ratio (D), $^{87}Sr/^{86}Sr$ ratios (E), and $^{4}He/CH_4$ (F) across the study area in relation to distance to the nearest shale gas well (m). No statistically significant relationships were observed between any of these geochemical tracers and distance to the nearest gas well were observed. However, the carbon isotopes of CH_4 ($\delta^{13}C\text{-}CH_4$) and C_1/C_2+ ratios had weak correlations with distance to the nearest shell gas wells shale gas well ($r=0.28$, $p<0.05$ and $r=0.27$, $p<0.05$, respectively). $^{87}Sr/^{86}Sr$ ratios were also significantly correlated with distance to the nearest shale gas well ($r=0.40$, $p<0.04$).

Fig. 10. Relationships between Cl (A), CH_4 (B), C_2H_6 and heavier aliphatic hydrocarbons (C), δ^7Li (D), $^{87}Sr/^{86}Sr$ (E), $\delta^{13}C\text{-}CH_4$ (F), $^4He/^{20}Ne$ (G), $CH_4/^{36}Ar$ (H), and $^4He/CH_4$ (I) in shallow groundwater wells before and after shale gas drilling and hydraulic fracturing in the study area. Dash lines represent a 1:1 line, indication no change in time. All of these geochemical tracers showed no changes in groundwater sampled post-shale gas development as compared to baseline values, indicating no impact from shale gas development.

REFERENCES

Aeschbach-Hertig W., El-Gamal H., Wieser M. and Palcsu L. (2008) Modeling excess air and degassing in groundwater by equilibrium partioning with a gas phase. *Water Resour. Res.* **44**, W08449.

Bain G.a.F. (1972) Water Resources of teh Little Kanawha River basin, West Virginia: West Virginia Geological and Economic Survey Basin Bulletin 2. 122.

Baldassare F.J., McCaffrey M.A. and Harper J.A. (2014) A geochemical context for stray gas investigations in the northern Appalachian Basin: Implications of analyses of natural gases from Neogene-through Devonian-age strata. *AAPG Bull.* **98**, 341-372.

Ballentine C.J., Burgess R. and Marty B., 2002. Tracing fluid origin, transport and interaction in the crust, In *Noble Gases in Geochemistry and Cosmochemistry (*eds. D. Porcelli, Ballentine, C.J. and R.Wieler, R.). pp. 539-614.

Ballentine C.J., Onions R.K., Oxburgh E.R., Horvath F. and Deak J. (1991) Rare-gas constraints on hydrocarbon accumulation, crustal degassing, and groundwater-flow in the Pannonian Basin *ESPL* **105**, 229-246.

Ballentine C.J. and O'Nions R.K. (1994) The use of He, Ne, and Ar isotopes to study hydrocarbon related fluid provenance, migration, mass balance in sedimentary basins. *In Geofluids: Origin, migration, and mass balance in sedimentary basins* (ed. J. Parnell). **78**, 347-361.

Bernard B.B., Brooks J.M.and Sackett W.M. (1976) Natural gas seepage in the Gulf of Mexico. *ESPL* **31**, 48-54.

Bernard B.B., 1978. Light hydrocarbons in marine sediments. Texas A&M University, College Station, TX.

Brett C.E., Goodman W.M., LoDuca S.T. and Lehmann D.F., 1996. Upper Ordovician and Silurian strata in western New York: Sequences, cycles and basin dynamics, Upper Ordovician and Silurian sequence stratigraphy and depositional environments in western New York: A field guide for the James Hall Symposium: Rochester, University of Rochester, pp. 71-120.

Busch K.W. and Busch M.A., 1997. Cavity Ringdown Spectroscopy: An Ultratrace Absorption Measurement Technique American Chemical Society Symposium Series. Oxford Press.

Capo R.C., Stewart B.W., Rowan E.L., Kohl C.A.K., Wall A.J., Chapman E.C., Hammack R.W. and Schroeder K.T. (2014) The strontium isotopic evolution of Marcellus Formation produced waters, southwestern Pennsylvania. *Int. J. Coal Geol.* **126**, 57-63.

Cathles L.M. (1990) Scales and effects of fluid-flow in the upper crust. *Science* **248**, 323-329.

Chapman E.C., Capo R.C., Stewart B.W., Kirby C.S., Hammack R.W., Schroeder K.T. and Edenborn H.M. (2012) Geochemical and strontium isotope characterization of produced waters from Marcellus Shale natural gas extraction. *Environ. Sci. Tech* **46**, 3545-3553.

Clayton C. (1991) Carbon isotope fractionation during natural gas generation from kerogen *Mar. Petrol. Geol.* **8**, 232-240.

Coleman D.D., Risatti J.B., Schoell, M. (1981) Fractionation of carbon and hydrogen isotopes by methane oxidising bacteria. *Geochim. Cosmochim. Acta* **45**, 1033-1037.

1261 Cuoco E., Tedesco D., Poreda R.J., Williams J.C., De Francesco S., Balagizi C. and
1262 Darrah T.H. (2013) Impact of volcanic plume emissions on rain water chemistry
1263 during the January 2010 Nyamuragira eruptive event: Implications for essential
1264 potable water resources. *J. Hazard. Mater.* **244**, 570-581.
1265 Darrah T.H. and Poreda R.J. (2012) Evaluating the accretion of meteoritic debris and
1266 interplanetary dust particles in the GPC-3 sediment core using noble gas and
1267 mineralogical tracers. *Geochim. Cosmochim. Acta* **84**, 329-352.
1268 Darrah T.H., Tedesco D., Tassi F., Vaselli O., Cuoco E., and Poreda R.J. (2013) Gas chemistry
1269 of the Dallol region of the Danakil depression in the Afar region of the northern-most
1270 East African Rift. *Chemical Geology* **339**, 16-29.
1271 Darrah T.H., Vengosh A., Jackson R.B., Warner N.R. and Poreda R.J. (2014) Noble
1272 gases identify the mechanisms of fugitive gas contamination in drinking-water
1273 wells overlying the Marcellus and Barnett Shales. *PNAS* **111**, 14076-14081.
1274 Darrah T.H., Jackson R.B., Vengosh A., Warner N.R. and Poreda R.J. (2015a) Noble
1275 Gases: A New Technique for Fugitive Gas Investigation in Groundwater.
1276 *Groundwater* **53**, 23-28.
1277 Darrah T.H., Jackson R.B., Vengosh A., Warner N.R., Whyte C.J., Walsh T.B., Kondash
1278 A.J. and Poreda R.J. (2015b) The evolution of Devonian hydrocarbon gases in
1279 shallow aquifers of the northern Appalachian Basin: insights from integrating
1280 noble gas and hydrocarbon geochemistry. *Geochim. Cosmochim. Acta* **170**.
1281 Dresel P.E. and Rose A.W. (2010) Chemistry and origin of oil and gas well brines in
1282 western Pennsylvania. *Open-File Report OFOG* **10**, 01.00.
1283 Dubacq B., Bickle M.J., Wigley M., Kampman N., Ballentine C.J. and Lollar B.S. (2012)
1284 Noble gas and carbon isotopic evidence for CO 2-driven silicate dissolution in a
1285 recent natural CO 2 field. *ESPL* **341**, 10-19.
1286 Eckhardt D.A.V. and Sloto R.A., 2012. Baseline groundwater quality in national park
1287 units within the Marcellus and Utica Shale gas plays, New York, Pennsylvania,
1288 and West Virginia, 2011. US Geological Survey, Washington, DC.
1289 Engelder T., Lash G.G. and Uzcátegui R.S. (2009) Joint sets that enhance production
1290 from Middle and Upper Devonian gas shales of the Appalachian Basin. *AAPG*
1291 *Bull* **93**, 857-889.
1292 Engle M.A. and Rowan E.L. (2014) Geochemical evolution of produced waters from
1293 hydraulic fracturing of the Marcellus Shale, northern Appalachian Basin: A
1294 multivariate compositional data analysis approach. *Int. J. Coal Geol.* **126**, 45-56.
1295 Etiope G, Baciu CL, Schoell M (2011) Extreme methane deuterium, nitrogen and helium
1296 enrichment in natural gas from the Homorod seep (Romania) *Chemical Geology* **280**, 89-
1297 96.
1298 Faill R.T. (1997a) A geologic history of the north-central Appalachians; Part 1,
1299 Orogenesis from the Mesoproterozoic through the Taconic Orogeny. *Am. J. Sci.*
1300 **297**, 551-619.
1301 Faill R.T. (1997b) A geologic history of the north-central Appalachians; Part 2, The
1302 Appalachian Basin from the Silurian through the Carboniferous. *Am. J. Sci.* **297**,
1303 729-761.
1304 Faber E and Stahl W (1984) Geochemical surface exploration for hydrocarbon in the Norht Sea.
1305 AAPG Bull. **68**, 363-386.
1306 Fontenot B.E., Hunt L.R., Hildenbrand Z.L., Carlton Jr D.D., Oka H., Walton J.L.,

Hopkins D., Osorio A., Bjorndal B. and Hu Q.H. (2013) An evaluation of water quality in private drinking water wells near natural gas extraction sites in the Barnett Shale Formation. *Environ. Sci. Tech.* **47**, 10032-10040.

Gilfillan S.M.V., Sherwood Lollar B., Holland G., Blagburn D., Stevens S., Schoell M., Cassidy M., Ding Z.J., Zhou Z., Lacrampe-Couloume G. and Ballentine C.J. (2009) Solubility trapping in formation water as dominant CO2 sink in natural gas fields. *Nature* **458**, 614-618.

Haluszczak L.O., Rose A.W. and Kump L.R. (2013) Geochemical evaluation of flowback brine from Marcellus gas wells in Pennsylvania, USA. *App. Geochem.* **28**, 55-61.

Harkness J.S., Dwyer G.S., Warner N.R., Parker K.M., Mitch W.A. and Vengosh A. (2015) Iodide, bromide, and ammonium in hydraulic fracturing and oil and gas wastewaters: Environmental implications. *Environ. Sci. Tech* **49**, 1955-1963.

Heaton T.H.E. and Vogel J.C. (1981) Excess air in groundwater. *J. of Hydrol.* **50**, 201-216.

Heilweil V.M., Grieve P.L., Hynek S.A., Brantley S.L., Solomon D.K. and Risser D.W. (2015) Stream measurements locate thermogenic methane fluxes in groundwater discharge in an area of shale-gas development. *Environ. Sci. Tech.* **49**, 4057-4065.

Hennen R.V., 1912. Doddridge and Harrison counties. WVGES, Wheeling News Litho. Co. Wheeling, WV.

Holocher J., Peeters F., Aeschbach-Hertig W., Hofer M., Brennwald M., Kinzelbach W. and Kipfer R. (2002) Experimental investigations of the formation of excess air in quasi-saturated porous media. *Geochim. Cosmochim. Acta* **66**, 4103-4117.

Holocher J., Peeters F., Aeschbach-Hertig W., Kinzelbach W. and Kipfer R. (2003) Kinetic model of gas bubble dissolution in groundwater and its implications for the dissolved gas composition. *Environ. Sci. Tech.* **37**, 1337-1343.

Hunt A.G., Darrah T.H. and Poreda R.J. (2012) Determining the source and genetic fingerprint of natural gases using noble gas geochemistry: A northern Appalachian Basin case study. *AAPG Bull.* **96**, 1785-1811.

Isotech. (2011) Collection of groundwater samples from domestic and municipal water wells for dissolved gas analysis, in: Isotech Laboratories, Chicago, IL.

Jackson R.B., Vengosh A., Darrah T.H., Warner N.R., Down A., Poreda R.J., Osborn S.G., Zhao K.G. and Karr J.D. (2013) Increased stray gas abundance in a subset of drinking water wells near Marcellus shale gas extraction. *PNAS* **110**, 11250-11255.

Jackson R.B., Vengosh A., Carey J.W., Davies R.J., Darrah T.H., O'Sullivan F. and Pétron G. (2014) The environmental costs and benefits of fracking. *Annu. Rev. Env. Resour.* **39**, 327-362.

Kampbell D.H. and Vandegrift S.A. (1998) Analysis of dissolved methane, ethane, and ethylene in ground water by a standard gas chromatographic technique. *J. Chromatogr. Sc.* **36**, 253-256.

Kang, M., Christian, S., Celia, M.A., Mauzerall, D.L., Bill, M., Miller, A.R., Chen, Y., Conrad, M.E., Darrah. T.H., and Jackson, R.B., (2016) Identification and characterization of high methane-emitting abanddoned oil and gas wells. *PNAS* **113**, 13636-13641.

Kessler J.D., Reeburgh W.S. and Tyler S.C. (2006) Controls on methane concentration and stable isotope (delta H-2-CH4 and delta C-13-CH4) distributions in the water columns of the Black Sea and Cariaco Basin. *Global Biogeochem.l Cy.* **20**, 366-

375.
Lauer N.E., Harkness J.S. and Vengosh A. (2016) Brine Spills Associated with Unconventional Oil Development in North Dakota. *Environ. Sci. Tech.* **50**, 5389-5397.
Lautz L.K., Hoke G.D., Lu Z., Siegel D.I., Christian K., Kessler J.D. and Teale N.G. (2014) Using discriminant analysis to determine sources of salinity in shallow groundwater prior to hydraulic fracturing. *Environ. Sci. Tech.* **48**, 9061-9069.
Lindsey B.D., Falls W.F., Ferrari M.J., Zimmerman T.M., Harned D.A., Sadorf E.M. and Chapman M.J. (2006) Factors affecting occurrence and distribution of selected contaminants in ground water from selected areas in the Piedmont Aquifer System, eastern United States, 1993-2003. USGS, Washington, DC.
Llewellyn G.T. (2014) Evidence and mechanisms for Appalachian Basin brine migration into shallow aquifers in NE Pennsylvania, U.S.A. *Hydrogeol. J.* **22**, 1055-1066.
Martin W.D. (1998) Geology of the Dunkard Group (Upper Pennsylvanian-Lower Permian) in Ohio, West Virignia, and Pennsylvania Bulletin 73, Columbus, OH, p. 49.
Milici R.C. and de Witt Jr W. (1988) The Appalachian Basin. *The Geology of North America* **2**, 427-469.
Millot R., Guerrot C. and Vigier N. (2004) Accurate and High‐Precision Measurement of Lithium Isotopes in Two Reference Materials by MC‐ICP‐MS. *Geostand. Geoanal. Res.* **28**, 153-159.
Molofsky L.J., Connor J.A., Wylie A.S., Wagner T. and Farhat S.K. (2013) Evaluation of Methane Sources in Groundwater in Northeastern Pennsylvania. *Ground Water* **51**, 333-349.
Moritz A., Helie J.F., Pinti D.L., Larocque M., Barnetche D., Retailleau S., Lefebvre R. and Gelinas Y. (2015) Methane Baseline Concentrations and Sources in Shallow Aquifers from the Shale Gas-Prone Region of the St. Lawrence Lowlands (Quebec, Canada). *Environ. Sci. Tech.* **49**, 4765-4771.
Osborn S.G., Vengosh A., Warner N.R. and Jackson R.B. (2011) Methane contamination of drinking water accompanying gas-well drilling and hydraulic fracturing. *PNAS* **108**, 8172-8176.
Phan T.T., Capo R.C., Stewart B.W., Macpherson G.L., Rowan E.L. and Hammack R.W. (2016) Factors controlling Li concentration and isotopic composition in formation waters and host rocks of Marcellus Shale, Appalachian Basin. *Chem. Geol.* **420**, 162-179.
Revesz K.M., Breen K.J., Baldassare A.J. and Burruss R.C. (2010) Carbon and hydrogen isotopic evidence for the origin of combustible gases in water-supply wells in north-central Pennsylvania. *App. Geochem.* **25**, 1845-1859.
Rice D.D. and Claypool G.E. (1981) Generation, accumulation, and resource potential of biogenic gas *AAPG Bull.* **65**, 5-25.
Rowe D. and Muehlenbachs K. (1999) Isotopic fingerprints of shallow gases in the Western Canadian Sedimentary Basin: Tools for remediation of leaking heavy oil wells. *Org. Geochem.* **30**, 861-871.
Ruhl L.S., Dwyer G.S., Hsu-Kim H., Hower J.C.and Vengosh A. (2014) Boron and strontium isotopic characterization of coal combustion residuals: validation of new environmental tracers. *Environ. Sci. Tech.* **48**, 14790-14798.

Ryder R.T., Trippi M.H., Swezey C.S., Crangle Jr R.D., Hope R.S., Rowan E.L. and Lentz E.E. (2012) Geologic Cross Section CC'Through the Appalachian Basin from Erie County, North-central Ohio, to the Valley and Ridge Province, Bedford County, South-central Pennsylvania. USGS, Washington, DC.

Schedl A., McCabe C., Montanez I.P., Fullagar P.D. and Valley J.W. (1992) Alleghenian regional diagenesis: A response to the migration of modified metamorphic fluids derived from beneath the Blue Ridge-Piedmont thrust sheet. *J. Geol.*, 339-352.

Schoell M. (1980) The hydrogen and carbon isotopic composition of methane from natural gases of various origins. *Geochim. Cosmochim. Acta* **44**, 649-661.

Schoell M. (1983) Genetic characterization of natural gases. *AAPG Bull.* **67**, 2225-2238.

Schoell M. (1988) Multiple origins of methane in the earth *Chem. Geol.***71**, 1-10.

Schon S.C. (2011) Hydraulic fracturing not responsible for methane migration. *PNAS* **108**, E664-E664.

Sharma S. and Baggett J.K. (2011) Application of carbon isotopes to detect seepage out of coalbed natural gas produced water impoundments. *App Geochem.* **26**, 1423-1432.

Sharma S., Mulder M.L., Sack A., Schroeder K.and Hammack R. (2014) Isotope approach to assess hydrologic connections during Marcellus Shale drilling. *Ground Water* **52**, 424-433.

Sherwood O.W., Rogers, J.D., Lackey G., Burke T.L., Osborn S.G., Ryan J.N. (2016) Groundwater methane in relation to oil and gas development and shallow coal seams in the Denver-Julesburg Basin of Colorado. *PNAS* 113(30), 8391-8396.

Shultz R. (1984). Ground-Water Hydrology of the Minor Tributary Basins of the Ohio River, West Virginia, prepared in cooperation with the West Virginia Department of Natural Resources Publication X-WVDNR-6. U.S. Geological Survey, Washington, DC.

Siegel D.I., Azzolina N.A., Smith B.J., Perry A.E. and Bothun R.L. (2015a) Methane Concentrations in Water Wells Unrelated to Proximity to Existing Oil and Gas Wells in Northeastern Pennsylvania. *Environ. Sci. Tech.* **49**, 4106-4112.

Siegel D.I., Smith B., Perry E., Bothun R. and Hollingsworth M. (2015b) Pre-drilling water-quality data of groundwater prior to shale gas drilling in the Appalachian Basin: Analysis of the Chesapeake Energy Corporation dataset. *App. Geochem.* **63**, 37-57.

Solomon D.K., Poreda R.J., Schiff S.L. and Cherry J.A. (1992) Tritium and He-3 as groundwater age tracers in the Borden aquifer. *Water Resour. Res.* **28**, 741-755.

Solomon D.K., Poreda R.J., Cook P.G. and Hunt A. (1995) Site characterization using H-3/He-3 groundwater ages, Cape Cod, MA. *Ground Water* **33**, 988-996.

Solomon D.K., Hunt A. and Poreda R.J. (1996) Source of radiogenic helium 4 in shallow aquifers: Implications for dating young groundwater. *Water Resour. Res.* **32**, 1805-1813.

Spivack A.J. and Edmond J.M. (1987) Boron isotope exchange between seawater and the oceanic crust. *Geochim. Cosmochim. Acta* **51**, 1033-1043.

Spivak-Birndorf L.J., Stewart B.W., Capo R.C., Chapman E.C., Schroeder K.T. and Brubaker T.M. (2012) Strontium isotope study of coal utilization by-products interacting with environmental waters. *J. Environ. Qual.* **41**, 144-154.

US Energy Information Association. (2014) *Annual Energy Outlook 2014*. U.S.

Department of Energy, Washington, DC.
US Geological Survey. (2011) *National field manual for the collection of water-quality data*. USGS, Washington, D.C.
Vengosh A., Lindberg T.T., Merola B.R., Ruhl L., Warner N.R., White A., Dwyer G.S. and Di Giulio R.T. (2013) Isotopic imprints of mountaintop mining contaminants. *Environ. Sci. Tech.* **47**, 10041-10048.
Vengosh A. (2014) Salinization and Saline Environments. In *Treatise on Geochemistry Second Edition* (eds. H.D. Holland and K.K. Turekian) Elsevier, Oxford. pp. 325-378.
Vengosh A., Jackson R.B., Warner N., Darrah T.H. and Kondash A. (2014) A critical review of the risks to water resources from unconventional shale gas development and hydraulic fracturing in the United States *Environ. Sci. Tech.* **48**, 8334-8348.
Wanty R.B. and Kharaka Y.K., 1997. USGS Research on Saline Waters Co-Produced with Energy Resources. US Geological Survey.
Warner N.R., Jackson R.B., Darrah T.H., Osborn S.G., Down A., Zhao K.G., White A. and Vengosh A. (2012) Geochemical evidence for possible natural migration of Marcellus Formation brine to shallow aquifers in Pennsylvania. *PNAS* **109**, 11961-11966.
Warner N.R., Christie C.A., Jackson R.B. and Vengosh A. (2013a) Impacts of shale gas wastewater disposal on water quality in Western Pennsylvania. *Environ. Sci. Tech.* **47**, 11849–11857
Warner N.R., Kresse T.M., Hays P.D., Down A., Karr J.D., Jackson R.B. and Vengosh A. (2013b) Geochemical and isotopic variations in shallow groundwater in areas of the Fayetteville Shale development, north-central Arkansas. *App. Geochem.* **35**, 207-220.

Warner N.R., Darrah T.H., Jackson R.B., Millot R., Kloppmann W. and Vengosh A. (2014) New tracers identify hydraulic fracturing fluids and accidental releases from oil and gas operations. *Environ. Sci. Tech.* **48**, 12552-12560.
Weiss R. (1971a) Effect of salinity on the solubility of argon in water and seawater. *Deep-Sea Res.* **17**, 721.
Weiss R. (1971b) Solubility of helium and neon in water and seawater. *J. Chem. Eng. Data* **16**, 235.
White J.S. and Mathes M.V. (2006) Dissolved-gas concentrations in ground water in West Virginia, 1997-2005. USGS Numbered Series 156.
Whiticar M.J., Faber E. and Schoell M. (1985) Hydrogen and carbon isotopes of C-1 to C-5 alkanes in natural gases. *AAPG Bull.* **69**, 316-316.
Whiticar M.J. and Faber E. (1986) Methane oxidation in sediment and water column environments—isotope evidence. *Org. Geochem.* **10**, 759-768.
Whiticar MR, Faber E, Whelan JK, and Simoneit BRT (1994) Thermogenic and bacterial hydrocarbon gases (Free and sorbed) in Middle Valley, Juan De Fuca Ridge, LEG 139 Proceedings of the Ocean Drilling Program, Scientific Results, **139**, 467-477.
Wunsch D.R. (1992) Ground-water geochemistry and its relationship to the flow system at an unmined site in the eastern Kentucky coal field. Kentucky Geological Survey Thesis Series 5.
WVGES, 2012. WVGES References about Devonian Shales.
Wyrick G.G. and Borchers J.W. (1981). Hydrologic effects of stress-relief fracturing in

an Appalachian valley. USGS Water Supply Paper 2177.
Zhou Z. and Ballentine C.J. (2006) He-4 dating of groundwater associated with hydrocarbon reservoirs. *Chem. Geol.* **226**, 309-327.
Ziemkiewicz P.F. and He Y.T. (2015) Evolution of water chemistry during Marcellus Shale gas development: A case study in West Virginia. *Chemosphere* **134**, 224-231

Tables

Table 1. Major chemistry for groundwater samples. All ratios are in molar units. Blank entries indicate no analysis for that constituent.

Sample ID[b]	Type	Co.[a]	Distance to well (m)	Cl (mg/L)	Br/Cl ($x10^{-3}$)	Na/Cl ($x10^{-3}$)	DIC (mg/L)	^{13}C-DIC (‰)	Ba (mg/L)	As (ppb)	Sr/Cl ($x10^{-3}$)	$^{87}Sr/^{86}Sr$	B/Cl ($x10^{-3}$)	δ^{11}B (‰)	Li/Cl ($x10^{-3}$)	δ^{7}Li (‰)
WV-1a	1	DD	3104	3		49.0	289	-16.50	0.17	6.95	31.7		86.4		10.5	
WV-1b	1	DD	3104	3		48.5	278		0.31	6.27	48.5		76.1		11.3	
WV-2a	1	DD	1485	1		39.1	146		0.19	28.45	56.2		47.6		9.2	
WV-2b	1	DD	1485	2		26.3	143		0.19	26.76	36.3		27.6		5.4	16
WV-3a	1	DD	1951	2		41.4	253	-14.54	0.33	20.69	49.9		35.9		11.3	
WV-3b	1	DD	1951	3		44.5	250		0.37	24.86	54.6		24.3		9.3	
WV-4	1	DD	513	3		13.1	193	-15.74	0.69	5.67	61.3		22.6		8.2	
WV-5	1	DD	513	9		2.8	167	-14.92	0.74	9.59	21.8		5.2		1.9	
WV-6	1	DD	1937	1		25.8	195	-15.61	0.50	15.50	130.8		61.4		21.6	
WV-7	1	DD	1944	1		4.8	42	-15.90	0.05	0.07	46.0		164		1.8	
WV-8a	1	DD	599	3		27.3	229	-11.85	0.46	2.46	96.7		50.1		17.6	
WV-8b	1	DD	599	12		20.9	504	-15.21	0.05	11.59	1.3		48.9		3.2	
WV-8c	1	DD	599	3		31.1	227		0.44	1.85	73.3		36.6		12.6	
WV-10a	1	DD	939	21		6.6	172	-16.93	0.25	7.45	4.5		12.2		2.0	
WV-10b	1	DD	939	11		48	836	-15.90	0.06	6.59	4.2		51.5		6.3	
WV-10c	1	DD	939	20		10	292	-18.4	0.25	8.25	4.7	0.7130	12.6		2.1	18
WV-11	1	DD	488	5		13.0	174	-15.44	0.43	8.27	24.3		23.8		6.2	
WV-11b	1	DD	488	5		7.1	145		0.41	6.25	24.0		14.1		4.9	
WV-11c	1	DD	488	4		15.3	161		0.39	6.42	32.2		20.7		6.8	
WV-12	1	DD	491	5		13.9	174		0.42	7.82	26.0		26.7		6.8	
WV-21	1	DD	1032	23		6.5	298	-19.88	0.37	0.71	4.9		12.2		2.2	
WV-22	1	DD	69	8		11.5	228	-20.17	0.00	1.02	31.0		24.1		6.3	
WV-25	2	DD		51	1.8	4.2	344	-17.29	0.52	2.33	5.5	0.7126	7.2	20	1.1	18
WV-27a	1	DD	752	20		13.7	446	-14.27	0.09	0.54	1.9		16.3		1.9	
WV-27b	1	DD	752	25		11.8	471	-13.3	0.13	0.63	1.6	0.7130	12.4		1.4	19
WV-29a	2	DD	1420	53	1.6	0.3	374	-15.38	0.02	6.49	<0.1		7.3		0.1	
WV-29b	1	DD	1421	32		0.1	323.93		0.02	4.53	<0.1		8.6		<0.1	
WV-29c	1	DD	1420	45		6.9	396	-14.9	0.00	3.86	0.0		8.0		0.8	20
WV-31a	1	DD	893	5		19.9	219	-15.92	0.64	0.03	47.4		44.7		11	
WV-31b	1	DD	893	5		21.0	172		0.53	0.04	50.3		48.9		11.9	
WV-32a	1	DD	1576	1		6.6	65	-19.08	0.18	0.33	47.4		67.1		8.2	
WV-32b	1	DD	1576	1		6.2	62		0.14	0.25	39.1		30.6		6.1	
WV-33	1	DD	542	1		40.9	319	-17.73	0.66	7.31	206.6		116		26.1	
WV-36a	2	DD	757	159	1.7	6.6	619	-4.27	0.28	11.82	1.6	0.7128	3.9	26	0.9	20
WV-36b	3	DD	757	58	3.1	1.0	322	-8.5	0.55	13.26	3.0	0.7129	2.3		0.1	
WV-36c	2	DD	757	696	1.9	1.3	632		0.00	7.73	0.3	0.7128	0.8	25	0.2	20
WV-37a	2	DD	1126	793	1.7	0.1			0.53	0.00	0.3		0.3		0.1	
WV-37b	2	DD	1126	83	2.5	3.4	328	-17.8	0.00	0.35	0.4	0.7128	3.9		0.7	20
WV-38a	2	DD	1677	110	2.2	2.4	312	-14.94	0.50	3.62	1.3		3.5	23	1.0	
WV-38b	3	DD	1677	660	3.3	1.0	323	-14.7	0.33	3.33	0.2	0.7128	0.7		0.2	18
WV-39a	1	DD	1085	32		6.8	378.23	-18.39	0.14	10.55	2.8	0.7129	6.0	16	0.7	15
WV-39b	1	DD	1085	32		2.9	373.00	-14.2	0.57	10.80	11.7	0.7129	5.8	13	1.9	15
WV-39c	1	DD	1085	42		3.2	172.00		0.57	7.20	8.8		4.2		1.2	
WV-40a	1	DD	1351	29		5.7	338	-17.22	0.38	0.67	10.6	0.7129	9.6	17	1.7	17
WV-40b	1	DD	1351	19		<0.1	334		0.24	0.53	16.1		14.3		2.3	
WV-40c	1	DD	1351	20		7.5	340	-16.9	0.32	0.60	16.1	0.7129	14.0		2.4	18
WV-41a	1	DD	938	4		5.0	245	-18.62	0.68	1.05	72.7		16.7	18	3.8	
WV-41b	1	DD	938	5		6.5	235		0.82	1.26	75.7		21.9		4.2	
WV-51a	3	DD	212	347	7.6	0.4	203	-14.7	2.08	37.26	1.7	0.7128	0.5		0.2	13
WV-51b	3	DD	212	172	3.6	0.8	230	-18.0	0.91	41.79	2.0	0.7128	1.0		0.3	
WV-52a	3	DD	61	540	3.9	1.5	448	-16.8	4.22	1.04	0.2	0.7127	1.2	20	0.2	20
WV-52b	2	DD	61	337	2.4	1.6	387	-17.1	0.00	2.54	0.2	0.7127	1.9	21	0.2	20
WV-53	1	DD	861	41		1.3	149.00	-14.3	0.38	3.16	3.0	0.7133	2.4		0.6	14
WV-54	1	DD	903	31		5.9	314.84	-17.3	0.11	18.93	1.2	0.7130	12.1	16	1.0	20
WV-55b	1	DD	1677	3		26.6	214		0.42	0.38	62.8		81.7		8.6	
WV-55c	1	DD	1677	4		17.6	216		0.33	0.71	38.4		38.8		4.0	
WV-56	1	DD	2133	38		3.6	240.02	-17.9	0.40	1.65	3.6	0.7129	8.9	14	0.8	18
WV-57	1	DD	2133	6		14.8	210		0.35	2.04	20.2		39.7		3.9	
WV-58a	3	DD	2167	773	8.7	1.0	252	-5.3	2.74	0.62	1.4	0.7132	0.5	18	0.2	16
WV-58b	3	DD	2167	900	3.7	0.9	258	-8.7	3.39	2.30	1.2	0.7132	0.4	22	0.2	
WV-59	2	DD	2133	80	2.2	4.8	480	-12.7	0.08	3.71	0.3	0.7129	7.1	19	0.4	20
WV-60b	1	DD	2165	28		5.6	282	-19.7	0.05	4.90	0.4		13.0	17	0.7	21
WV-60c	1	DD	2165	29		7.4	298	-21.5	0.00	3.71	0.4		14.7		0.7	21
WV-61	1	DD	2222	30		2.4	193.84	-16.4	0.57	14.62	6.8	0.7121	6.6		1.0	18
WV-62b	1	DD	2107	17		4.2	191		0.58	6.82	9.8		10.0		1.4	
WV-62c	1	DD	2107	13		7.1	168		0.47	6.06	9.8		11.2		1.4	
WV-63	1	DD	2088	21		3.3	199		0.68	6.77	11.7		7.1		1.6	
WV-64a	3	DD	2258	383	4.2	1.2	251	-19.0	1.09	1.10	1.2	0.7130	1.4		0.2	18
WV-64b	3	DD	2258	509	3.4	1.2		-20.4	1.98	26.21	1.6	0.7130	0.9	18	0.2	18
WV-65	1	DD	1533	15		4.1	195		0.42	1.87	10.8		7.8		2.0	
WV-66b	1	DD	495	3		5.1	128		0.08	1.10	27.7		6.1		10.3	
WV-66c	1	DD	495	5		3.4	148		0.10	0.24	21.1		4.2		8.0	
WV-101b	2	DD	744	88	0.5	2.5	277		0.24	1.84	1.1	0.7129	2.8		0.4	21
WV-101c	2	DD	744	80	0.2	2.6	287	-18.8	0.18	2.19	1.2	0.7129	3.5		0.4	21
WV-102	1	DD	737	8		3.8	204		0.50	3.41	18.5		10.1		2.7	

WV-103	1	DD	737	11		10.8	191		0.02	6.57	<0.1		7.4		0.2 10.4	
WV-104	1	DD	1514	2		36.5	221		0.66	1.99	58.6		84.2			
WV-105	1	DD	813	9		16.0	260		0.29	0.03	8.2		33.5		5.0	
WV-106	1	H	1011	2		39.6	313		0.42	1.66	178.4		47.9		16.2	
WV-107	1	DD	2107	3		4.9	181		0.64	0.44	209.0		52.0		11.6	
WV-108b	1	DD	755	4		14.8	221		0.17	1.22	73.0		35.9		9.8	
WV-108c	1	DD	723	3		24.8	246		0.21	1.11	83.9		36.8		10.7	
WV-109b	1	DD	929	4		14.6	232		0.78	0.00	71.0		33.4		10.5	
WV-109c	1	DD	929	3		30.0	238		0.77	0.00	96.7		46.8		13.9	
WV-110	1	T	526	2		3.9	74		0.10	1.05	28.3		36.6		0.7	
WV-111	1	T	503	3		24.5	199		0.11	7.92	26.6		50.9		3.9	
WV-112	1	DD	1223	2		20.4	201		0.52	4.82	120.7		28.0		15.8	
WV-113	1	DD	1265	8		0.9	118		0.21	0.26	5.6		2.4		7.5	
WV-116b	2	DD	5180	79	2.5	3.1	350		0.07	9.86	0.2		3.6		0.5	20
WV-116c	2	DD	5180	73	2.1	4.4	370	-18.5	0.04	12.10	0.2	0.7130	4.4	17	0.6	19
WV-117	1	DD	378	12		1.3	92		0.55	4.01	8.9		8.2		0.9	
WV-300	1	DD	1658	1		47.1	279		0.31	0.12	414.0		280		45.3	
WV-301b	1	DD	650	28		4.7	236	-13.1	0.57	9.48	8.8	0.7128	10.3		2.0	14
WV-301c	1	DD	650	48		3.2	249.00	-15.2	0.35	19.39	2.9	0.7128	6.7		0.9	17
WV-302b	1	DD	516	27		2.8	177	-18.1	0.59	19.18	7.2	0.7128	4.5		1.2	14
WV-302c	1	DD	516	2		28.0	169		0.47	22.83	61.1	0.7128	42.7		12.3	14
WV-303b	1	DD	552	14		3.9	154		0.45	12.96	14.3		10.1		2.8	
WV-303c	1	DD	552	18		3.0	160		0.46	9.84	10.5		5.0		2.0	
WV-304	1	DD	457	7		9.7	193		0.95	3.47	56.3		16.8		4.2	
WV-305	1	DD	542	<1		159.7	154		0.39	10.71	481.5		461		90.2	
WV-306	1	DD	542	<1		5.4	361		0.04	0.14	18.7		90.2	23	3.1	
WV-308	1	DD	1701	1		57.6	194		0.67	0.59	393.3		107		41.2	
WV-309	1	DD	1932	14		4.0	305		0.26	0.10	4.8		28.4		2.3	
WV-311	1	DD	1587	<1		169.8	161		0.75	1.39	1355		576		103.9	
WV-312	1	DD	1408	<1		47.1	186		0.33	0.04	586.0		223		56.5	
WV-313	2	DD	906	59	1.8	1.9	334		0.09	1.27	0.4	0.7127	12.6	16	0.8	20
WV-314b	2	H	389	2366	2.2	0.3	161	-14.4	0.77	4.39	0.5	0.7129	0.2	20	0.2	19
WV-314c	2	H	389	2232	1.8	0.9	492	-14.8	2.88	3.69	0.5	0.7129	0.2	17	0.2	19
WV-315	1	DD	2125	1		47.7	424		0.18	2.81	129.3		65.6		18.4	
WV-316	1	DD	2196	9		27.0	483		0.01	4.69	2.3		52.1		4.7	
WV-317	2	DD	2336	54	1.8	5.0	361	-14.8	0.02	4.92	1.2	0.7125	9.2	19	1.1	20
WV-318	1	DD	1114	1		8.0	56		0.04	0.00	30.5		40.4		3.3	
WV-319	1	DD	1117	<1		38.9	132		0.10	0.18	301.8		216		28.8	
WV-320	1	DD	912	2		73.1	246		0.00	16.83	<0.1		92.2		0.1	
WV-321	1	DD	830	5		3.7	261		0.39	0.44	85.6		17.3		20.8	
WV-322	1	DD	744	3		4.3	214		0.00	6.82	0.6		12.3		4.3	
WV-323	1	H	1025	47		2.3	252.00	-16.8	0.19	0.79	9.2	0.7133	2.7	13	1.1	16
WV-324b	1	H	964	24		2.3	188	-17.1	0.43	0.30	7.4	0.7131	3.8		1.4	15
WV-324c	1	H	964	37		0.8	182	-19.3	0.44	0.34	4.7		1.8		0.8	
WV-325	1	H	834	3		15.4	221		0.38	9.90	37.9		33.4		8.1	
WV-326	1	H	467	3		10.8			0.26	0.42	68.8		32.4		5.4	
WV-327	1	R	765	6		12.8	290		0.67	1.12	91.1		60.9		11.4	
WV-329	1	R	925	3		18.2	239		1.13	4.85	181.7		86.0		15.6	
WV-400	1	T	261	3		4.9	114		0.10	0.17	29.1		45.4		3.3	
WV-401	1	T	874	2		62.3	287	-18.4	0.12	0.17	84.5		134		14.3	
WV-412	1	DD	141	26		8.3	322	-16.2	0.00	0.28	<0.1		8.3		0.1	
WV-414	1	DD	912	6		22.6	246		0.21	0.43	20.9		35.0		5.3	
WV-417	1	DD	1177	21		12.3	400	-15.2	0.24	2.45	8.9	0.7127	20.1		2.5	
WV-427	1	R	615	5		22.9	337	-19.7	0.92	27.89	92.5		34.0		8.8	
WV-428	1	R	402	7		33.8	248	-18.9	0.22	15.58	10.7		64.9		5.4	
WV-429	1	DD	277	1		131.3	256	-20.6	0.10	3.50	25.1		273		25.1	
WV-435	1	H	184	3		<0.1	218		0.39	1.60	78.6		23.9		10.9	
WV-501	1	W	521	5		5.8	239		0.38	2.60	21.1		52.2		4.8	
WV-502	1	W	772	17		2.6	159		0.25	0.31	9.3		7.2		0.6	
WV-503	3	W	675	159	3.1	0.9	145	-19.6	1.41	15.70	1.8	0.7129	0.6		0.2	16
WV-504	1	T	478	5		5.3	193		0.24	2.58	34.7		23.8		4.5	
WV-505	1	DD	1806	5		38.0	328	-11.2	0.00	0.47	15.6		77.0		7.9	
WV-511	1	H	334	2		10.9	206		0.45	0.71	98.3		34.0		13.0	
WV-512	1	H	393	28		1.3	262	-19.5	0.80	3.01	11.3		2.3		0.8	
WV-514	1	H	840	6		1.9	340	-17.9	0.02	0.00	27.5		14.4		7.9	
WV-515	1	DD	1161	37		5.7	330.00	-21.2	0.52	1.37	7.4	0.7128	5.8		1.3	16
WV-516	1	DD	847	22		3.4	239	-21.4	0.79	8.13	14.1	0.7129	6.7		1.7	11
WV-517	1	DD	883	21		11.4	289	-18.0	0.09	0.00	1.9	0.7126	14.6	15	2.9	20
WV-519	1	DD	1397	20		1.9	224	-16.7	0.15	0.00	18.1		6.8		2.8	
WV-602	1	R		1		113.0	311		0.32	10.72	99.0		155		33.8	

[a]Timeline samples are labeled alphabetically (a = pre-drill, b or c are consecutive samples post-drill).
[b]County: DD=Doddridge, H=Harrison, R=Ritchie, T=Tyler, W=Wetzel

Table 2. Dissolved hydrocarbon gas chemistry for groundwater samples. Blank entries indicate no analysis for that constituent.

Sample ID*	[CH_4] (ccSTP/L)	[C_2H_6] (ccSTP/L)	[C_3H_8] (ccSTP/L)	[i-C_4H_{10}] (ccSTP/L)	[n-C_4H_{10}] (ccSTP/L)	[i-C_5H_{12}] (ccSTP/L)	[n-C_5H_{12}] (ccSTP/L)	C_1/C_2+	$\delta^{13}C$-CH_4 (‰)	$\delta^{13}C$-C_2H_6 (‰)
WV-1a	0.34	2.81E-05	b.d.l.	b.d.l.	b.d.l.	b.d.l.	b.d.l.	12048	-70.90	
WV-1b	0.09	b.d.l.	b.d.l.	b.d.l.	b.d.l.	b.d.l.	b.d.l.			
WV-2a	0.01	b.d.l.	b.d.l.	b.d.l.	b.d.l.	b.d.l.	b.d.l.			
WV-2b	0.00	b.d.l.	b.d.l.	b.d.l.	b.d.l.	b.d.l.	b.d.l.			
WV-3a	2.74	1.96E-04	b.d.l.	b.d.l.	b.d.l.	b.d.l.	b.d.l.	14025	-93.25	
WV-3b	15.33	1.22E-03	b.d.l.	b.d.l.	b.d.l.	b.d.l.	b.d.l.	12578	-91.14	-34.2
WV-4	0.13	1.04E-05	b.d.l.	b.d.l.	b.d.l.	b.d.l.	b.d.l.	12547	-70.03	
WV-5	0.04	b.d.l.	b.d.l.	b.d.l.	b.d.l.	b.d.l.	b.d.l.			
WV-6	0.59	3.70E-05	b.d.l.	b.d.l.	b.d.l.	b.d.l.	b.d.l.	16022	-87.56	
WV-7	0.00	b.d.l.	b.d.l.	b.d.l.	b.d.l.	b.d.l.	b.d.l.		-52.86	
WV-8a	0.02	b.d.l.	b.d.l.	b.d.l.	b.d.l.	b.d.l.	b.d.l.		-73.61	
WV-8b	0.15	1.71E-05	b.d.l.	b.d.l.	b.d.l.	b.d.l.	b.d.l.	8746	-59.55	
WV-8c	0.02	b.d.l.	b.d.l.	b.d.l.	b.d.l.	b.d.l.	b.d.l.		-70.15	
WV-10a	0.39	3.95E-05	b.d.l.	b.d.l.	b.d.l.	b.d.l.	b.d.l.	9767	-67.62	
WV-10b	0.07	6.24E-06	b.d.l.	b.d.l.	b.d.l.	b.d.l.	b.d.l.	11343	-64.19	
WV-10c	0.23	1.85E-05	b.d.l.	b.d.l.	b.d.l.	b.d.l.	b.d.l.	12146	-69.84	
WV-11a	0.37	3.54E-05	b.d.l.	b.d.l.	b.d.l.	b.d.l.	b.d.l.	10550	-95.40	
WV-11b	0.41	3.10E-05	b.d.l.	b.d.l.	b.d.l.	b.d.l.	b.d.l.	13065	-95.95	
WV-11c	0.19	1.44E-05	b.d.l.	b.d.l.	b.d.l.	b.d.l.	b.d.l.	13145	-77.55	
WV-12	0.28	2.81E-05	b.d.l.	b.d.l.	b.d.l.	b.d.l.	b.d.l.	9880	-95.40	
WV-21	2.48	2.24E-04	b.d.l.	b.d.l.	b.d.l.	b.d.l.	b.d.l.	11031	-50.59	
WV-22	0.97	1.69E-04	b.d.l.	b.d.l.	b.d.l.	b.d.l.	b.d.l.	5750	-35.06	
WV-25	0.08	b.d.l.	b.d.l.	b.d.l.	b.d.l.	b.d.l.	b.d.l.			
WV-27a	8.81	1.54E-03	3.45E-06	b.d.l.	b.d.l.	b.d.l.	b.d.l.	5703	-62.85	-35.6
WV-27b	7.81	1.27E-03	3.44E-05	b.d.l.	b.d.l.	b.d.l.	b.d.l.	5985	-61.89	-36.2
WV-29a	2.39	6.01E-04	b.d.l.	b.d.l.	b.d.l.	b.d.l.	b.d.l.	3968	-69.41	
WV-29b	0.92	b.d.l.	b.d.l.	b.d.l.	b.d.l.	b.d.l.	b.d.l.		-66.85	
WV-29c	2.36	4.75E-04	4.31E-06	b.d.l.	b.d.l.	b.d.l.	b.d.l.	4924	-59.36	
WV-31a	0.99	8.15E-05	b.d.l.	b.d.l.	b.d.l.	b.d.l.	b.d.l.	12145	-57.74	
WV-31b	1.35	b.d.l.	b.d.l.	b.d.l.	b.d.l.	b.d.l.	b.d.l.		-53.46	
WV-32a	0.02	b.d.l.	b.d.l.	b.d.l.	b.d.l.	b.d.l.	b.d.l.			
WV-32b	0.00	b.d.l.	b.d.l.	b.d.l.	b.d.l.	b.d.l.	b.d.l.		-40.43	
WV-33	0.37	b.d.l.	b.d.l.	b.d.l.	b.d.l.	b.d.l.	b.d.l.		-95.08	
WV-36a	27.99	1.42E-02	6.64E-05	b.d.l.	b.d.l.	b.d.l.	b.d.l.	1959	-64.35	-38.6
WV-36b	29.89	1.29E-02	6.65E-04	4.21E-07	3.85E-07	b.d.l.	b.d.l.	2201		-38.0
WV-36c	18.45	8.55E-03	1.65E-05	b.d.l.	b.d.l.	b.d.l.	b.d.l.	2154	-66.63	-38.6
WV-37a	4.44	9.82E-04	5.24E-07	b.d.l.	b.d.l.	b.d.l.	b.d.l.	4522	-67.36	
WV-37b	5.01	1.16E-03	5.98E-05	b.d.l.	b.d.l.	b.d.l.	b.d.l.	4114	-65.91	
WV-38a	13.41	5.27E-03	4.55E-05	b.d.l.	b.d.l.	b.d.l.	b.d.l.	2522	-65.07	-36.8
WV-38b	12.78	5.12E-03	9.56E-05	b.d.l.	b.d.l.	b.d.l.	b.d.l.	2453	-61.20	-38.2
WV-39a	0.00	b.d.l.	b.d.l.	b.d.l.	b.d.l.	b.d.l.	b.d.l.		-31.91	
WV-39b	0.02	b.d.l.	b.d.l.	b.d.l.	b.d.l.	b.d.l.	b.d.l.			
WV-39c	d.n.r.	d.n.r.	d.n.r.	d.n.r.	d.n.r.	d.n.r.	d.n.r.			
WV-40a	0.58	6.58E-05	b.d.l.	b.d.l.	b.d.l.	b.d.l.	b.d.l.	8765	-63.73	
WV-40b	3.15	2.87E-04	b.d.l.	b.d.l.	b.d.l.	b.d.l.	b.d.l.	10988		
WV-40c	1.62	1.64E-04	b.d.l.	b.d.l.	b.d.l.	b.d.l.	b.d.l.	9896		
WV-41a	0.00	b.d.l.	b.d.l.	b.d.l.	b.d.l.	b.d.l.	b.d.l.			
WV-41b	0.00	b.d.l.	b.d.l.	b.d.l.	b.d.l.	b.d.l.	b.d.l.		-67.46	
WV-51a	1.84	2.78E-04	1.46E-06	b.d.l.	b.d.l.	b.d.l.	b.d.l.	6580	-82.80	
WV-51b	1.37	1.84E-04	3.14E-07	b.d.l.	b.d.l.	b.d.l.	b.d.l.	7423	-86.41	
WV-52a	9.26	1.81E-03	1.36E-05	b.d.l.	b.d.l.	b.d.l.	b.d.l.	5086	-79.65	-37.0
WV-52b	6.66	1.38E-03	6.21E-05	b.d.l.	b.d.l.	b.d.l.	b.d.l.	4617	-76.90	
WV-53	0.03	b.d.l.	b.d.l.	b.d.l.	b.d.l.	b.d.l.	b.d.l.		-71.82	
WV-54	0.01	b.d.l.	b.d.l.	b.d.l.	b.d.l.	b.d.l.	b.d.l.		-59.05	
WV-55b	2.05	1.43E-04	b.d.l.	b.d.l.	b.d.l.	b.d.l.	b.d.l.	14326	-58.48	
WV-55c	0.01	4.82E-07	b.d.l.	b.d.l.	b.d.l.	b.d.l.	b.d.l.	12956		
WV-56	0.03	b.d.l.	b.d.l.	b.d.l.	b.d.l.	b.d.l.	b.d.l.			
WV-57	0.02	b.d.l.	b.d.l.	b.d.l.	b.d.l.	b.d.l.	b.d.l.		-19.23	
WV-58a	25.52	8.50E-03	2.01E-05	b.d.l.	b.d.l.	b.d.l.	b.d.l.	2995	-50.69	-37.1
WV-58b	28.82	9.22E-03	4.25E-06	b.d.l.	b.d.l.	b.d.l.	b.d.l.	3123	-47.89	-37.6
WV-59	8.45	1.41E-03	4.95E-06	b.d.l.	b.d.l.	b.d.l.	b.d.l.	5961	-67.77	
WV-60b	0.35	b.d.l.	b.d.l.	b.d.l.	b.d.l.	b.d.l.	b.d.l.		-57.67	
WV-60c	4.16	b.d.l.	b.d.l.	b.d.l.	b.d.l.	b.d.l.	b.d.l.		-60.28	
WV-61	2.28	3.48E-04	1.59E-06	b.d.l.	b.d.l.	b.d.l.	b.d.l.	6518	-49.33	-38.8
WV-62b	1.19	9.01E-05	b.d.l.	b.d.l.	b.d.l.	b.d.l.	b.d.l.	13258	-46.26	
WV-62c	0.64	b.d.l.	b.d.l.	b.d.l.	b.d.l.	b.d.l.	b.d.l.		-47.31	
WV-63	0.03	b.d.l.	b.d.l.	b.d.l.	b.d.l.	b.d.l.	b.d.l.			
WV-64a	2.05	4.43E-04	1.26E-06	b.d.l.	b.d.l.	b.d.l.	b.d.l.	4612	-78.70	
WV-64b	3.68	7.76E-04	7.35E-05	b.d.l.	b.d.l.	b.d.l.	b.d.l.	4326	-73.07	
WV-65	0.01	b.d.l.	b.d.l.	b.d.l.	b.d.l.	b.d.l.	b.d.l.		-28.24	
WV-66b	0.00	b.d.l.	b.d.l.	b.d.l.	b.d.l.	b.d.l.	b.d.l.		-65.11	
WV-66c	0.00	b.d.l.	b.d.l.	b.d.l.	b.d.l.	b.d.l.	b.d.l.		-72.46	
WV-101b	0.27	5.06E-05	b.d.l.	b.d.l.	b.d.l.	b.d.l.	b.d.l.	5365	-44.23	
WV-101c	0.24	3.68E-05	b.d.l.	b.d.l.	b.d.l.	b.d.l.	b.d.l.	6524	-47.59	
WV-102	0.16	b.d.l.	b.d.l.	b.d.l.	b.d.l.	b.d.l.	b.d.l.		-77.31	
WV-103	0.14	1.10E-05	b.d.l.	b.d.l.	b.d.l.	b.d.l.	b.d.l.	12625	-74.77	
WV-104	0.11	b.d.l.	b.d.l.	b.d.l.	b.d.l.	b.d.l.	b.d.l.		-73.18	
WV-105	5.72	3.63E-04	b.d.l.	b.d.l.	b.d.l.	b.d.l.	b.d.l.	15749	-78.45	-35.0
WV-106	0.04	b.d.l.	b.d.l.	b.d.l.	b.d.l.	b.d.l.	b.d.l.			
WV-107	0.00	b.d.l.	b.d.l.	b.d.l.	b.d.l.	b.d.l.	b.d.l.			
WV-108b	0.01	b.d.l.	b.d.l.	b.d.l.	b.d.l.	b.d.l.	b.d.l.		-50.26	
WV-108c	0.00	b.d.l.	b.d.l.	b.d.l.	b.d.l.	b.d.l.	b.d.l.			
WV-109b	0.07	b.d.l.	b.d.l.	b.d.l.	b.d.l.	b.d.l.	b.d.l.		-48.88	
WV-109c	0.01	b.d.l.	b.d.l.	b.d.l.	b.d.l.	b.d.l.	b.d.l.			
WV-110	0.04	b.d.l.	b.d.l.	b.d.l.	b.d.l.	b.d.l.	b.d.l.		-57.05	

WV-111	0.04	b.d.l.	b.d.l.	b.d.l.	b.d.l.	b.d.l.	b.d.l.		-71.44	
WV-112	0.01	b.d.l.	b.d.l.	b.d.l.	b.d.l.	b.d.l.	b.d.l.			
WV-113	0.06	b.d.l.	b.d.l.	b.d.l.	b.d.l.	b.d.l.	b.d.l.			
WV-116b	0.96	3.20E-04	6.16E-06	b.d.l.	b.d.l.	b.d.l.	b.d.l.	2932	-58.38	
WV-116c	0.65	1.99E-04	b.d.l.	b.d.l.	b.d.l.	b.d.l.	b.d.l.	3257	-55.76	
WV-117	0.07	b.d.l.	b.d.l.	b.d.l.	b.d.l.	b.d.l.	b.d.l.		-91.36	
WV-300	0.00	b.d.l.	b.d.l.	b.d.l.	b.d.l.	b.d.l.	b.d.l.			
WV-301b										
WV-301c	6.66	4.92E-04	7.47E-07	b.d.l.	b.d.l.	b.d.l.	b.d.l.	13527	-69.11	
WV-302b	2.02	b.d.l.	b.d.l.	b.d.l.	b.d.l.	b.d.l.	b.d.l.			
WV-302c	0.02	b.d.l.	b.d.l.	b.d.l.	b.d.l.	b.d.l.	b.d.l.			
WV-303b	1.05	1.17E-04	b.d.l.	b.d.l.	b.d.l.	b.d.l.	b.d.l.	8975		
WV-303c	0.24	2.52E-05	b.d.l.	b.d.l.	b.d.l.	b.d.l.	b.d.l.	9357		
WV-304	2.65	2.80E-04	b.d.l.	b.d.l.	b.d.l.	b.d.l.	b.d.l.	9457		
WV-305	4.37	b.d.l.	b.d.l.	b.d.l.	b.d.l.	b.d.l.	b.d.l.			
WV-306	0.02	b.d.l.	b.d.l.	b.d.l.	b.d.l.	b.d.l.	b.d.l.			
WV-308	2.24	2.33E-04	b.d.l.	b.d.l.	b.d.l.	b.d.l.	b.d.l.	9645		
WV-309	2.14	2.17E-04	b.d.l.	b.d.l.	b.d.l.	b.d.l.	b.d.l.	9845		
WV-311	0.04	b.d.l.	b.d.l.	b.d.l.	b.d.l.	b.d.l.	b.d.l.			
WV-312	0.22	b.d.l.	b.d.l.	b.d.l.	b.d.l.	b.d.l.	b.d.l.			
WV-313	7.41	5.99E-03	2.34E-05	b.d.l.	b.d.l.	b.d.l.	b.d.l.	1232		
WV-314b	36.87	3.70E-02	1.42E-04	2.68E-06	2.24E-06	4.65E-07	4.32E-07	992		-39.0
WV-314c	21.46	1.95E-02	9.55E-05	5.55E-07	6.21E-07	b.d.l.	b.d.l.	1097	-69.45	-38.3
WV-315	0.03	b.d.l.	b.d.l.	b.d.l.	b.d.l.	b.d.l.	b.d.l.			
WV-316	6.85	7.16E-04	b.d.l.	b.d.l.	b.d.l.	b.d.l.	b.d.l.	9568		-35.1
WV-317	9.16	9.28E-03	7.95E-05	b.d.l.	b.d.l.	b.d.l.	b.d.l.	979		
WV-318	0.03	b.d.l.	b.d.l.	b.d.l.	b.d.l.	b.d.l.	b.d.l.			
WV-319	0.03	b.d.l.	b.d.l.	b.d.l.	b.d.l.	b.d.l.	b.d.l.			
WV-320	2.14	2.20E-04	b.d.l.	b.d.l.	b.d.l.	b.d.l.	b.d.l.	9752		
WV-321	1.87	1.38E-04	b.d.l.	b.d.l.	b.d.l.	b.d.l.	b.d.l.	13615		
WV-322	0.09	b.d.l.	b.d.l.	b.d.l.	b.d.l.	b.d.l.	b.d.l.			
WV-323	5.20	2.05E-03	5.68E-07	b.d.l.	b.d.l.	b.d.l.	b.d.l.	2540		
WV-324b	1.65	1.90E-04	b.d.l.	b.d.l.	b.d.l.	b.d.l.	b.d.l.	8714		
WV-324c	0.03	b.d.l.	b.d.l.	b.d.l.	b.d.l.	b.d.l.	b.d.l.		-40.38	
WV-325	0.57	4.91E-05	b.d.l.	b.d.l.	b.d.l.	b.d.l.	b.d.l.	11548		
WV-326	2.36	3.59E-04	b.d.l.	b.d.l.	b.d.l.	b.d.l.	b.d.l.	6579		
WV-327	3.14	2.77E-04	b.d.l.	b.d.l.	b.d.l.	b.d.l.	b.d.l.	11355		
WV-329	1.35	1.09E-04	b.d.l.	b.d.l.	b.d.l.	b.d.l.	b.d.l.	12355		
WV-400	0.07	b.d.l.	b.d.l.	b.d.l.	b.d.l.	b.d.l.	b.d.l.		-34.36	
WV-401	0.00	b.d.l.	b.d.l.	b.d.l.	b.d.l.	b.d.l.	b.d.l.			
WV-412	2.60	5.07E-04	b.d.l.	b.d.l.	b.d.l.	b.d.l.	b.d.l.	5136	-60.93	
WV-414	0.02	b.d.l.	b.d.l.	b.d.l.	b.d.l.	b.d.l.	b.d.l.		-48.40	
WV-417	0.29	3.26E-05	b.d.l.	b.d.l.	b.d.l.	b.d.l.	b.d.l.	8780	-65.30	
WV-427	0.02	b.d.l.	b.d.l.	b.d.l.	b.d.l.	b.d.l.	b.d.l.		-70.68	
WV-428	0.02	b.d.l.	b.d.l.	b.d.l.	b.d.l.	b.d.l.	b.d.l.		-51.72	
WV-429	0.01	b.d.l.	b.d.l.	b.d.l.	b.d.l.	b.d.l.	b.d.l.		-54.78	
WV-435	0.01	b.d.l.	b.d.l.	b.d.l.	b.d.l.	b.d.l.	b.d.l.			
WV-501	0.74	b.d.l.	b.d.l.	b.d.l.	b.d.l.	b.d.l.	b.d.l.		-63.74	
WV-502	0.01	b.d.l.	b.d.l.	b.d.l.	b.d.l.	b.d.l.	b.d.l.		-54.28	
WV-503	0.70	5.95E-05	b.d.l.	b.d.l.	b.d.l.	b.d.l.	b.d.l.	11727	-60.40	
WV-504	0.08	b.d.l.	b.d.l.	b.d.l.	b.d.l.	b.d.l.	b.d.l.		-52.95	
WV-505	1.12	b.d.l.	b.d.l.	b.d.l.	b.d.l.	b.d.l.	b.d.l.		-58.55	
WV-511	0.00	b.d.l.	b.d.l.	b.d.l.	b.d.l.	b.d.l.	b.d.l.		-58.67	
WV-512	0.00	b.d.l.	b.d.l.	b.d.l.	b.d.l.	b.d.l.	b.d.l.		-68.27	
WV-514	0.00	b.d.l.	b.d.l.	b.d.l.	b.d.l.	b.d.l.	b.d.l.		-61.49	
WV-515	0.89	b.d.l.	b.d.l.	b.d.l.	b.d.l.	b.d.l.	b.d.l.		-59.03	
WV-516	1.99	b.d.l.	b.d.l.	b.d.l.	b.d.l.	b.d.l.	b.d.l.		-74.17	
WV-517	1.77	b.d.l.	b.d.l.	b.d.l.	b.d.l.	b.d.l.	b.d.l.		-60.94	
WV-519	0.19	b.d.l.	b.d.l.	b.d.l.	b.d.l.	b.d.l.	b.d.l.		-66.24	
WV-602	0.01	b.d.l.	b.d.l.	b.d.l.	b.d.l.	b.d.l.	b.d.l.			

[a]Timeline samples are labeled alphabetically (a = pre-drill, b or c are consecutive samples post-drill).

Table 3. Dissolved major and noble gas chemistry for groundwater samples. Blank entries indicate no analysis for that constituent.

Sample ID*	[N_2] (ccSTP/L)	[^{4}He] (x10^{-6} ccSTP/L)	[^{20}Ne] (x10^{-6} ccSTP/L)	[^{36}Ar] (x10^{-6} ccSTP/L)	^{3}He/^{4}He (R/Ra)	^{20}Ne/^{22}Ne	^{40}Ar/^{36}Ar	^{38}Ar/^{36}Ar	^{20}Ne/^{36}Ar	^{4}He/CH_4 (x10^{-6})	3H (T.U.)
WV-1a	13.00	46.5	169.8	1031.4	0.984	9.801	295.1	0.1896	0.165	137.3	
WV-1b	13.54	51.1	174.7	1098.1	0.961	9.811	295.7	0.1901	0.159	539.2	
WV-2a	10.99	43.0	125.5	895.4	0.914	9.803	295.3	0.1884	0.140	7002	
WV-2b	16.95	39.5	169.0	1234.5	1.021	9.781	295.4	0.1869	0.137	18453	
WV-3a	11.70	62.1	143.6	952.5	0.842	9.790	295.6	0.1886	0.151	22.6	
WV-3b	12.62	87.6	163.6	1069.1	0.851	9.772	295.4	0.1855	0.153	5.7	
WV-4	10.46	47.7	146.9	936.1	0.965	9.808	295.5	0.1881	0.157	366	
WV-5	13.78										
WV-6	11.95	45.2	136.0	946.3	1.014	9.815	295.8	0.1905	0.144	76.2	
WV-7	10.95	42.2	162.5	1004.4	1.006	9.785	296.4	0.1864	0.162	9894	
WV-8a	16.43	61.3	361.7	1346.6	0.871	9.782	295.3	0.1891	0.269	3648	5.4
WV-8b	15.48	67.1	342.1	1341.6	0.881	9.777	295.6	0.1897	0.255	450.0	6.3
WV-8c	15.99	57.5	358.0	1376.0	0.861	9.796	295.1	0.1894	0.260	3672	7.0
WV-10a	13.03	51.5	181.7	1044.5	0.912	9.791	295.3	0.1886	0.174	133.3	6.1
WV-10b	12.68	47.7	172.7	1032.0	0.905	9.804	295.7	0.1887	0.167	674.3	7.7
WV-10c	12.43	41.6	183.4	1023.4	0.921	9.776	295.2	0.1876	0.179	184.8	
WV-11a	14.35	81.1	183.5	1087.5	0.920	9.820	294.8	0.1857	0.169	217.3	
WV-11b	14.94	61.2	180.4	1100.5	0.881	9.802	295.7	0.1857	0.164	151.1	4.7
WV-11c	14.70	70.0	186.7	1036.4	0.875	9.824	295.7	0.1866	0.180	368.4	7.0
WV-12	14.65	72.2	192.1	1118.3	0.902	9.802	295.7	0.1874	0.172	259.6	
WV-21	11.56	63.4	141.2	962.8	0.946	9.791	295.7	0.1867	0.147	25.6	
WV-22	10.67	63.5	135.5	974.4	0.834	9.814	295.7	0.1866	0.139	65.5	
WV-25	12.64	6746.0	261.1	1020.3	0.045	9.863	295.4	0.1865	0.256	83284	
WV-27a	11.41	6315.0	402.4	897.9	0.021	9.817	299.0	0.1866	0.448	716.7	
WV-27b	9.84	5269.8	289.6	998.2	0.020	9.821	301.6	0.1896	0.290	675.1	4.7
WV-29a	10.26	8451.1	135.0	878.2	0.022	9.821	295.8	0.1904	0.154	3543	
WV-29b	10.97	7245.7	150.7	981.2	0.042	9.764	295.6	0.1897	0.154	7904	7.0
WV-29c	11.02	5146.7	158.4	944.3	0.036	9.771	295.6	0.1884	0.168	2181	
WV-31a	12.65	48.0	150.1	986.1	0.985	9.779	295.5	0.1879	0.152	48.5	5.0
WV-31b	14.21	79.5	153.4	1148.5	0.940	9.802	296.2	0.1896	0.134	58.7	
WV-32a	13.97	82.1	147.0	1131.3	0.841	9.777	295.7	0.1877	0.130	5334	
WV-32b	14.68	71.2	143.1	1020.5	0.831	9.795	295.3	0.1871	0.140	22631	
WV-33	17.07	48.0	157.2	1257.2	1.006	9.792	295.4	0.1896	0.125	129.7	
WV-36a	10.09	91451.7	506.5	926.3	0.021	9.827	307.4	0.1890	0.547	3268	
WV-36b	10.41	101214.1	568.5	831.9	0.019	9.851	306.2	0.1866	0.683	3387	
WV-36c	10.78	96874.4	498.5	947.4	0.023	9.830	303.4	0.0186	0.526	5250	
WV-37a	11.32	3979.7	261.1	942.0	0.030	9.781	297.1	0.1874	0.277	895.6	
WV-37b	11.82	4026.7	234.7	963.7	0.036	9.789	296.1	0.1877	0.243	803.1	3.5
WV-38a	10.25	67154.7	438.5	868.3	0.019	9.831	299.1	0.1876	0.505	5008	3.0
WV-38b	12.45	54658.0	387.7	1074.6	0.025	9.762	298.0	0.1895	0.361	4276	2.5
WV-39a	14.16	868.0	219.4	1120.1	0.106	9.796	295.9	0.0187	0.196	242776	
WV-39b	13.59	961.4	206.8	1095.9	0.104	9.802	296.1	0.1904	0.189	47129	3.5
WV-39c											
WV-40a	12.05	128.1	169.2	1056.6	0.781	9.821	295.7	0.1904	0.160	222.3	
WV-40b	11.87	102.1	176.5	1033.9	0.792	9.802	295.1	0.1867	0.171	32.4	
WV-40c	12.02	119.7	163.6	1030.3	0.831		295.1	0.1874	0.159	73.7	5.1
WV-41a	11.99	61.2	146.1	946.8	0.871	9.777	295.7	0.1890	0.154	28588	
WV-41b	14.15	61.1	149.5	1148.6	0.970	9.761	296.4	0.1869	0.130	74099	4.1
WV-51a	13.87	4789.7	394.6	892.3	0.023	9.824	297.1	0.1874	0.442	2600	
WV-51b	14.24	6021.4	385.5	964.4	0.020	9.831	298.0	0.1841	0.400	4408	4.7
WV-52a	10.72	357154.6	601.1	769.3	0.019	9.851	298.5	0.1904	0.781	38558	5.1
WV-52b	9.98	298647.5	442.7	887.6	0.018	9.871	299.0	0.1877	0.499	44836	6.2
WV-53	12.14	436.4	172.7	1222.4	0.084		295.6	0.1901	0.141	16543	
WV-54	10.90	102.4	132.5	961.5	0.698		295.8	0.1899	0.138	11856	
WV-55b	12.15	41.7	132.4	927.1	0.874	9.781	295.7	0.1896	0.143	20.4	3.2
WV-55c	10.95	53.5	151.4	918.6	0.934	9.760	295.5	0.1897	0.165	8574	
WV-56	11.62	235.4	131.4	1031.8	0.180		296.0	0.1898	0.127	7954	
WV-57	20.50										
WV-58a	12.46	214324.1	1196.8	1070.7	0.018	9.914	308.8	0.1891	1.118	8398	3.7
WV-58b	13.21	193214.7	384.1	1116.2	0.023	9.897	306.5	0.1886	0.344	6705	3.0
WV-59	11.57	1326.4	235.5	1007.9	0.031	9.805	297.6	0.1900	0.234	157.0	
WV-60b	14.75	127.8	153.5	927.6	0.832	9.795	295.5	0.1878	0.165	368.3	
WV-60c	14.22	502.3	224.4	1156.5	0.190	9.824	296.5	0.1901	0.194	120.8	
WV-61	10.41	7698.5	173.0	983.1	0.020		295.6	0.1875	0.176	3376	
WV-62b	14.02	72.2	132.1	919.2	0.847	9.791	295.4	0.1866	0.144	60.4	
WV-62c	14.52	63.4	190.2	999.6	0.920	9.804	294.6	0.1901	0.190	99.3	2.0
WV-63	12.14	53.5	129.9	990.3	0.861	9.780	295.3	0.1866	0.131	1776	
WV-64a	14.16	7255.0	239.4	966.4	0.021	9.779	297.4	0.1876	0.248	3538	
WV-64b	13.88	8967.7	249.5	963.6	0.031	9.761	298.4	0.1879	0.259	2439	
WV-65	12.14	49.8	142.2	996.4	0.924	9.799	295.4	0.1894	0.143	4387	
WV-66b	12.18	68.5	160.1	970.9	0.871	9.778	296.1	0.1904	0.165	27665	
WV-66c	13.55	67.1	161.2	1099.1	0.931	9.791	295.4	0.1884	0.147	20884	
WV-101b	12.14	978.6	204.6	873.0	0.030	9.790	297.1	0.1864	0.234	3606	5.7
WV-101c	11.97	1021.4	215.7	917.2	0.021	9.804	297.0	0.1843	0.235	4251	8.3
WV-102											
WV-103	11.15	51.6	137.4	907.5	0.911	9.787	295.0	0.1893	0.151	371.7	
WV-104											
WV-105	11.55	59.9	124.4	905.2	0.868		295.7	0.1904	0.137	10.5	
WV-106	13.49	43.5	136.0	1020.5	0.972	9.801	295.7	0.1864	0.133	1058	
WV-107											
WV-108b	14.24	79.5	182.4	1006.1	0.801	9.824	295.7	0.1876	0.181	6011	
WV-108c											
WV-109b	12.84	43.1	179.7	937.0	0.957	9.806	295.6	0.1894	0.192	605	
WV-109c	12.68	46.2	176.5	968.8	0.986	9.791	295.3	0.1867	0.182	3729	
WV-110	19.15	72.4	143.0	1326.1	0.931	9.785	295.2	0.1861	0.108	1827	

WV-111	13.54	43.7	153.0	964.6	0.979	9.799	295.4	0.1876	0.159	1001	4.7
WV-112	12.20	80.1	136.4	1030.4	0.803	9.821	295.4	0.1881	0.132	14195	4.4
WV-113	11.90										
WV-116b	12.01	815.4	249.6	932.6	0.196	9.802	296.1	0.1886	0.268	852.5	7.1
WV-116c	11.84	906.2	241.7	1089.0	0.163	9.790	298.0	0.1904	0.222	1399	2.7
WV-117	13.45										
WV-300											
WV-301b											
WV-301c	14.01	75.1	168.7	969.5	0.751	9.810	295.1	0.1890	0.174	11.3	4.7
WV-302b	12.96	103.2	192.2	1097.6	0.852	9.779	296.0	0.1876	0.175	51.1	3.0
WV-302c	12.35	63.1	171.6	1037.6	0.951	9.780	295.3	0.1869	0.165	2951	
WV-303b	12.75	54.7	175.4	1053.0	0.965	9.795	295.7	0.1898	0.167	51.9	
WV-303c	13.06	61.1	183.5	1009.3	0.981	9.776	295.0	0.1890	0.182	259.4	5.6
WV-304	10.69	53.6	128.8	933.4	0.822	9.767	294.5	0.1866	0.138	20.2	
WV-305											
WV-306											
WV-308	11.72	53.2	147.5	1018.6	0.930	9.821	295.6	0.1843	0.145	23.7	
WV-309	12.66	68.4	138.0	962.1	0.831	9.804	295.6	0.1865	0.143	32.0	
WV-311	17.24	50.0	132.5	1232.4	0.981		295.7	0.1880	0.108	1259	
WV-312	13.95	60.8	146.0	988.0	0.975	9.811	295.6	0.1878	0.148	281.7	7.2
WV-313	9.97	72156.4	269.5	900.4	0.017	9.851	301.3	0.1880	0.299	9735	3.5
WV-314b	12.61	154214.6	452.4	931.4	0.019	9.821	300.1	0.1890	0.486	4183	3.1
WV-314c	12.03	243142.4	406.8	923.2	0.019	9.842	299.4	0.1892	0.441	11328	4.7
WV-315	11.66	46.2	143.4	982.0	0.924	9.797	295.4	0.1883	0.146	1711	5.2
WV-316	10.99	56.6	141.2	962.9	0.931		295.4	0.1899	0.147	8.3	8.1
WV-317	8.94	96548.4	204.7	702.3	0.023	9.794	299.6	0.1877	0.291	10536	2.7
WV-318	12.99	39.0	137.6	861.5	0.826	9.757	295.3	0.1875	0.160	1258	6.5
WV-319	11.49	60.0	137.9	930.8	0.964	9.764	295.4	0.1899	0.148	1764	5.0
WV-320	10.45	70.0	136.0	1036.6	0.921	9.800	295.6	0.1874	0.131	32.7	
WV-321	10.59	42.5	138.0	1114.5	0.981	9.791	296.5	0.1886	0.124	22.7	7.5
WV-322	11.59	49.4	153.9	995.6	0.952	9.787	295.7	0.1877	0.155	568.3	3.5
WV-323	9.69	2154.4	163.4	825.9	0.037	9.842	295.4	0.1851	0.198	414.5	
WV-324b	12.87	90.2	157.2	963.8	0.687	9.786	295.3	0.1888	0.163	54.6	
WV-324c	13.24	206.2	214.5	1335.3	0.398	9.789	295.4	0.1899	0.161	7800	
WV-325	11.50	55.0	136.0	976.1	0.942	9.792	294.8	0.1886	0.139	97.0	
WV-326	11.50	53.5	161.6	946.8	0.942	9.821	295.7	0.1909	0.171	22.7	
WV-327	16.69	72.7	127.0	1233.6	0.694	9.831	295.6	0.1879	0.103	23.1	
WV-329	12.97	42.7	126.0	919.8	0.980	9.802	295.3	0.1881	0.137	31.6	8.4
WV-400	11.95	51.6	143.5	979.2	0.941	9.798	296.1	0.1882	0.147	767.8	6.0
WV-401	11.95	65.1	130.0	946.8	0.880	9.802	295.7	0.1879	0.137	30429	6.6
WV-412	13.84	8270.0	324.8	940.1	0.036	9.762	299.4	0.1874	0.345	3179	2.5
WV-414	11.98										
WV-417	11.64	61.4	147.0	907.1	0.765	9.801	294.8	0.1894	0.162	215.0	7.4
WV-427	12.50	47.0	132.0	941.8	0.964	9.805	295.9	0.1899	0.140	1922	
WV-428	10.15										
WV-429	12.14	51.2	124.5	972.4	0.894	9.795	295.6	0.1879	0.128	5697	
WV-435	11.29	49.0	163.4	919.8	0.962	9.797	295.7	0.1881	0.178	8999	7.5
WV-501	14.66	59.5	168.4	1221.2	0.981	9.795	295.1	0.1895	0.138	80.2	2.1
WV-502	19.65	37.5	358.0	1320.6	0.979	9.820	294.9	0.1905	0.271	6608	
WV-503	13.70	635.8	241.2	1153.3	0.045	9.795	296.5	0.1899	0.209	911.5	
WV-504	12.64	52.2	156.5	1010.6	0.964	9.790	295.4	0.1905	0.155	692.0	3.5
WV-505	13.75	76.4	146.5	1188.1	0.950	9.760	294.7	0.1897	0.123	68.2	
WV-511	11.82	80.0	146.2	1216.5	0.940	9.781	296.0	0.1891			
WV-512	13.25	145.4	189.5	1157.1	0.846	9.801	295.5	0.1895	0.164	29786	4.1
WV-514	14.15	51.1	176.4	1192.6	0.960	9.764	295.0	0.1865	0.148	99770	2.4
WV-515	12.96	301.5	223.2	1279.5	0.405	9.804	296.5	0.1904	0.174	339.2	
WV-516	13.06	197.9	189.6	1040.6	0.345	9.805	294.6	0.1879	0.182	99.5	2.7
WV-517	14.05	59.5	179.5	1033.4	1.002	9.782	295.1	0.1876	0.174	33.7	2.5
WV-519	13.21	67.4	154.6	1082.6	0.964	9.790	296.0	0.1880	0.143	346.0	1.9
WV-602											

[a]Timeline samples are labeled alphabetically (a = pre-drill, b or c are consecutive samples post-drill).

Table 4. Water chemistry for surface water associated with the flowback spill in Tyler County and leaks from the two injection well sites. All ratios are in molar units. Blank entries indicate no analysis for that constituent

Sample ID	Sample Descriptions	Date Sampled	Cl (mg/L)	Br/Cl ($x10^{-3}$)	Li (ppb)	B (ppb)	V (ppb)	Cr (ppb)	As (ppb)	Se (ppb)	Sr (ppb)	Mo (ppb)	Ba (ppb)	$\delta^{11}B$ (‰)	$\delta^{7}Li$ (‰)	$^{87}Sr/^{86}Sr$
WV Flowback n = 13	From Ziemkiewicz and He (2015)		42683	4.8				ND	0.08	ND	1365		515			
Tyler - 1	Spill water in Field	1/3/14	18087	6.8	14151	25737	221	679	50.0	282	769376	289	53119	27	11	0.7098
Tyler - 2	Spill water in Field	1/6/14	2133	4.0	841	1600	16.5	51.8	3.4	20.9	55009	25.1	1837	28	14	0.7096
Tyler - 3	Pool by well pad	1/6/14	1031	5.6	413	790	8.1	26.0	2.2	12.8	27067	29.9	975	27	14	0.7096
Tyler - 4	Creek at runoff point	1/6/14	14	3.9	2.65	14.9	0.3	0.7	0.1	0.7	210	3.4	35.3			0.7111
Tyler - 5	Creek upstream	1/6/14	2	ND	0.3	8.6	0.2	0.3	0.1	0.4	67.2	1.7	27.5			
Tyler - 6	Run-off into Creek	2/23/14	669	3.9	197	340	5.3	69.1	5.2	89.0	8269	ND	601.0			0.7098
Tyler - 7	Big Run Creek by pad	2/23/14	21	3.7	3.0	19.6	0.2	0.7	0.2	0.7	267	0.1	44.7			
Tyler - 8	Big Run Creek	2/23/14	6	2.7	0.5	10.0	0.2	0.3	0.2	0.5	74.3	ND	27.8			
Tyler - 9	Middle Island Creek	2/23/14	9	2.5	0.6	9.0	0.2	0.4	0.2	0.6	61.0	ND	27.7			
Tyler - 10	Effluent from well pad	8/29/14	918	4.5	2.2	233	4.9	14.4	3.7	7.0	12519	3.8	1102			0.7095
Lochgully -1	Downstream Creek 1	9/14/13	575	2.1	11.6	0.4	2.5	<DL	<DL	<DL	2068	<DL		20		
Lochgully -2	Downstream Creek 2	9/14/13	367	3.0	33.9	24.1	1.4	<DL	<DL	<DL	1296	<DL				
Hall - 1	Upstream	12/18/13	16	2.7	0.7	20.4	0.4	0.9	0.1	ND	302	ND	74.0			
Hall - 2	Downstream 1	12/18/13	95	4.4	1.0	48.8	1.0	2.7	0.2	0.6	617	ND	127			0.7113
Hall - 3	Downstream 2	12/17/13	80	3.2	0.7	38.7	0.9	2.3	0.2	ND	526	ND	106			0.7113
WV-327	Groundwater well	12/17/13	6	1.8	12.4	105	0.4	0.1	1.1	ND	1247	1.2	765			
WV-329	Groundwater well	12/17/13	3	2.7	10.1	89.0	ND	0.1	4.9	ND	1487	0.7	1450			

ND = value below detection

Figure 1

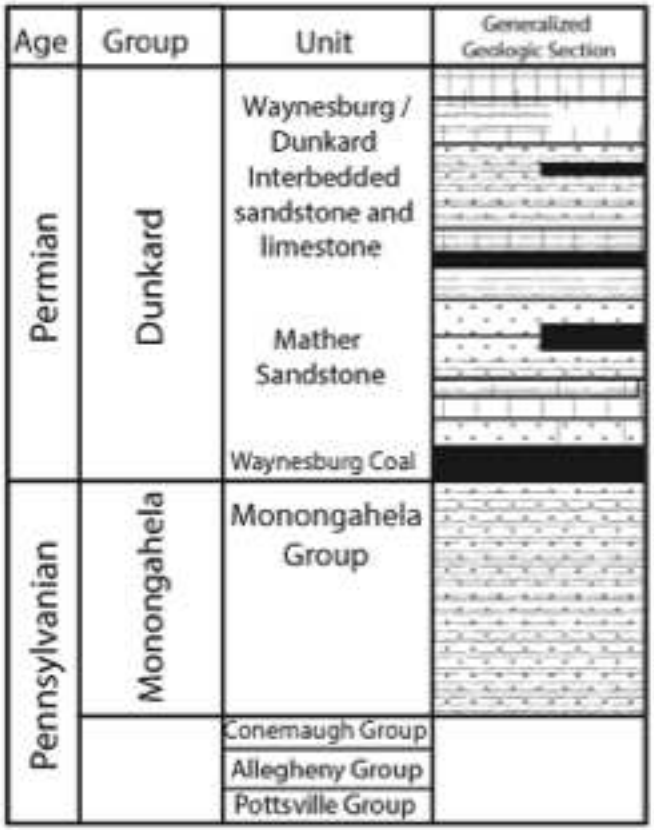

Figure 1

Figure 2

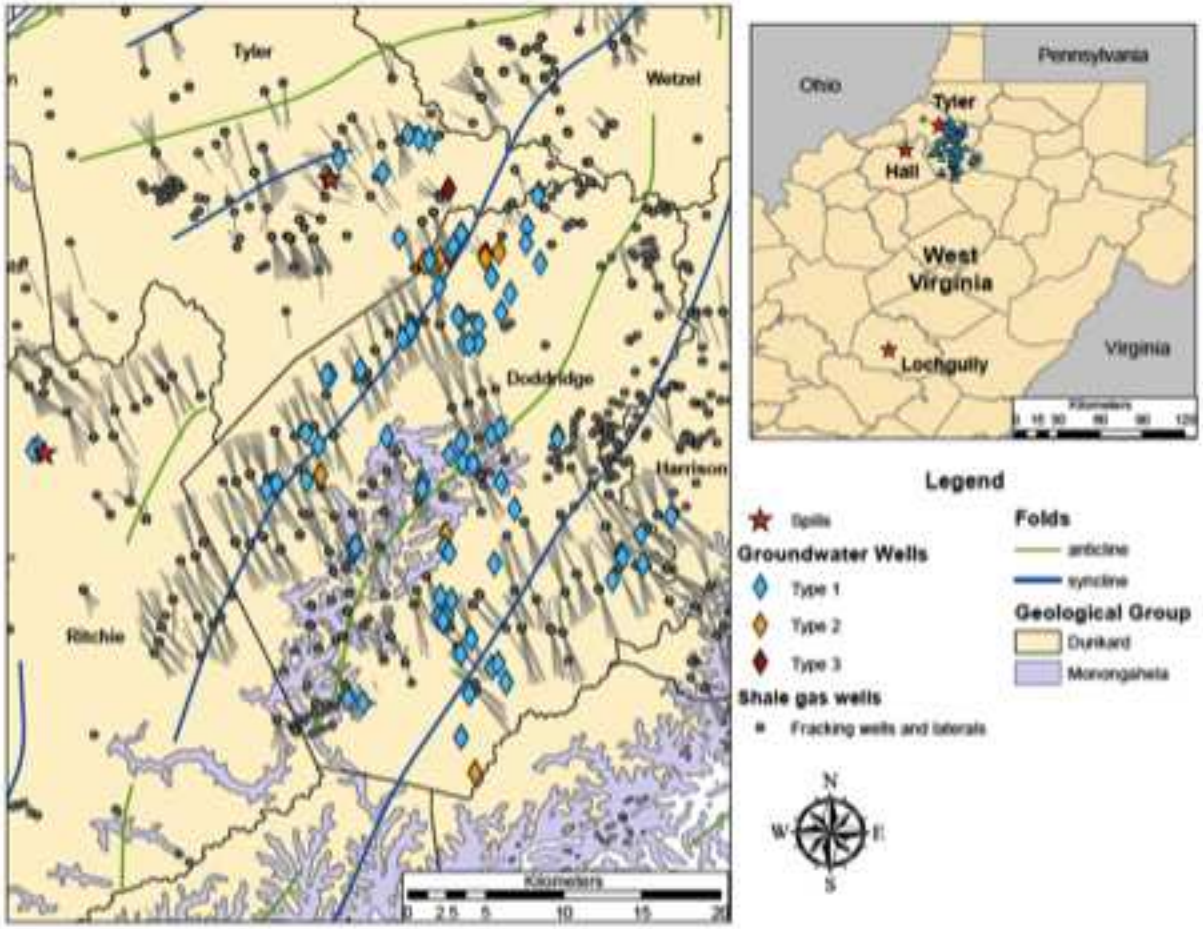

Figure 2

Figure 3

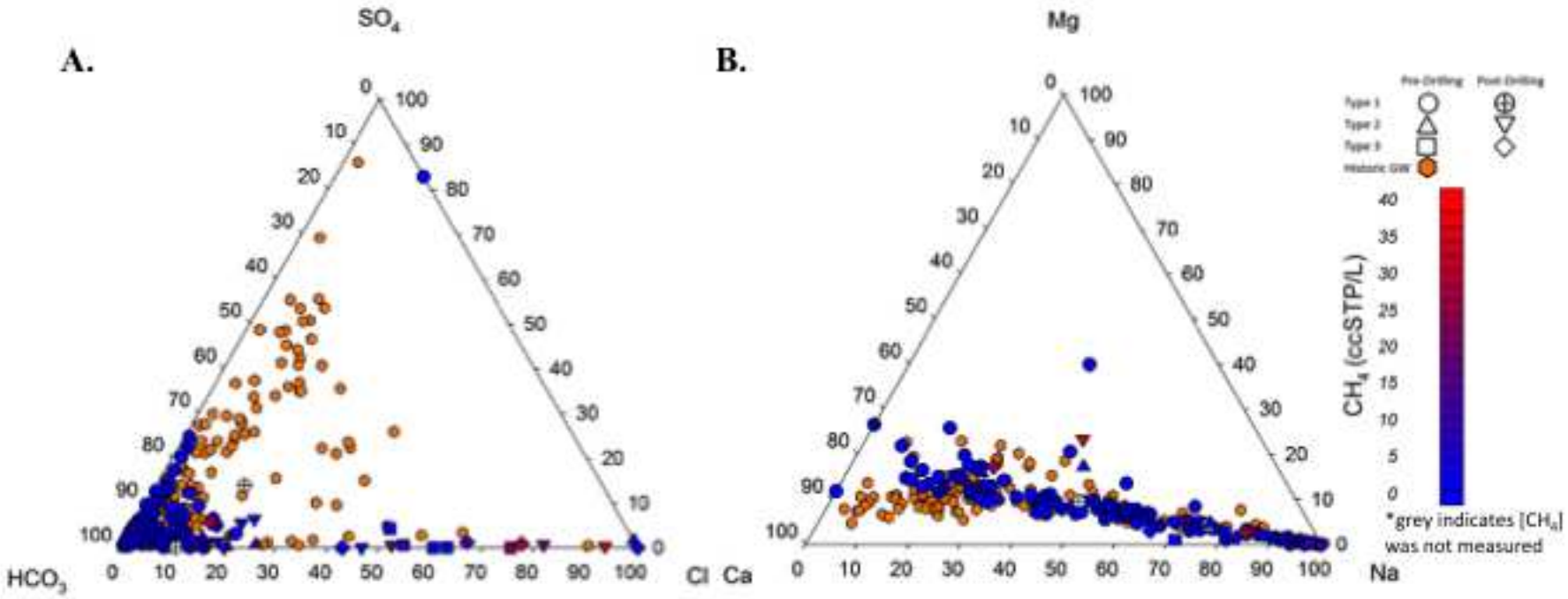

Figure 3

Figure 4

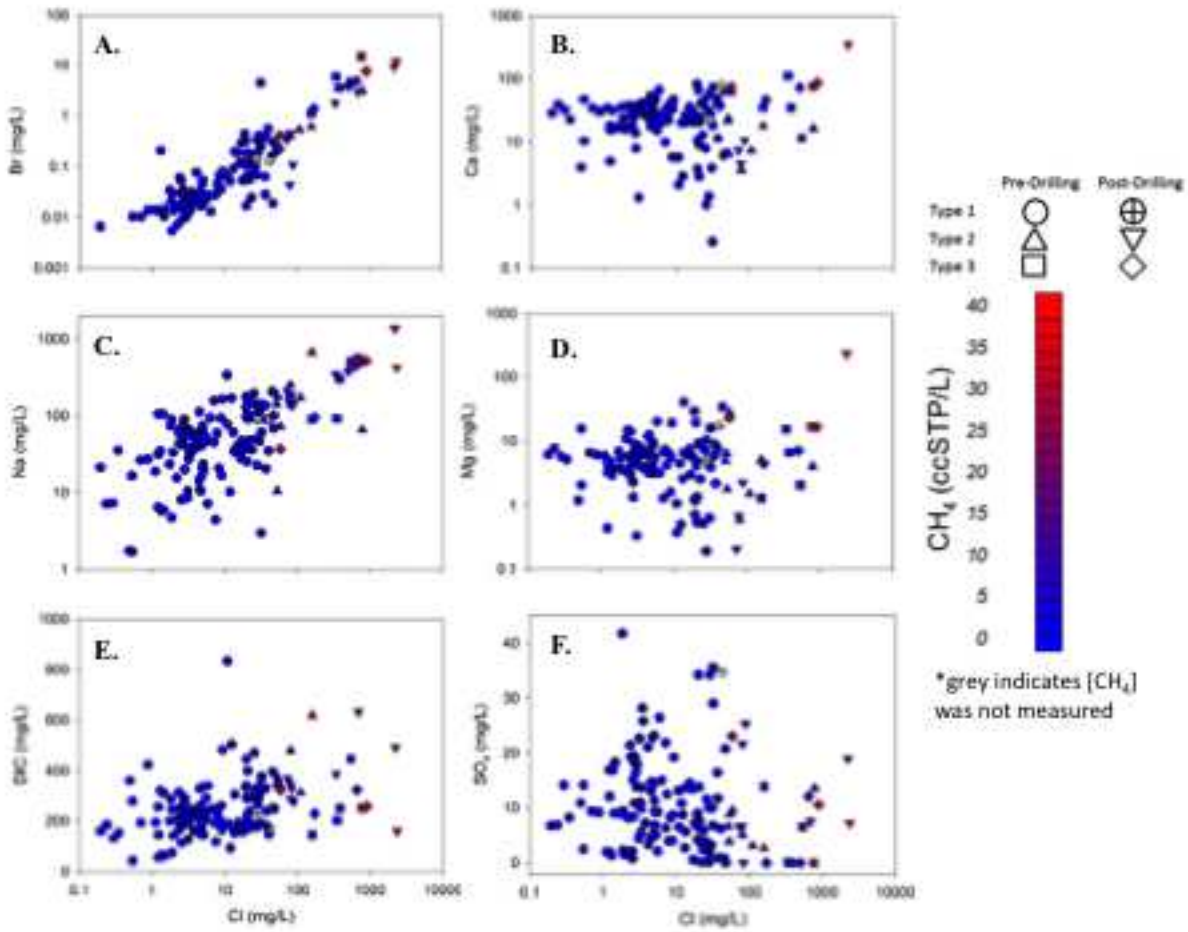

Figure 4

Figure 5

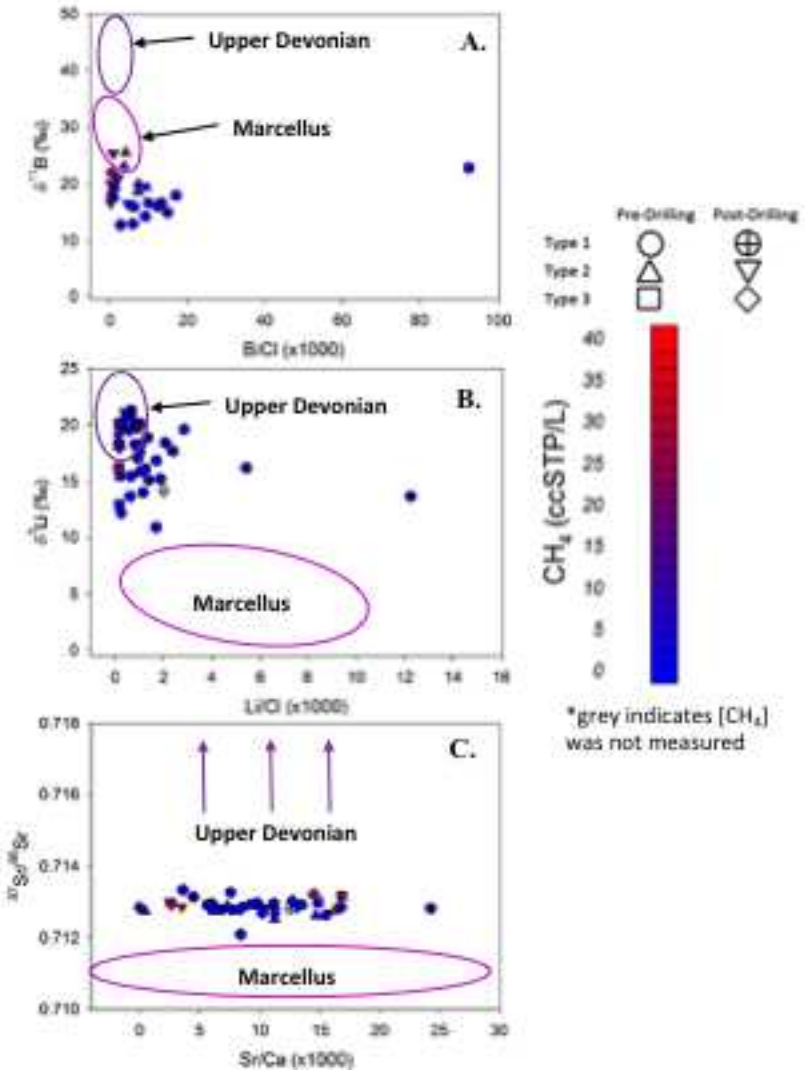

Figure 5

Figure 6

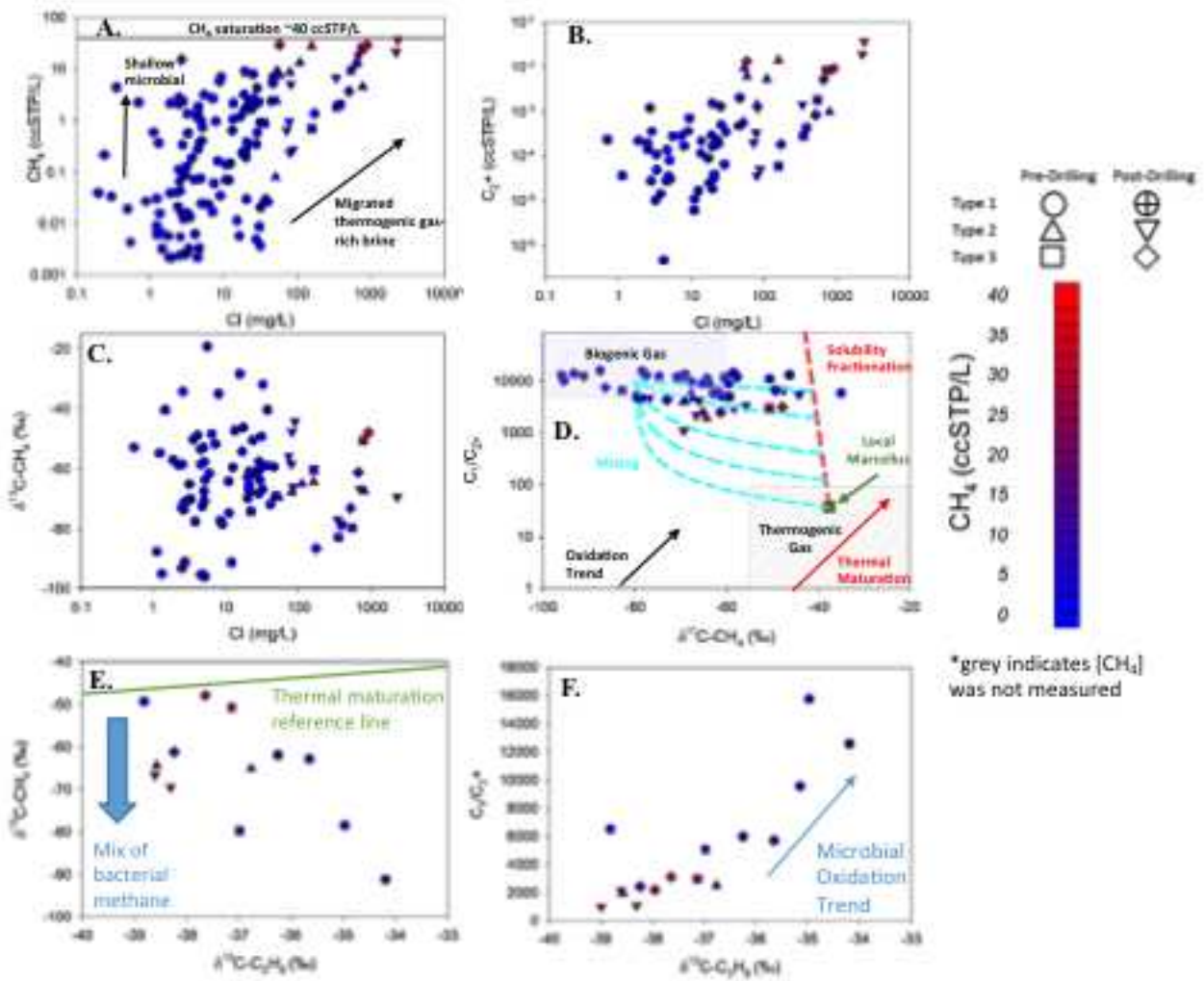

*grey indicates [CH_4] was not measured

Figure 6

Figure 7

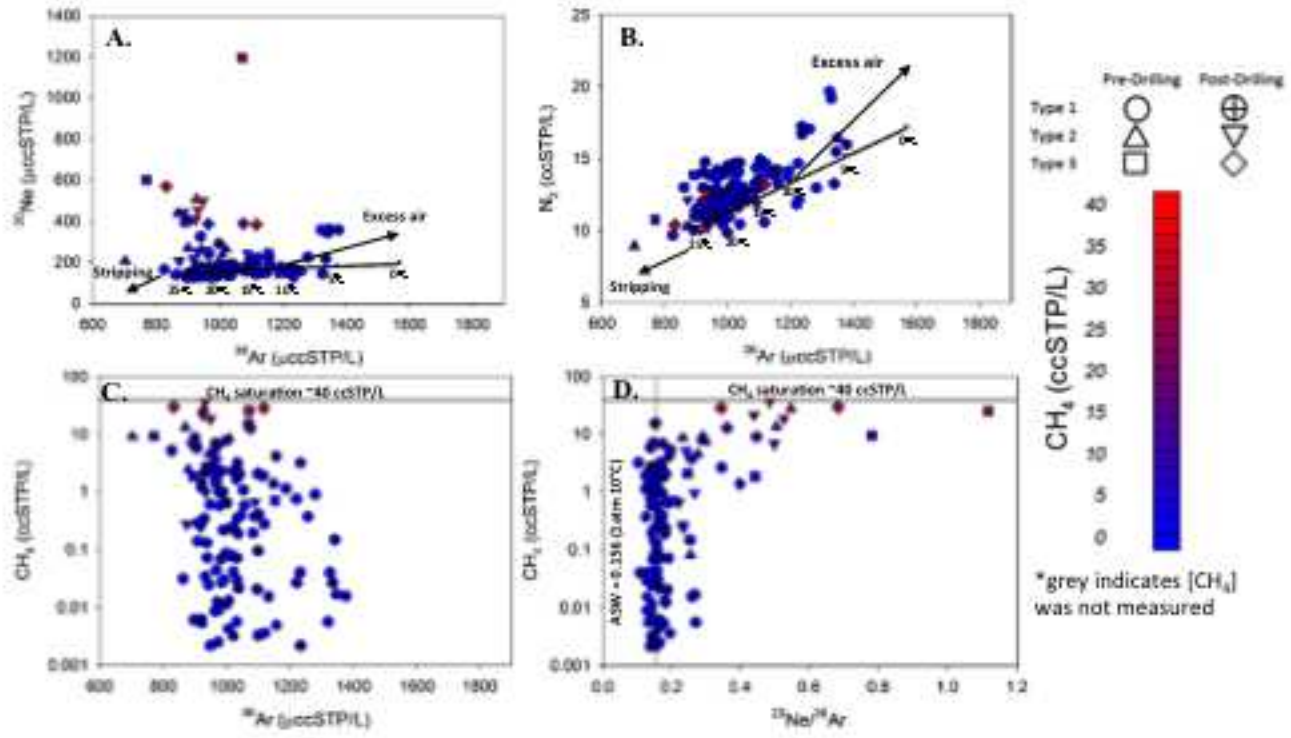

Figure 7

Figure 8

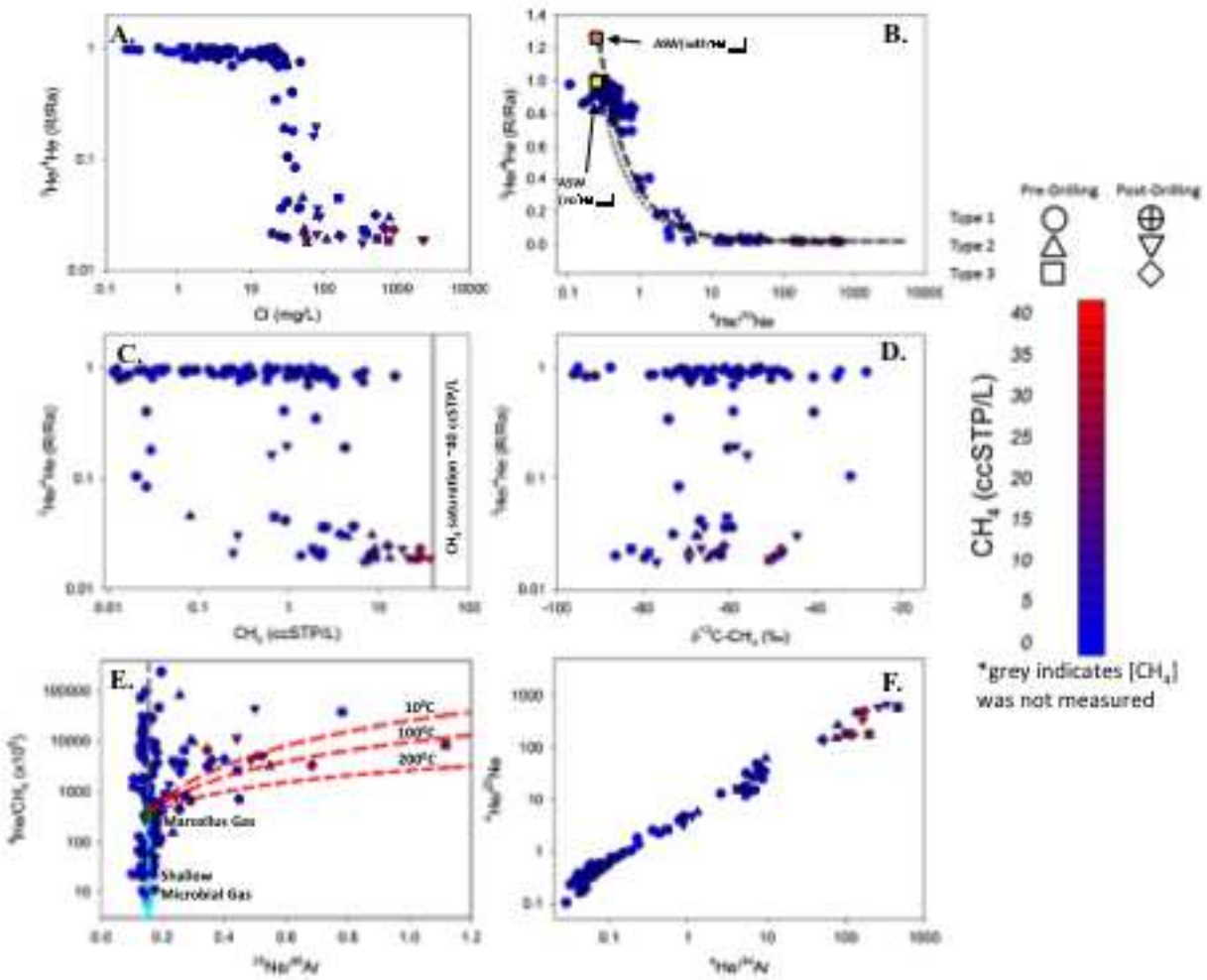

Figure 8

Figure 9

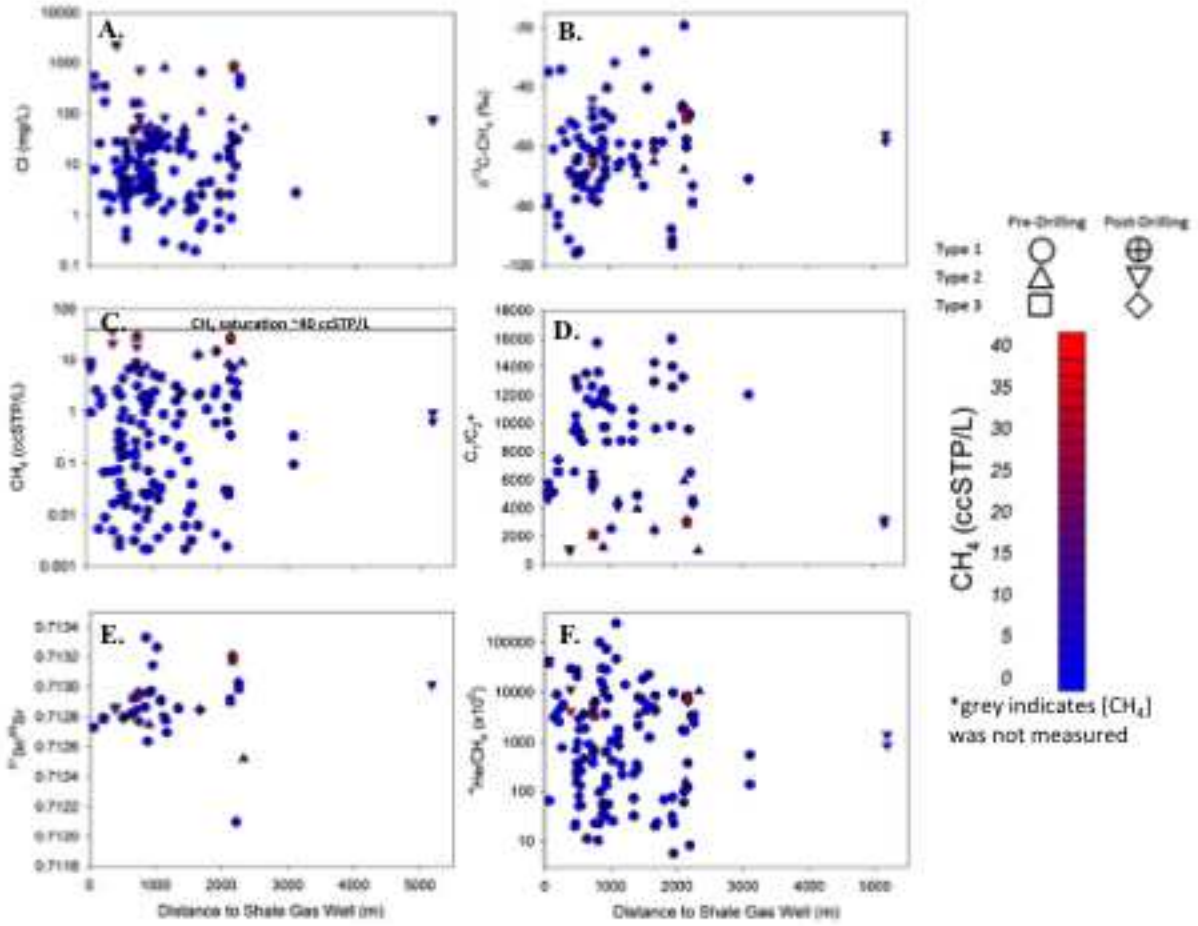

Figure 9

Figure 10

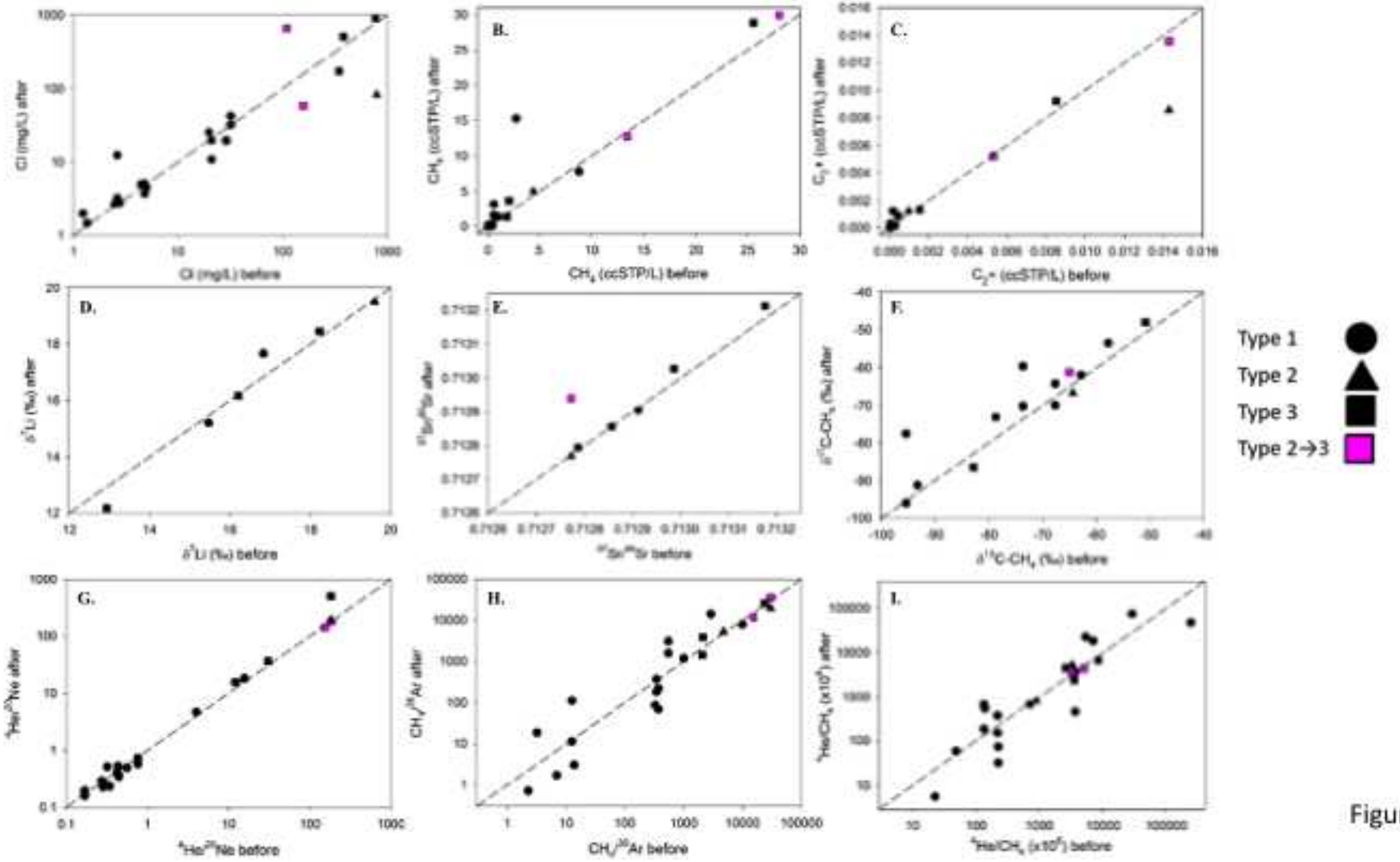

Figure 10